K O N I N K L I J K N E D E R L A N D S
M E T E O R O L O G I S C H I N S T I T U U T

D e B i l t

WETENSCHAPPELIJK RAPPORT

W.R. 74-11

L.C. Heijboer
and
A.W. den Exter Blokland

The inclusion of Latent heat in a three-level model with filtered equations and its influence upon the development of depressions

De Bilt, 1974

Publikatienummer: K.N.M.I. W.R. 74-11 (M.O.)

U.D.C.: 551.509.313:
551.515.1

Table of contents

		Page
1.	Introduction	1
2.	The dry model	3
	2.1. Basic equations	3
	2.2. The construction of a surfaceprog.	6
3.	The moist model	7
	3.1. The splitting procedure	7
	3.2. The parameterization of D_m and its consequences	10
	3.3. The amount of heating due to condensation	12
	3.4. The correction of the stream functions at 300, 500 and 850 mbar due to condensation	15
	3.5. Some further remarks about the parameterization of D_m and the related ω_m profile	16
	3.6. The effect of the chosen vertical distribution of D_m and latent heat on the prognosis	17
4.	Results	18
5.	Summary and conclusion	21
6.	List of symbols	23
7.	Literature	24

The inclusion of latent heat in a three-level model with filtered equations and its influence upon the development of depressions

by L.C. Heijboer and A.W. den Exter Blokland

1. Introduction

At the Royal Netherlands Meteorological Institute a three-level quasi-geostrophic filtered equations model has been in operational use since 1971. The model in its present form was developed by L.C. Heijboer. Its special features are a characteristic vertical parameterization of the divergence of the horizontal wind, which makes it possible to do without a specification of the vertical parameterization of the wind. In addition to this, the final equations have been amended in a special way, so as to keep the thickness patterns in phase with the absolute topography of 500 mbar.

The details of the model will be amply discussed in a forthcoming publication [3]; here, only a short survey of the equations used is given in chapter 2, with some explanatory notes, but without any derivations. The three forecast levels are 300, 500 and 850 mbar, while an extrapolation to 1000 mbar is made to obtain a surface prognosis. So far this model does not include the release of latent heat due to the condensation of water vapour; therefore it is called the "dry model".

The present report deals with a "moist model" in which latent heat is taken into account. The way it is done is described in chapter 3. In this chapter the three fundamental equations: the vorticity equation, the thermodynamic equation and the continuity equation are introduced again, this time with a heating term in the thermodynamic equation. They form the basis of the moist model. The solution of this model can easily be compared with that of the dry version. While the equations are linear in the relevant terms, expressions for the difference between the solutions can be found by simply subtracting the vorticity and the thermodynamic equation of the dry model from the corresponding equations of the moist model, as is shown in paragraph 3.1.

In this expression the difference D_m between the "moist" and the "dry" divergence appears besides terms related to the release of latent heat.
In paragraph 3.2. an assumption about the vertical profile of D_m is made. Using the continuity equation, this leads to an expression for the differences between the solution of the moist and the dry version at the three levels 850, 500 and 300 mbar.
Further, knowledge of the amount of heating is necessary; this amount is derived from a precipitation forecast in a way shown in paragraph 3.3.
Finally, in paragraph 3.4 the differences between the moist and the dry solutions at 850, 500 and 300 mbar are expressed as functions of the released latent heat. These differences are considered as corrections to the solution of the dry model to obtain the solution of the moist one. The corrections are applied at each time step of the computation, so that the corrected solution, a set of stream functions, serves as initial for the next time step.
In the paragraphs 3.5 and 3.6 some remarks are made concerning the relation between the vertical profiles of D_m and the vertical velocity and of the effect of the parameterization of D_m - together with assumptions about the released latent heat - on the moist solution.
In chapter 4 forecasts with the moist model are discussed and compared with those of the dry model. The results of the selected cases in this report clearly indicate that the main cause of development of frontal waves at sea level is the release of latent heat.

-o-o-o-o-o-o-

2. The dry model

2.1 Basic equations

The three-level model at present in operational use at the Royal Netherlands Meteorological Institute is a filtered equations model based on the following well-known formulas:
(Coordinates x,y,p)

Simplified vorticity equation:

$$\nabla^2 \dot{\psi} + J(\psi, \eta) + f_o D = 0 \qquad (1)^*$$

Thermodynamic equation:

$$\frac{\partial \dot{\psi}}{\partial p} + J\left(\psi, \frac{\partial \psi}{\partial p}\right) + \frac{\sigma}{f_o} \omega = 0 \qquad (2)$$

ψ is the quasi-geostrophic stream function;

$$\psi = \frac{gz}{f_o}$$

The right side of (2) is put equal to zero, because no heating whatsoever is considered in the dry model. In paragraph 3.1 the thermodynamic equation appears again with a heating term included.

Continuity equation:

$$D + \frac{\partial \omega}{\partial p} = 0 \qquad (3)$$

The model is based on the assumption that the vorticity equation (1) is exactly fulfilled at 850, 500 and 300 mbar, thus:

(The suffix $_{8.5}$ refers to 850 mbar, etc.).

---

* See list of symbols on page 23

$$\left.\begin{aligned} \nabla^2 \dot{\psi}_{8.5} + J\ (\psi_{8.5}, \eta_{8.5}) + f_o D_{8.5} &= 0 \\ \nabla^2 \dot{\psi}_5 + J\ (\psi_5, \eta_5) + f_o D_5 &= 0 \\ \nabla^2 \dot{\psi}_3 + J\ (\psi_3, \eta_3) + f_o D_3 &= 0 \end{aligned}\right\} \quad (4)$$

Between 850 and 500 mbar the quasi-geostrophic stream function is supposed to vary according to:

$$\psi = \psi_5 - A(p)\left[\psi_5 - \psi_{8.5}\right] + B(p)$$

with $A(p_{8.5}) = 1$, $A(p_5) = 0$, $B(p_{8.5}) = B(p_5) = 0$

(This implies that the geostrophic wind V_g can be given by:

$$V_g = V_{g_5} - A(p)\ \left[V_{g_5} - V_{g_{8.5}}\right]$$

Similarly between 500 and 300 mbar. Therefore, when (2) is integrated over the two layers 850 - 500 mbar and 500 - 300 mbar, respectively, we obtain:

$$\left.\begin{aligned} \dot{\psi}'_{8.5} + J\ (\psi_5, \psi'_{8.5}) - \frac{\sigma'_{8.5}}{f_o} \int_{p_5}^{p_{8.5}} \omega dp &= 0 \\ \dot{\psi}'_3 + J\ (\psi_5, \psi'_3) - \frac{\sigma'_3}{f_o} \int_{p_3}^{p_5} \omega dp &= 0 \quad , \end{aligned}\right\} \quad (5)$$

where

$$\psi'_{8.5} \equiv \psi_5 - \psi_{8.5}, \qquad \psi'_3 \equiv \psi_3 - \psi_5 \ ,$$

$\sigma'_{8.5}$ and σ'_3 are mean stability indices for the lower and upper layer respectively.

The functions A(p) and B(p) do not appear in (4) and (5); obviously no further specification of this parameterization is necessary.

The method of resolution of the set of equations (4), (5) and (3) is based on the introduction of a realistic parameterization of D along the vertical. With the logical supposition that $\omega_{10} = \omega_0 = 0$, (3) leads to

$$\int_{p_0}^{p_{10}} D \, dp = 0, \tag{6}$$

which is a constraint on this parameterization.
Then, with the help of (3), (6) and an accepted D-profile, ω, $D_{8.5}$, D_5 and D_3 can be eliminated from (4) and (5).
Furthermore, a special correction is applied in (5) to keep the forecast thickness pattern consistent with the 500 mbar forecast, introducing an additional stream function ψ_5^* (see [3]).
The lengthy and cumbersome computations which are necessary to obtain the final result are not given in the present report. They will be described in [3]. The resulting partial differential equations with the unknown functions $\dot{\psi}'_{8.5}$, $\dot{\psi}'_3$ (instead of $\dot{\psi}_{8.5}$, $\dot{\psi}_3$), $\dot{\psi}_5$ and $\dot{\psi}_5^*$, are:

$$\left.\begin{aligned}
(\nabla^2 - a_{00})\,\dot{\psi}'_{8.5} &= -J(\psi_5, \nabla^2\psi'_{8.5} - a_{00}\,\psi'_{8.5} + a_{01}\,\psi'_3) \\
&\quad - J(\psi'_{8.5}, \eta_5 - \nabla^2\psi'_{8.5}) - a_{01}\,\dot{\psi}_3 \\
&\quad - a_{05}\,\dot{\psi}_5^* + a_{04}\,J(\psi_5, \nabla^2\psi_5) \\
(\nabla^2 - a_{10})\,\dot{\psi}'_3 &= -J(\psi_5, \nabla^2\psi'_3 - a_{10}\,\psi'_3 + a_{11}\,\psi_{8.5}) \\
&\quad - J(\psi'_3, \eta_5 + \nabla^2\psi'_3) - a_{11}\,\dot{\psi}_{8.5} \\
&\quad - a_{15}\,\dot{\psi}_5^* + a_{14}\,J(\psi_5, \nabla^2\psi_5) \\
\nabla^2\dot{\psi}_5 &= -J(\psi_5, \eta_5 - a_0\,\psi'_{8.5} + a_1\,\psi'_3) \\
&\quad + a_0\,\dot{\psi}'_{8.5} - a_1\,\dot{\psi}'_3 \\
\nabla^2\dot{\psi}_5^* &= -J(\psi_5, \eta_5)
\end{aligned}\right\} \tag{7}$$

The a's are constants, which are dependent upon the parameterization of D and the chosen values of $\sigma_{8.5}$ and σ'_3.

Models of the same structure are found in [1] and [4] .
However, there are differences and in particular the final equations in those articles do not contain the terms with the constants a_{05}, a_{04}, a_{15}, a_{14} and the equation for $\nabla^2 \dot{\psi}$.
The execution is performed on a grid with a mesh width of 375 km on 60° N and with time steps of one hour.

2.2. The construction of a surface prog

Finally, the surface prog is derived from the 500 and 850 mbar progs as follows (assuming below 500 mbar a saturated adiabatic lapse rate):

$$p_{surf} = 0.125 \{ (\psi_5 - 1.25\psi'_{8.5}) \frac{f_o}{g} - 310 \} + 1000$$

(p_{surf} : surface pressure in mbar)
The inaccuracy of this approximation can generally be neglected. Only over land, in cases of extreme deviations from the assumed vertical temperature profile in the boundary layer the differences may be unacceptable.

3. The moist model

3.1. The splitting procedure

The basic equations are introduced again, this time with a heating term included:

Simplified vorticity equation:

$$\nabla^2 \dot{\psi} + J(\psi,\eta) + f_o D = 0 \tag{1}$$

Thermodynamic equation:

$$\frac{\partial \dot{\psi}}{\partial p} + J(\psi, \frac{\partial \psi}{\partial p}) + \frac{\sigma}{f_o} \omega = h \tag{8}$$

h is a heating term resulting from the condensation of water vapour; see for its value paragraph 3.3, formula (21).

Continuity equation:

$$D + \frac{\partial \omega}{\partial p} = 0 \tag{3}$$

(5) becomes:

$$\left.\begin{aligned} \dot{\psi}'_{8.5} + J(\psi_5, \psi'_{8.5}) - \frac{\sigma'_{8.5}}{f_o} \int_{p_5}^{p_{8.5}} \omega \, dp = H'_{8.5} \\ \dot{\psi}'_3 + J(\psi_5, \psi'_3) - \frac{\sigma'_3}{f_o} \int_{p_3}^{p_5} \omega \, dp = H'_3 \end{aligned}\right\} \tag{9}$$

where

$$H'_{8.5} = -\int_{p_5}^{p_{8.5}} h dp \quad \text{and} \quad H'_3 = -\int_{p_3}^{p_5} h dp \tag{10}$$

Consider the equations (1), (4) , (8) and (9).
Let $\dot{\psi}$, D and ω belong to the moist version and $\dot{\psi}_d$, D_d and ω_d to the dry version. The quantity $\dot{\psi}_m$ will be defined as the difference between $\dot{\psi}$ and $\dot{\psi}_d$:

$$\dot{\psi}_m = \dot{\psi} - \dot{\psi}_d$$

and accordingly

$$\omega_m = \omega - \omega_d, \quad D_m = D - D_d.$$

$\dot{\psi}_m$ is simply the correction, which should be added to the solution of the dry version of the equations to get the solution of the moist version. To find expressions for $\dot{\psi}_m$ we consider first the vorticity equation (1) in the moist case, where $\dot{\psi}$ and D satisfy the equation:

$$\nabla^2 \dot{\psi} + J(\psi,\eta) + f_o D = 0 \qquad (1)$$

Furthermore, in the dry case $\dot{\psi}_d$ and D_d satisfy this equation, so that:

$$\nabla^2 \dot{\psi}_d + J(\psi,\eta) + f_o D_d = 0 \qquad (1)$$

(Note that the Jacobian here is $J(\psi,\eta)$ and not $J(\psi_d, \eta_d)$.
In both equations the initial stream function is the same, the solutions $\dot{\psi}$ (with D) and $\dot{\psi}_d$ (with D_d) differ in general. Evidently, during the course of the computation with the moist model, the stream function will differ from the solution of the computation with the dry version. When applying (1), however, the "history" of the stream function is irrelevant. See further the Introduction and p.15.)
Subtraction gives:

$$\nabla^2 \dot{\psi}_m + f_o D_m = 0 \qquad (11)$$

a formula which applies at the three chosen levels 850, 500 and 300 mbar, thus:

$$\left.\begin{aligned} \nabla^2 \dot{\psi}_{8.5_m} &= - f_o D_{8.5_m} \\ \nabla^2 \dot{\psi}_{5_m} &= - f_o D_{5_m} \\ \nabla^2 \dot{\psi}_{3_m} &= - f_o D_{3_m} \end{aligned}\right\} \quad (12)$$

Handling the thermodynamic equations (9) in the same way:

$$\dot{\psi}'_{8.5} + J(\psi_5,\psi'_{8.5}) - \frac{\sigma'_{8.5}}{f_o} \int_{p_5}^{p_{8.5}} \omega dp = H'_{8.5}$$

$$\dot{\psi}_{8.5_d} + J(\psi_5,\psi'_{8.5}) - \frac{\sigma'_{8.5}}{f_o} \int_{p_5}^{p_{8.5}} \omega_d dp = 0$$

$$\dot{\psi}'_{8.5_m} - \frac{\sigma'_{8.5}}{f_o} \int_{p_5}^{p_{8.5}} \omega_m dp = H'_{8.5}$$

and analogous to this:

$$\dot{\psi}'_{3_m} - \frac{\sigma'_3}{f_o} \int_{p_3}^{p_5} \omega_m dp = H'_3$$

or:

$$\left.\begin{aligned} \dot{\psi}_{5_m} - \dot{\psi}_{8.5_m} &= H'_{8.5} + \frac{\sigma'_{8.5}}{f_{o'}} \int_{p_5}^{p_{8.5}} \omega_m dp \\ \dot{\psi}_{3_m} - \dot{\psi}_{5_m} &= H'_3 + \frac{\sigma'_3}{f_o} \int_{p_3}^{p_5} \omega_m dp \end{aligned}\right\} \quad (13)$$

Because D,ω and D_d, ω_d satisfy (3), evidently D_m, ω_m do also,

thus: $D_m + \frac{\partial \omega}{\partial p}_m = 0$ (14)

with $\omega_{10_m} = \omega_{0_m} = 0$ we get:

$$\int_{p_0}^{p_{10}} D_m dp = 0. \quad (15)$$

We want to solve $\dot{\psi}_{8.5_m}$, $\dot{\psi}_{5_m}$ and $\dot{\psi}_{3_m}$ from (12), (13) and (15).

In order to do this, we have to make some assumptions about the D_m's in (12) and the right sides of the equations (13), which will be discussed in the following paragraphs.

3.2. The parameterization of D_m and its consequences

As said before (p.5) a certain parameterization of D as a function of p enables us to solve the ψ's from the set of equations (4), (5) and (3). Heijboer [3] will show such a parameterization for the dry model. We shall now define a profile for D_m, with emphasis upon physical consistency and simplicity as follows (see fig. 1):

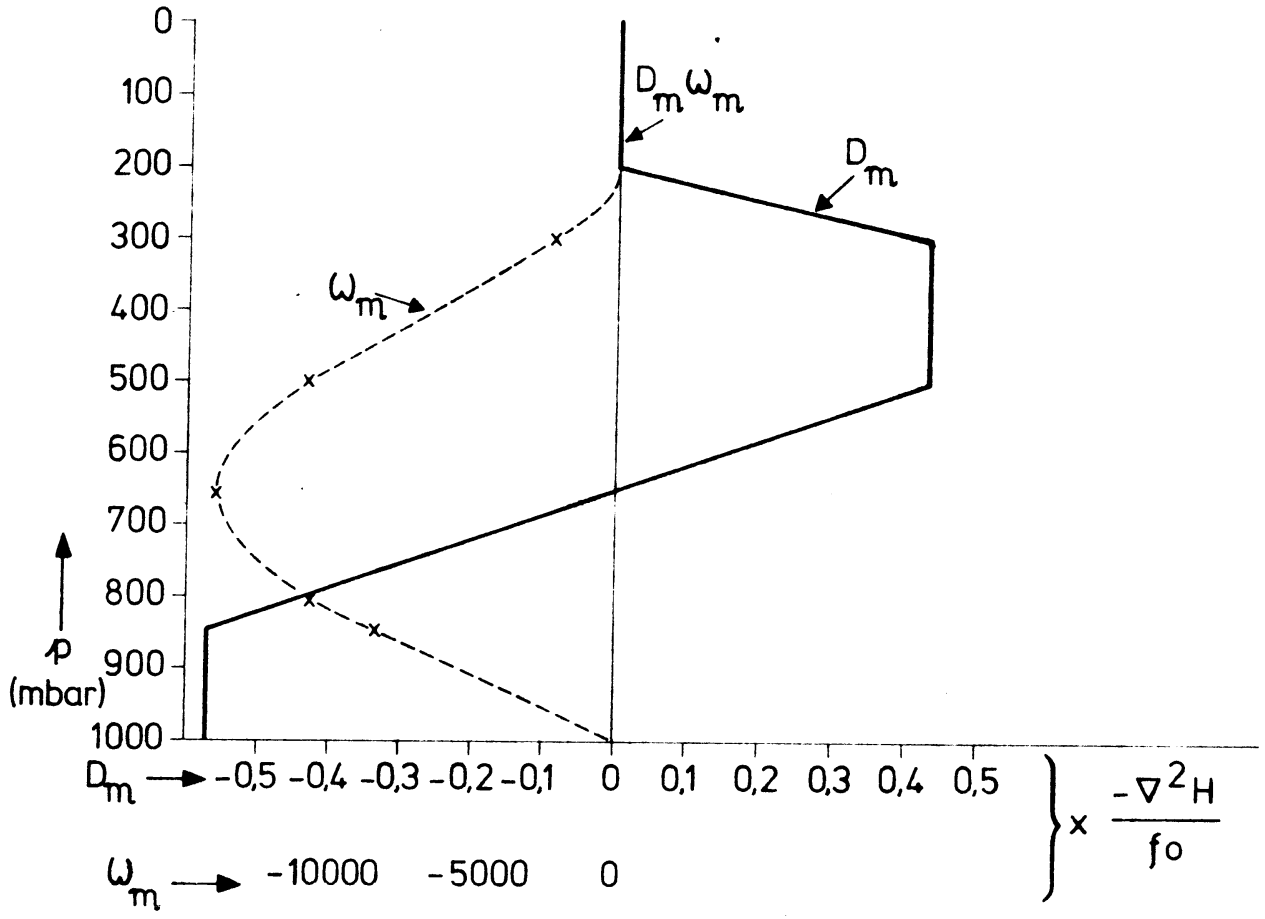
0
100
200
300
400
500
600
700
800
900
1000
p
(mbar)
$D_m\omega_m$
D_m
ω_m
D_m → -0,5 -0,4 -0,3 -0,2 -0,1 0 0,1 0,2 0,3 0,4 0,5
ω_m → -10000 -5000 0
$\times \frac{-\nabla^2 H}{f_o}$

fig.1

D_m is kept constant and equal to $D_{8.5_m}$ between 850 and 1000 mbar, thus:

$$D_{10_m} = D_{8.5_m}$$

and from 200 mbar upwards

$$D_m = 0$$

With the trapezoidal rule applied to (15):(pressure in mbar):

$$\left(\int_0^{200} + \int_{200}^{300} + \int_{300}^{500} + \int_{500}^{850} + \int_{850}^{1000} \right) D_m \, dp =$$

$$100 \frac{D_{3_m}}{2} + 200 \left(\frac{D_{3_m} + D_{5_m}}{2} \right) + 350 \left(\frac{D_{5_m} + D_{8.5_m}}{2} \right)$$

$$+ 150 \left(\frac{D_{8.5_m} + D_{8.5_m}}{2} \right) = 0 \quad \text{or}$$

$$6 D_{3_m} + 11 D_{5_m} + 13 D_{8.5_m} = 0$$

In the following paragraphs 3.3, 3.4 and 3.5 it will be shown that the postulated D_m profile is as given in fig. 1.

After substitution from (12):

$$\nabla^2 (6\dot{\psi}_{3_m} + 11 \dot{\psi}_{5_m} + 13 \dot{\psi}_{8.5_m}) = 0 \qquad (16)$$

While in the computational scheme all $\dot{\psi}_m$'s on the boundary are assumed to be equal to zero (the boundary being located, as much as possible, in regions where this assumption is approximately true), the form in (16) between brackets also is put equal to zero on the boundary.

Thus, according to a well-known theorem of the theory of the LAPLACE - equations, the solution of (16) is:

$$6\,\dot{\psi}_{3_m} + 11\,\dot{\psi}_{5_m} + 13\,\dot{\psi}_{8.5_m} = 0 \qquad (17)$$

3.3 The amount of heating due to condensation

First the amount of heating in the layer between 850 and 500 mbar will be considered. When an atmospheric layer is saturated and the temperature lapse rate $\frac{\partial T}{\partial p}$ is moist adiabatic, the terms $\frac{\sigma}{f_o}\,\omega$ and h in the thermodynamic equation (8) cancel out, thus

$$\frac{\sigma}{f_o}\,\omega = \frac{\sigma}{f_o}\,(\omega_d + \omega_m) = h,$$

According to (10) this leads to:

$$-\frac{\sigma'_{8.5}}{f_o}\int_{p_5}^{p_{8.5}} (\omega_d + \omega_m)\,dp = H'_{8.5} \qquad (18)$$

After substitution of (18), the first equation of (13) becomes:

$$\dot{\psi}_{5_m} - \dot{\psi}_{8.5_m} = \frac{-\sigma'_{8.5}}{f_o}\int_{p_5}^{p_{8.5}} \omega_d\,dp \qquad (19)$$

Define $\dot{\psi}_{5_m} - \dot{\psi}_{8.5_m}$ as H. Then

$$H \equiv \frac{-\sigma'_{8.5}}{f_o}\int_{p_5}^{p_{8.5}} \omega_d\,dp$$

In principle, this H can be calculated straightforwardly from (5) (on page 4), thus

$$H = -\{\,\dot{\psi}'_{8.5_d} + J(\psi_5, \psi'_{8.5})\,\} \qquad (20)$$

Experimental forecasts with H defined in this way appeared to be rather unsuccesful - probably because the amount of condensed water vapour was overestimated. A reason for this failure may be that at the beginning of a period of rain the conditions mentioned above - complete saturation and a moist adiabatic lapse rate - are not fulfilled yet. Applying (20) in that case certainly means an over-estimation of condensation. Therefore, in this experiment H is derived from the amount of precipitation. The way this amount is computed is described by den Exter Blokland [2] . The method consists of a determination, from time step to time step, of the amount of precipitable water of the column of air from 850 to 500mbar, in grid points. When this amount exceeds the saturation value, or a percentage thereof say 80% -, the surplus rains out.

Let P be the amount of precipitation, per second and per unit of cross-section, which is determined in this way.

The computation of P is performed with a "dry" version of the baroclinic model, where the computed vertical velocity is ω_d. So it is acceptable to use this amount of precipitation to replace the $-\sigma'_{8.5}/f_o \int \omega_d \, dp$ in (19). It should be noted that the amount of precipitation calculated in combination with a "dry" model, thus with ω_d, is lower than the amount calculated with $\omega = \omega_d + \omega_m$; the latter giving a better estimate of the real amount because ω is a better estimate of the vertical velocity in the actual atmosphere. Virtually the precipitation forecast gives a too small amount but this amount fits in the computational scheme that we use in this report for the determination of $\dot{\psi}_m$.

The initial state of the threedimensional humidity distribution is obtained by analysing radiosonde observations.

The considered column of air - as mentioned before - extends from 850 to 500 mbar. Suppose that the portion of P that condenses between p and $p + \Delta p$ amounts to $(ap + b) P \Delta p$, with

$$\int_{p_5}^{p_{8.5}} (ap + b)\, dp = 1,$$

(follows from the definition of P)

and $a = 13.10^{-10}$ (dimension $kg^{-2}\ m^2 s^4$)

$b = -59.10^{-6}$ (dimension $kg^{-1}\ m\ s^2$).

The evaluation of a and b is discussed by den Exter Blokland, [2] paragraph 3.1 and 3.2. It depends on the relation between the maximum specific humidity and p and should be considered here as a mere estimation of the relative amount of condensed vapour along the vertical axis p. So, h in (8) becomes:

$$h = \frac{-gRL}{f_o c_p} \frac{(ap + b)}{p} p \qquad (21)$$

and H:

$$H = \left[\frac{gRL}{f_o c_p} \int_{p_5}^{p_{8.5}} \frac{(ap + b)}{p} dp \right] P = \dot{\psi}_{5_m} - \dot{\psi}_{8.5_m} \qquad (22)$$

When the amount of precipitation is expressed in cm - and the other quantities in SI units - the constant in (22) between brackets is approximately 10^7.

Now, the second equation of (13) will be considered. In the experiments discussed here the right-hand side is put equal to zero. This is justified by the assumption that, in case of precipitation, some condensation will occur above 500mbar also, thus H_3' will be positive, while ω_m is supposed to be negative. Since the two terms on the right side of the equation are of opposite sign, we assume that their sum is at least one order of magnitude smaller than $\dot{\psi}_{3_m}$ and $\dot{\psi}_{5_m}$. Clearly this reasoning is entirely different from the one applied to the lower layer, which led to (22). The difference is explained by the fact, that complete saturation in combination with a moist adiabatic lapse rate is considered to be unlikely throughout the entire layer from 500 to 300mbar. Otherwise, when one wants to treat the upper layer similarly to the lower, one might substitute a fraction of H, say 10% or less, for the right hand side. For the water vapour content above 500 mbar is much smaller than below.

3.4. The correction of the stream functions at 300, 500 and 850 mbar due to condensation.

With the foregoing specifications $\dot{\psi}_{3_m}$, $\dot{\psi}_{5_m}$, and $\dot{\psi}_{8.5_m}$ can be solved from (13), (17) and (22):

$$6\,\dot{\psi}_{3_m} + 11\,\dot{\psi}_{5_m} + 13\,\dot{\psi}_{8.5_m} = 0 \qquad (17)$$

$$\dot{\psi}_{5_m} - \dot{\psi}_{8.5_m} = H$$

$$\dot{\psi}_{3_m} - \dot{\psi}_{5_m} = 0$$

where $H = 10^7 P$.

The solution is:

$$\dot{\psi}_{3_m} = \dot{\psi}_{5_m} = 0.43\ H,\ \dot{\psi}_{8.5_m} = -\ 0.57\ H \qquad (23)$$

These values are simply added to the outcome of a computation with the dry version to obtain the result of the moist version, with latent heat incorporated. This is done after every time step Δ t. Let the value of ψ_5 at t in the grid point (i,j) be ψ_5 (i,j,t). Then first the value at t + Δ t is determined with the dry model; call this value ψ_{5_d} (i,j,t + Δ t). Next the correction is applied and the final value of ψ_5 becomes:

$$\psi_5 (i,j,t + \Delta t) = \psi_{5_d} (i,j,t + \Delta t) + \Delta t \times 0.43\ H(i,j,t + \Delta t)$$

where H(i,j,t + Δ t) is derived from the precipitation, computed with the dry model, over the period t to t + Δ t.

ψ_5 (i,j,t + Δ t) serves as the initial value for the computation over the next period from t + Δ t to t + 2 Δ t, first with the dry model, followed by a correction Δ t x 0.43 H(i,j,t + 2 Δ t) to get the next value ψ_5 (i,j,t + 2 Δ t). Similarly, with the appropriate corrections, ψ_3 and $\psi_{8.5}$ are computed.

Evidently, in grid points where no precipitation is forecast, the correction is zero.

3.5. Some further remarks about the parameterization of D_m and the related ω_m profile

From (12) follows:

$$D_m = \frac{-\nabla^2 \dot{\psi}_m}{f_o}$$

With the parameterization of D_m mentioned in 3.2 and the consequent results as given in (23) it follows that:

$$D_{3_m} = D_{5_m} = -0.43\ \nabla^2 H,$$

$$D_{8.5_m} = 0.57\ \nabla^2 H\ ;$$

while supposing a linear relation between the specified levels, the D_m profile can be constructed as shown in fig.1.
From (14) and $\omega_{o_m} = 0$ follows:

$$\omega_m (p) = -\int_{p_o}^{p} D_m\, dp$$

With the chosen D_m this leads to:

If $p \leq 200$ mbar, then $\omega_m (p) = 0$,

Furthermore, keeping in mind that in SI units the unit of pressure is 0.01 mbar (= 1 Newton/m^2 = 1 Pascal):

$$\omega_{3_m} = \frac{2150\ \nabla^2 H}{f_o},$$

$$\omega_{5_m} = \frac{10750\ \nabla^2 H}{f_o}$$

$$\omega_{8.5_m} = \frac{8300\ \nabla^2 H}{f_o},$$

and again

$$\omega_{10_m} = 0.$$

The extreme value of ω is found at approximately 650 mbar where

$$\omega_m = \frac{13980\ \nabla^2 H}{f_o}$$

This profile, which is partly linear and partly parabolic, is also drawn in fig. 1.

The values of H are non-negative with a maximum within the area of heaviest precipitation. The Laplacian $\nabla^2 H$ will be negative around that maximum, and probably over practically the whole precipitation zone. Therefore, in fig. 1 the shown D_m and ω_m profiles are supposed to agree with reality in "weather-active" regions.

3.6. <u>The effect of the chosen vertical distribution of D_m and latent heat on the prognosis.</u>

Of course, a different D_m profile can be used, and can be combined with other estimations of the amount of latent heat in the two atmospheric layers.

To investigate how those suppositions affect the final product, an experiment was performed with quite different assumptions as follows:

$$D_{10_m} = 0.5 D_{8.5_m}$$

and

$$D_{0_m} = 0.$$

Then, from (15), with the trapezoidal rule:

$$\frac{300}{2} D_{3_m} + \frac{200}{2} (D_{3_m} + D_{5_m}) + \frac{350}{2} (D_{5_m} + D_{8.5_m})$$

$$+ \frac{150}{2} (D_{8.5_m} + 0.5 D_{8.5_m}) = 0,$$

which leads, similarly as in 3.2., to:

$$20\ \dot{\psi}_{3_m} + 22\ \dot{\psi}_{5_m} + 23\ \dot{\psi}_{8.5_m} = 0 \qquad (24)$$

The treatment of the thermodynamic equations (13) will be slightly different too. Suppose:

$$\left.\begin{aligned} \dot{\psi}_{5_m} - \dot{\psi}_{8.5_m} &= H \\ \dot{\psi}_{3_m} - \dot{\psi}_{5_m} &= 0.05\ H \end{aligned}\right\} \qquad (25)$$

where in the second equation (25) the right hand term 0.05H is a guess based on the considerations that some condensation in the higher layer is likely to occur in a way similar to that in the lower layer, but with a much smaller amount of condensing water vapour. The solution of (24) and (25) is:

$$\dot{\psi}_{3_m} = 0.39H,\ \dot{\psi}_{5_m} = 0.34H,\ \dot{\psi}_{8.5_m} = -0.66H$$

Forecasts with these values instead of those from (23) were performed. No significant difference in quality could be observed.

4. Results

Examples of forecasts with the dry and the moist model, for 24 hours ahead, are presented on pp 25 - 27 , together with initial and verification charts.

Both the surface pressure and the 500 mbar moist model forecast of 4 November 1972, for 24 hours ahead, are succesful. Only the low near Nova Scotia on the surface prog is not in agreement with reality. But with the dry model the forecast for that area is incorrect too; the fact that the deviations are smaller than with the moist model is hardly a proof of superiority, because the dry model in general does not allow large deepenings. On the surface analysis of 1200 GMT, 4 November 1972 - outside the area shown here - a flat low of 1013mbar is located at about 37N - 77W. This low moves within 24 hours to 36 N - 68W, deepening about 4 mbar.
It corresponds to the depression erroneously forecast near Nova Scotia. It is easily understood that a low, the movement of which is forecast incorrectly with the help of the dry model, leads to a "moist" forecast with incorrect deepening.

From 12 to 13 November 1972 a frontal wave over the Atlantic developed into a deep low, associated with a gale over the southern part of the North Sea and adjacent coastal areas. The dry model failed to forecast the strong deepening and consequently missed the gale. The moist model, with latent heat incorporated along the lines described in 2, succeeded in forecasting the developments quite well. Especially after a forecast period of 24 hours the expected positions and the central values of the pressure are in a fair agreement with reality. In general, the differences between the two 500mbar forecasts are not so important. Atfirst sight, the moist model looks less preferable because the wave over western Europe is too pronounced. This phenomenon is found again in the thickness progs. However, looking at them the suspicion arises that a difference in phase exists between the moist prog and the verification chart, which could account for the difference between the 500 mbar patterns as well.

The moist surface forecast of 11 December 1972, for 24 hours ahead, is much better than the dry prognosis. During 24 hours two depressions considerably deepened over the Atlantic - the moist version predicts this fairly well. On 500 mbar too the moist forecast is to be preferred.

In the prognosis for 0000 GMT, 15 December 1972, based upon the weather situation of 24 hours before, the central pressure of the low on the Atlantic is perfectly forecast with the moist model. But the position is inaccurate and at the bottom of the chart erroneous ridges of high pressure show up. Associated with them, an enormous high is formed in the 500 mbar + 24 moist forecast. Computational instability is the main reason for this failure, as shown by an experiment with halved time steps.

On 23 December 1972 a depression moved from Nova Scotia towards the centre of the Atlantic, deepening about 40 mbar within 24 hours. Here again the dry model fails, the moist model is reasonably good. A well-marked distinction between the qualities of the two 500 mbar progs is hard to make.

Regarding the thickness charts, when strictly comparing the numerical values, the dry model is better. The pattern of the isolines of the moist model, however, looks more like reality.

On 11 January 1973, the strong cyclogenesis on the Atlantic, resulting in a deep depression SW of Iceland, is correctly forecast by the moist model. At the bottom of the chart the moist forecast, however, is highly unrealistic, as on 15 December 1972. An experiment with halved time steps proved that computational instability was not the reason. Probably, an incorrect initialization of the specific humidity, combined with a too high value of the vertical velocity and with boundary errors, caused this failure of the moist model.

The severe gale on 2 April 1973 was not correctly forecast with the moist model, the central pressure being not deep enough. However, this forecast is far superior to the forecast with the dry model, which hardly shows a depression at all. Here again, at 500 mbar the dry forecast is better. It could be possible that in reality much more latent heat was freed than is accounted for in the moist model.

In fig. 2, p 58 , the set of graphs presents a comparison between the observed pressure tendencies and the forecasts with the dry and the moist model. In fig. 3, p 61 , the observed and forecast tracks to 36 hours ahead are shown.

5. Summary and conclusion.

A method is presented wherein latent heat resulting from the condensation of water vapour is incorporated in a three level quasi-geostrophic filtered equations model. The amount of latent heat is directly derived from the amount of precipitation, which is determined with the help of a simple model, in which in cases of supersaturation the condensate rains out completely.

The essential of the method is that after every time step the parameters of each of the three levels 300, 500 and 850 mbar are first computed without latent heat, whereafter a correction due to latent heat is applied. The correction is found by splitting the solution of the complete set of equations - with latent heat included - into a so-called dry and moist part. The dry part is determined by solving the set of equations without latent heat ; the method of solution is not discussed in this report. The manner according to which the moist part is computed is described. It appears to be a simple and straightforward calculation; one only needs to parameterize the moist part of divergence along the vertical.

From the forecast 500 and 850 mbar data an approximate surface chart is constructed.

Examples of prognosis of surface pressure, the height of 500 mbar and 850 mbar - 500 mbar thickness, are shown and compared with the forecasts without latent heat.

Our conclusion is that latent heat, due to the condensation of water vapour, is one of the principal causes - if not the principal cause - for the deepening of surface lows. The major cause of the opposite phenomenon, the filling of (deep) lows, is most likely friction. Friction is not included in the experiments under discussion, and also in the precipitation forecast a permanent supply of water vapour is assumed, which is certainly not true over land. Therefore, in some cases the deepening continues too long. The thickness forecasts of the moist model sometimes produce a good picture of warm tongues and therefore enable the meteorologist to locate fronts better.

It appears that the model requires an accurate analysis with respect to positions and intensities of troughs and ridges and of the moisture distribution, because an incorrect initialization of the upper-air humidity

or a wrong location of the areas of ascending vertical velocities may cause spurious deepenings, which occasionally tend to increase beyond limits. In fact, one of the experiments, not presented here, showed such a failure, resulting in forecasting an enormous depression which did not occur at all.

It can be noticed that a direct solution of the complete set of equations with latent heating, without use of a splitting procedure, might be possible. To do so, the value of the amount of heating has to be known, a value which depends on the solution to be found. Though there are ways to estimate the heating term fairly well, in this report another method is preferred that appears to give some promising results without requiring time consuming extra computations.

To complete the model, friction and a device to control the supply of water vapour should be incorporated; such a model would be suited for inclusion into an operational numerical prediction program.

6. List of symbols

c_p	Specific heat of dry air at constant pressure
f	CORIOLIS parameter
f_o	Value for the CORIOLIS parameter at 45^o N.
g	Acceleration of gravity
i,j	Grid point coordinates
p	Pressure
t	Time
x,y,z	Space coordinates
D	Horizontal divergence
$J(\ldots, \ldots)$	Jacobian
L	Latent heat
R	Gas constant for dry air
η	Absolute vorticity; here = $\nabla^2 \psi + f$
σ	Static stability parameter
ω	$\frac{dp}{dt}$; vertical velocity in x,y,p - system
Δ	Finite difference
ψ	Stream function; here = $\frac{gz}{f_o}$
∇^2	Horizontal Laplacian; $\frac{\partial^2}{\partial x^2} + \frac{\partial^2}{\partial y^2}$.

7. Literature

1. BENGTSSON, L. and MOEN L. (1971): Satellite and computer applications to synoptic meteorology: An operational system for numerical weather prediction. World Meteorological Organization publication. WMO 283, pp65 - 88.

2. EXTER BLOKLAND, A.W. den (1972): Experimenten met het numeriek opstellen van neerslagverwachtingen (with English summary). Royal Netherlands Meteorological Institute. Wetenschappelijk rapport van het Kon. Nederlands Meteorologisch Instituut. W.R. 72 - 8.

3. HEIJBOER, L.C. (-): Design of a barocline three level quasi-geostrophic model: (To be published in the series "Mededelingen en Verhandelingen" of the Royal Netherlands Meteorological Institute).

4. Speciale Projectgroep Numerieke Voorspelmethoden (1969): Beschrijving van Programma's voor de EL - X8. Royal Netherlands Meteorological Institute. Wetenschappelijk rapport van het Kon. Nederlands Meteorologisch Instituut. W.R. 69 - 3.

EXAMPLES OF FORECASTS

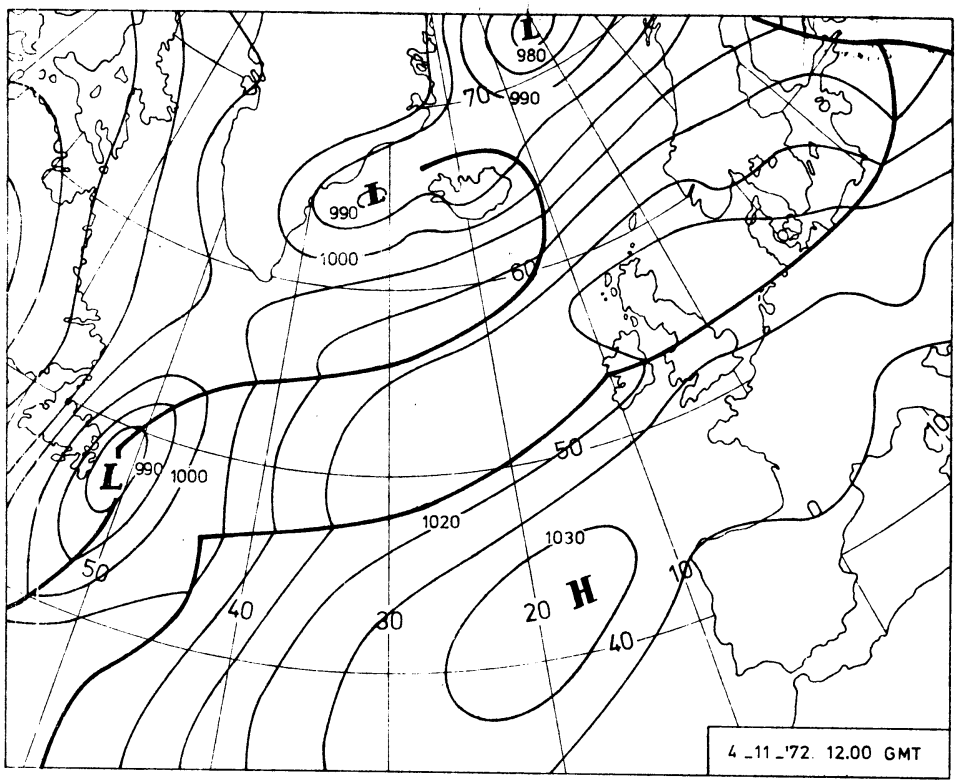

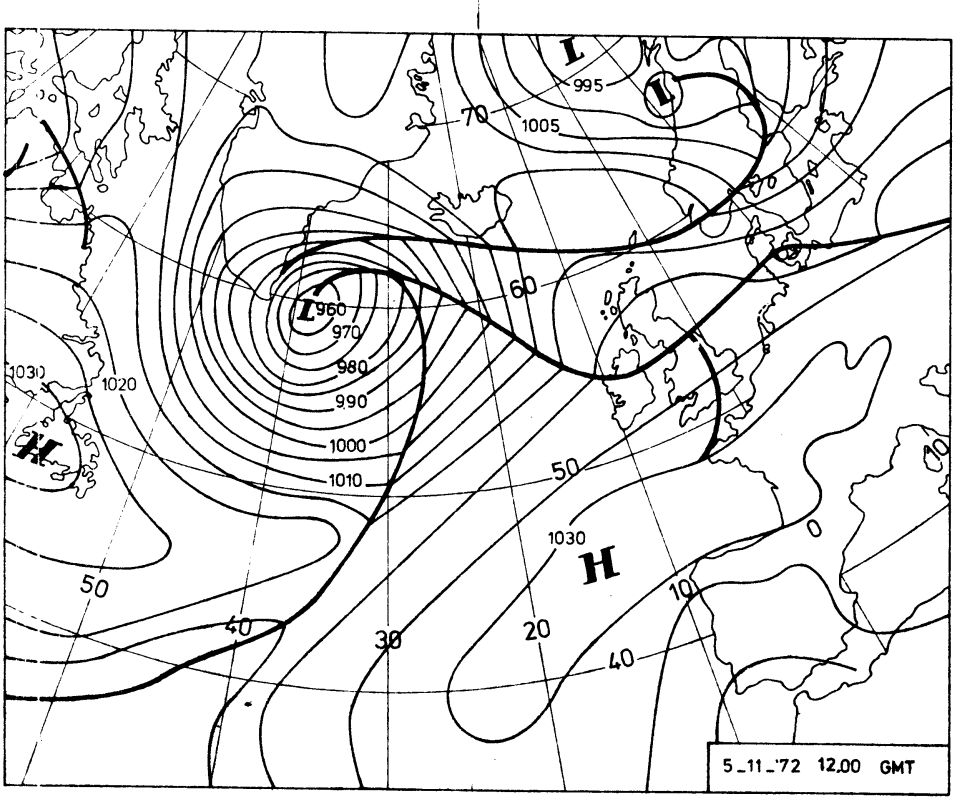

SURFACE ANALYSIS

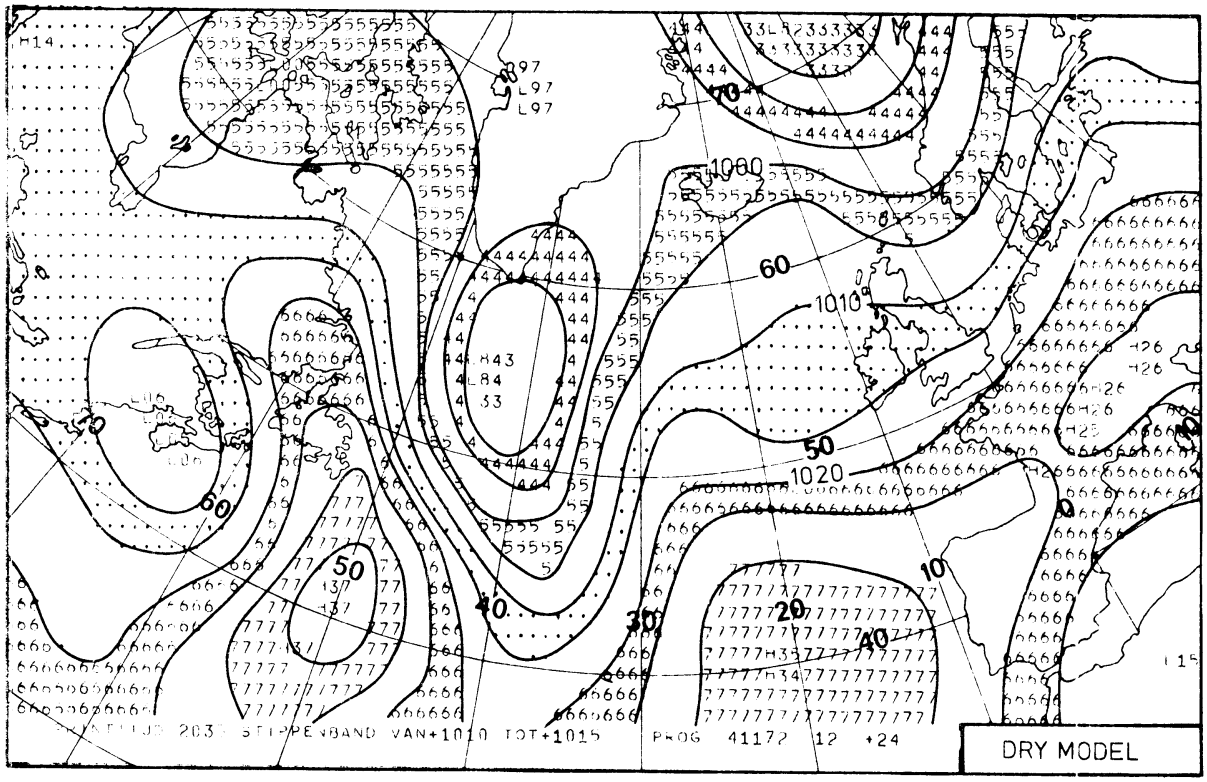

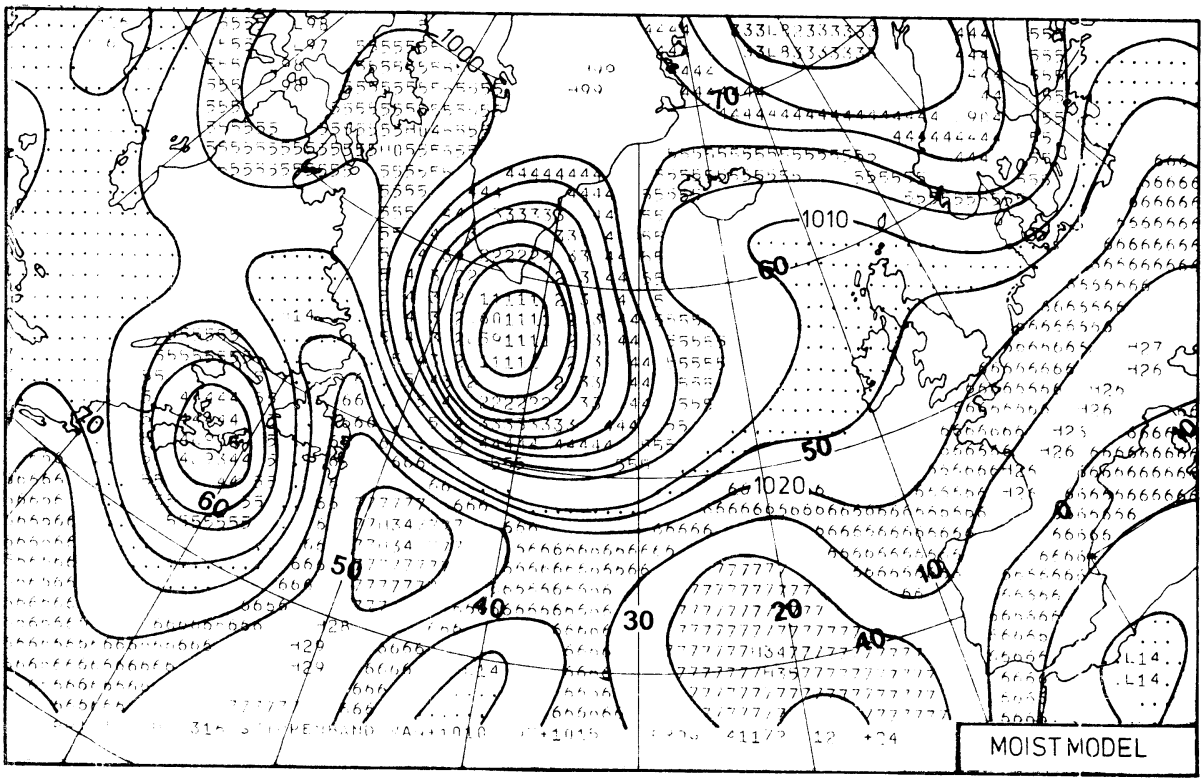

SURFACE +24 PROG, VALID 1200 GMT, 5-11-'72

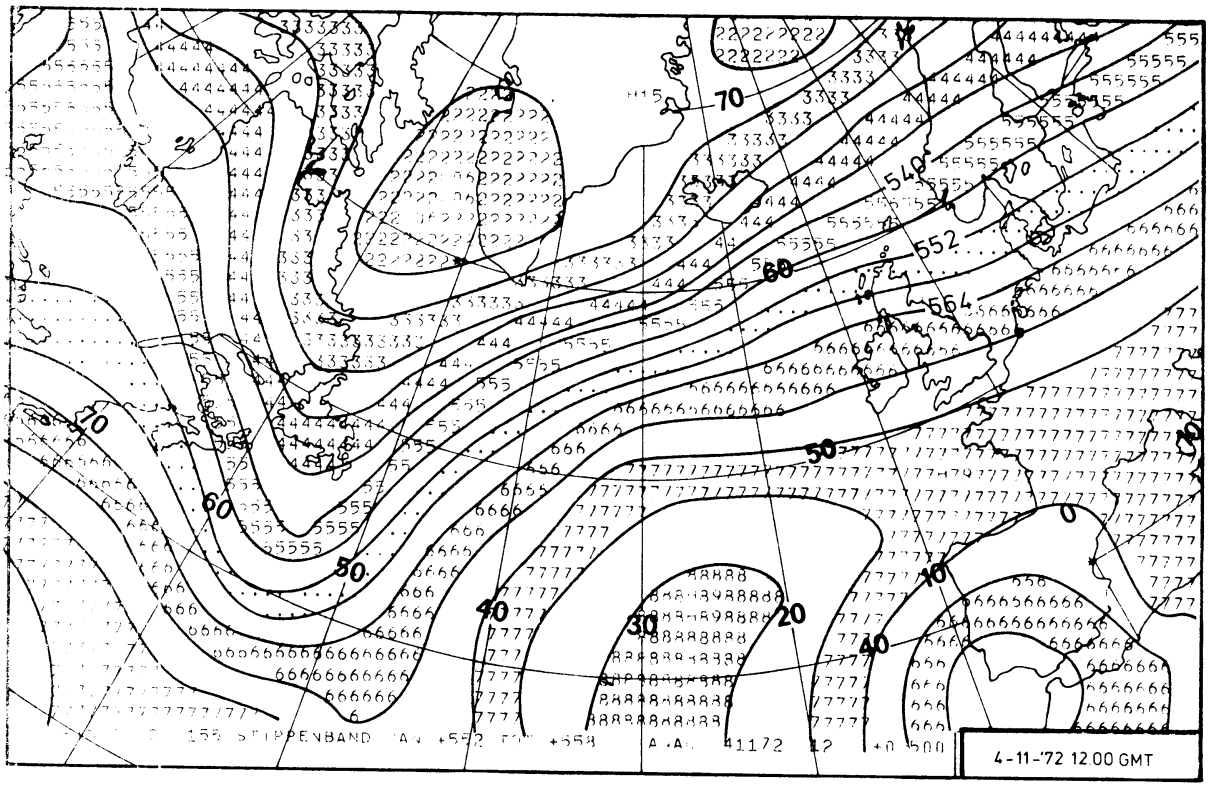

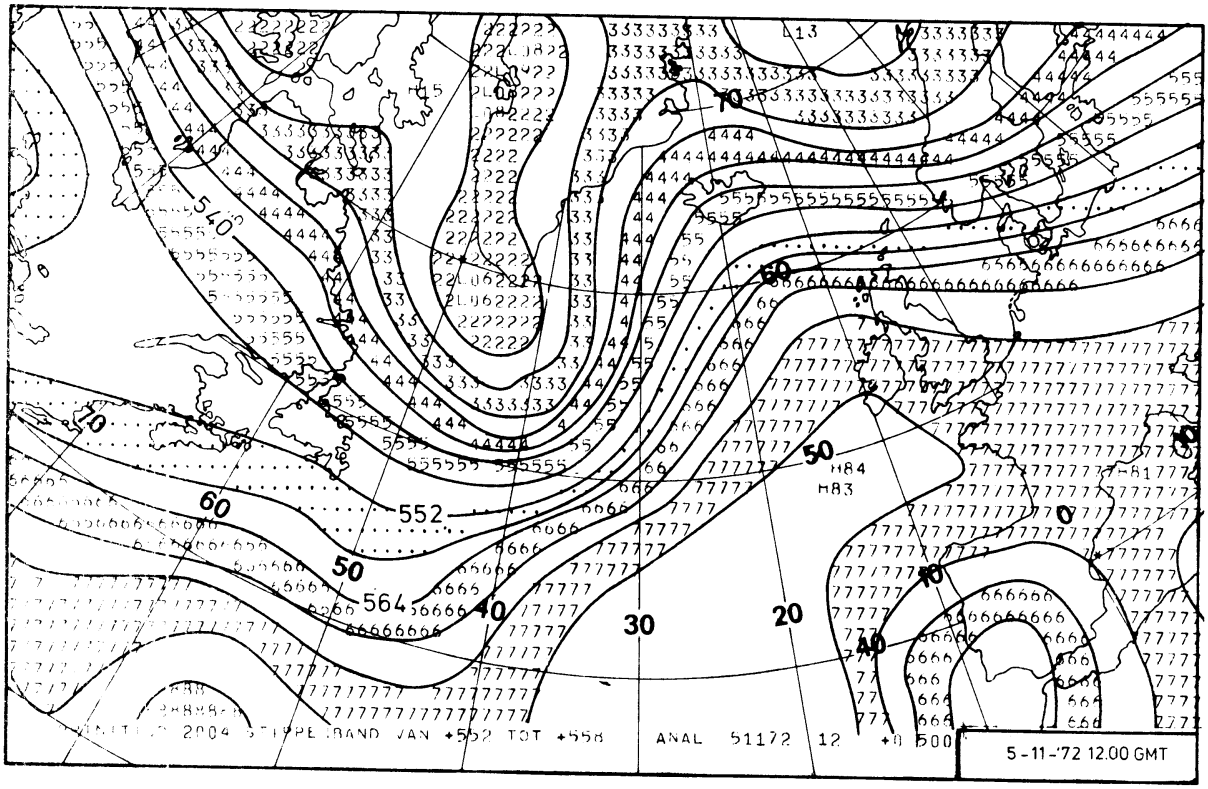

500MBAR ANALYSIS 1200 GMT

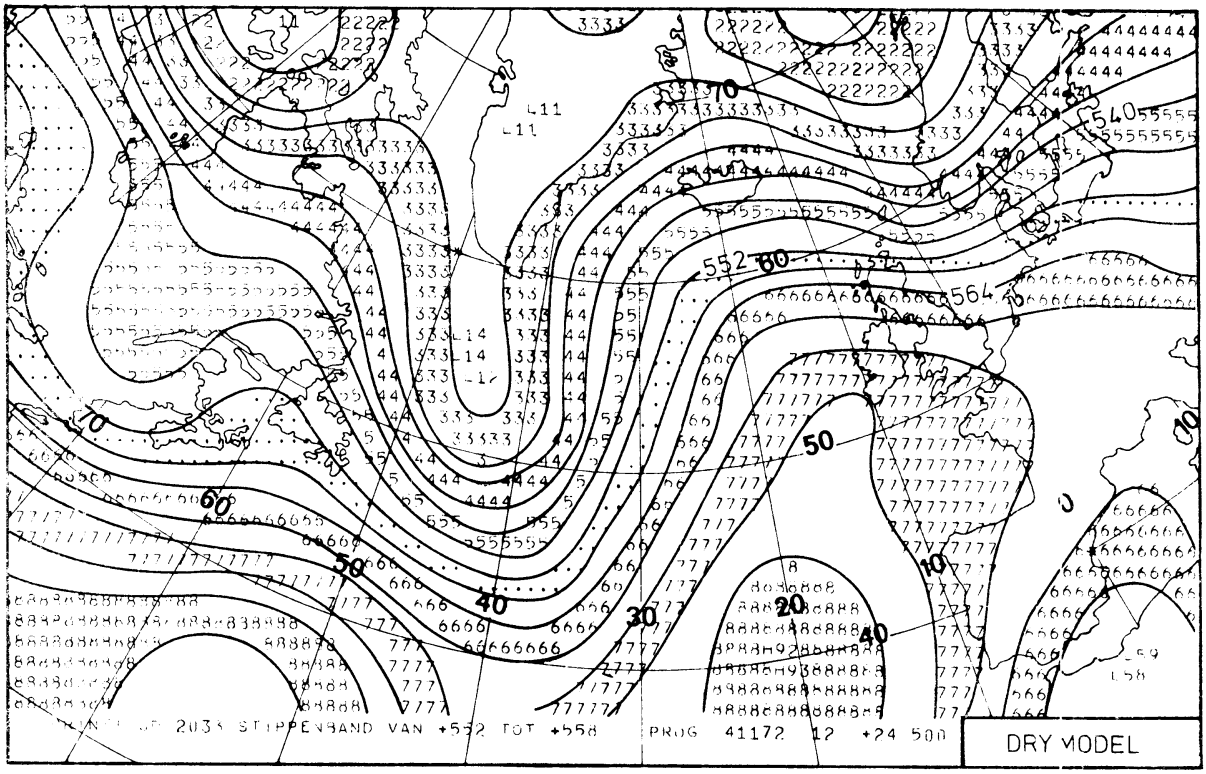

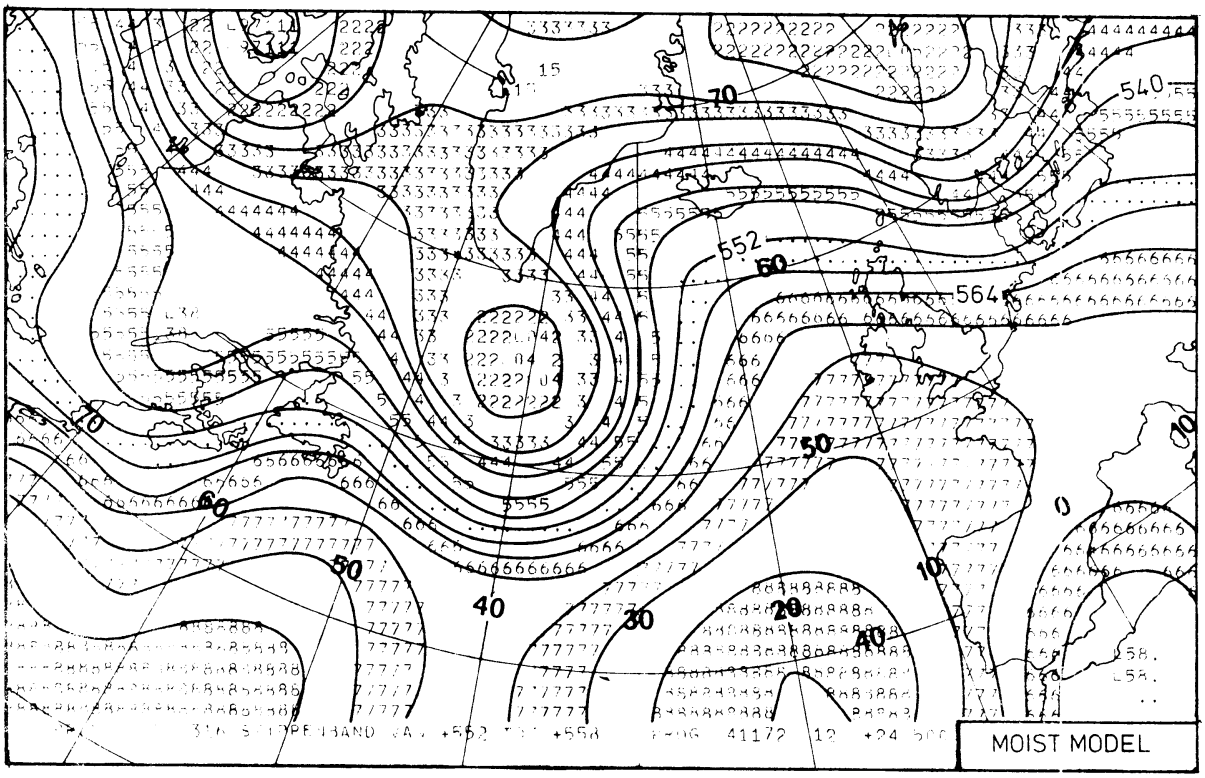

500 MBAR + 24 PROG, VALID 1200 GMT, 5-11-'72

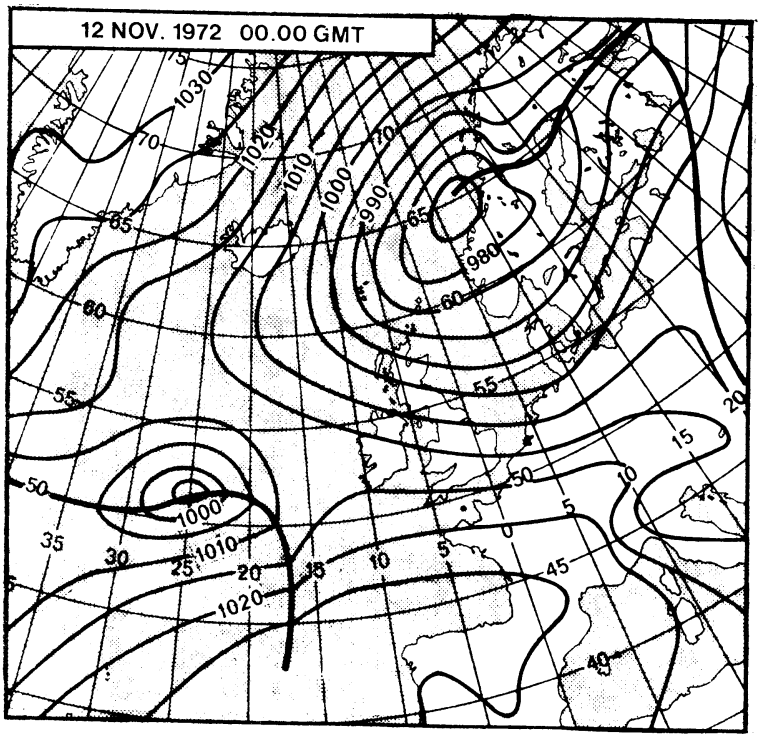

SURFACE ANALYSIS, 00.00 GMT 12-11-'72

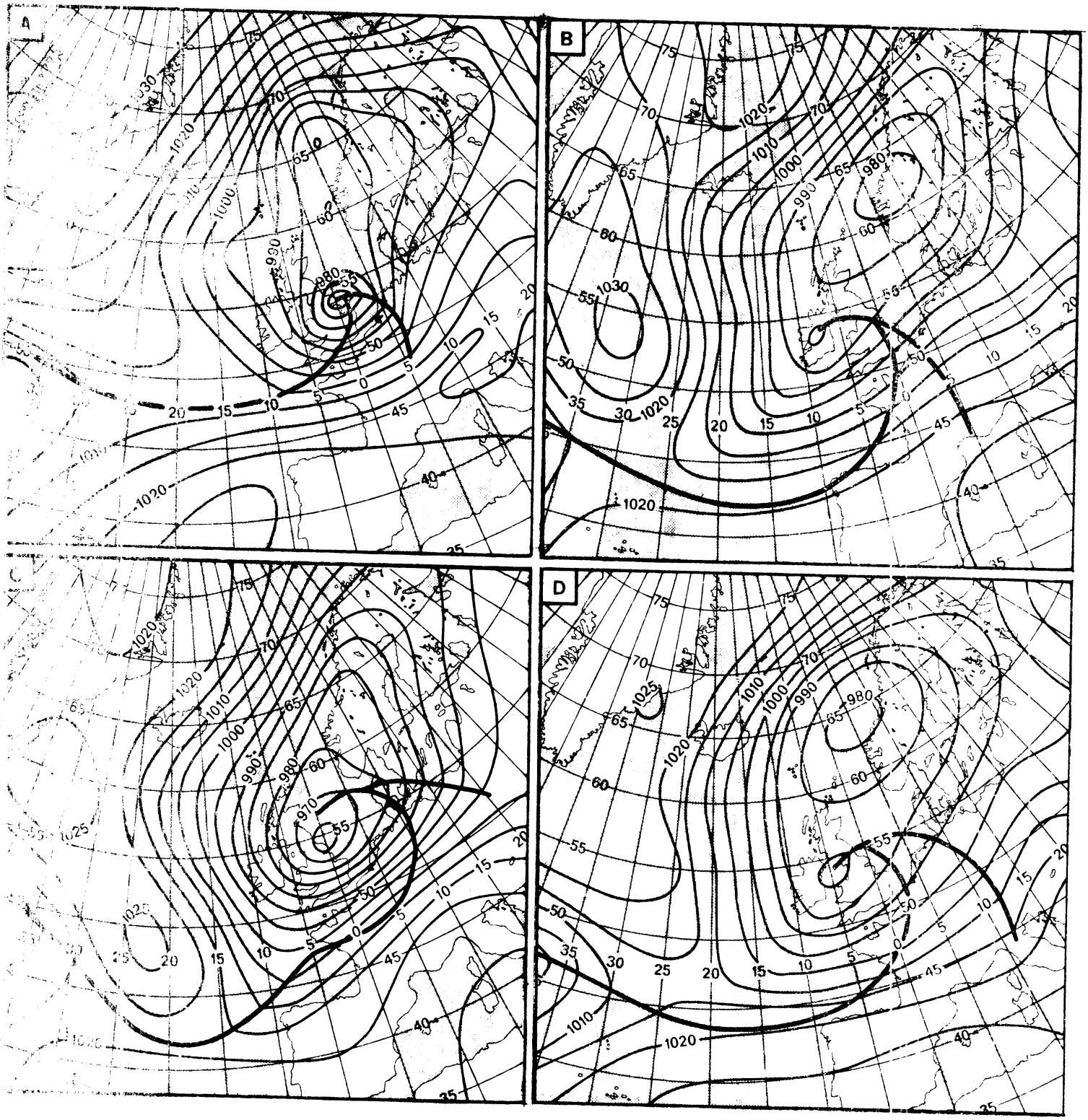

SURFACE ANALYSIS 00.00 GMT. 13 11 '72
SURFACE + 24 PROG. DRY MODEL
SURFACE + 24 PROG. MOIST MODEL } valid 00.00 GMT 13-11- '72
SURFACE + 12 PROG. DRY MODEL

...gs. the fronts are drawn on a subjective manner. Agreement, as much as possible, was sought with forecasts ... thickness 850 - 500 mbar and the vertical velocity (not shown in this report).
... + 12 dry model prog is surpassed by the + 24 moist model one.

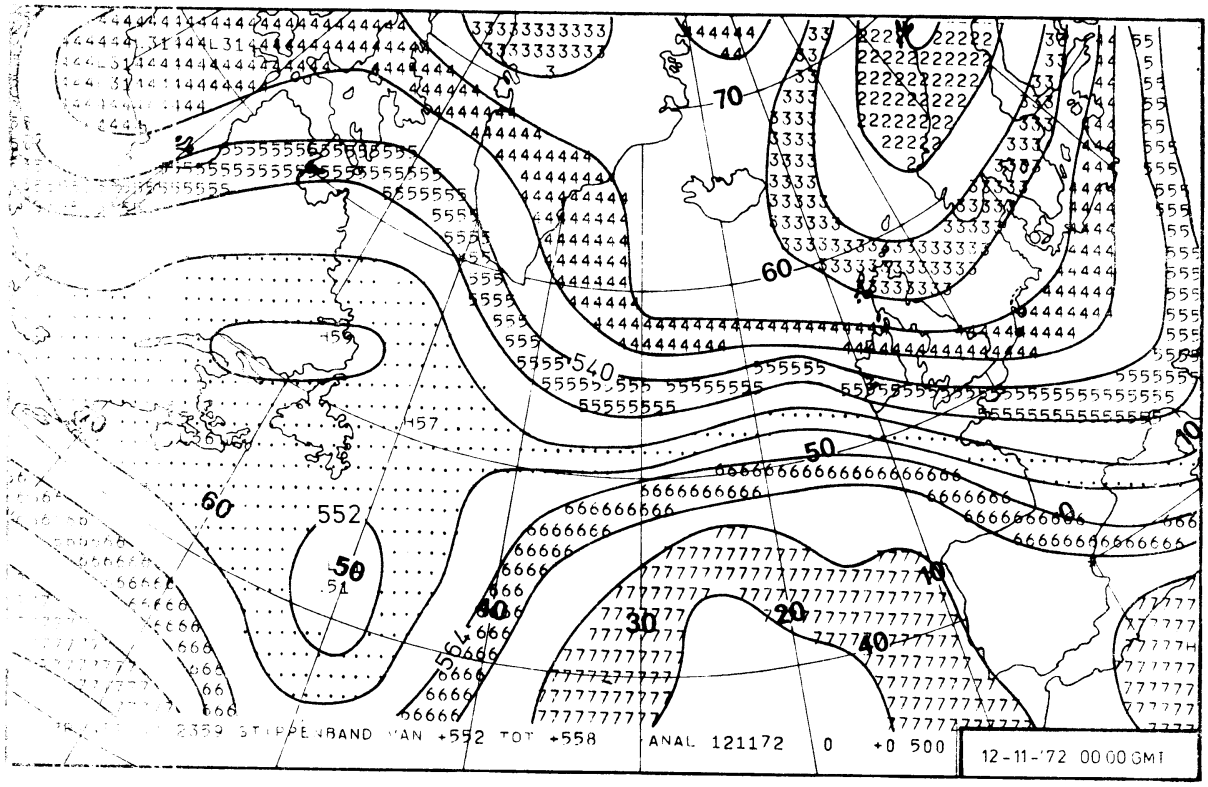

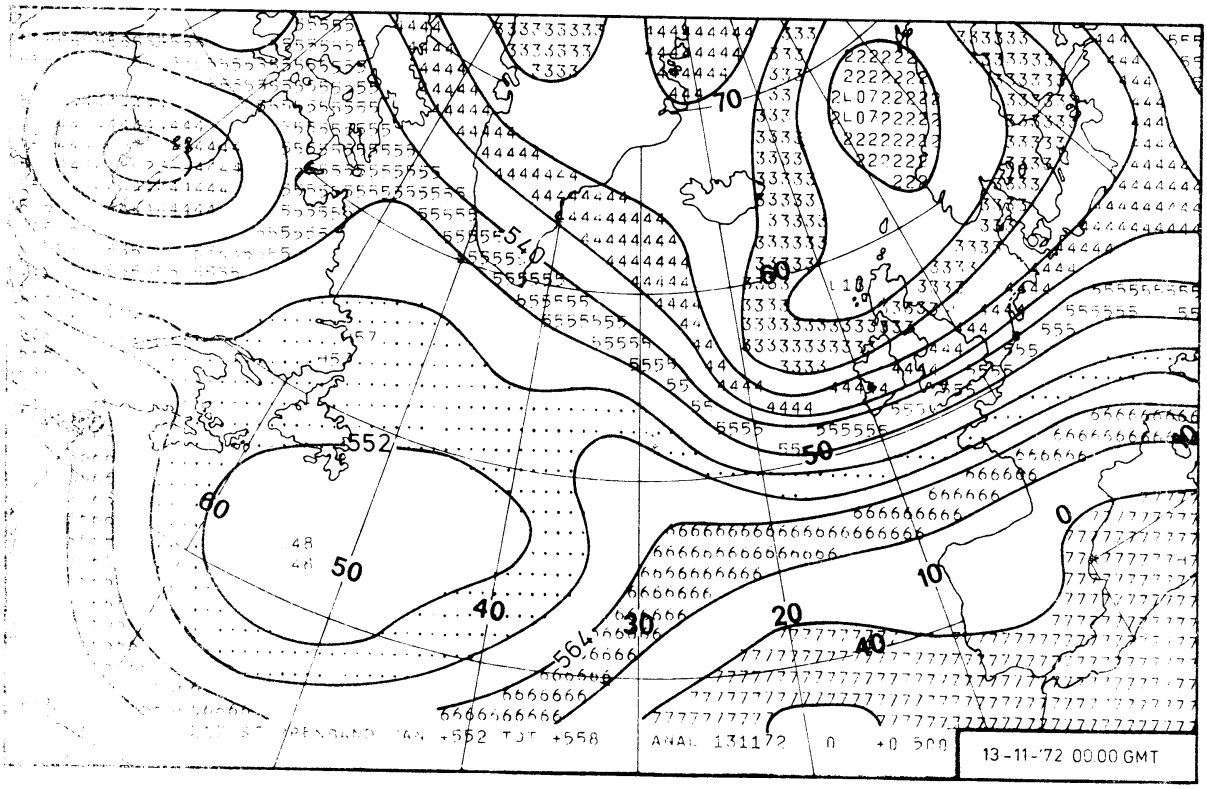

500 MBAR ANALYSIS 00.00 GMT

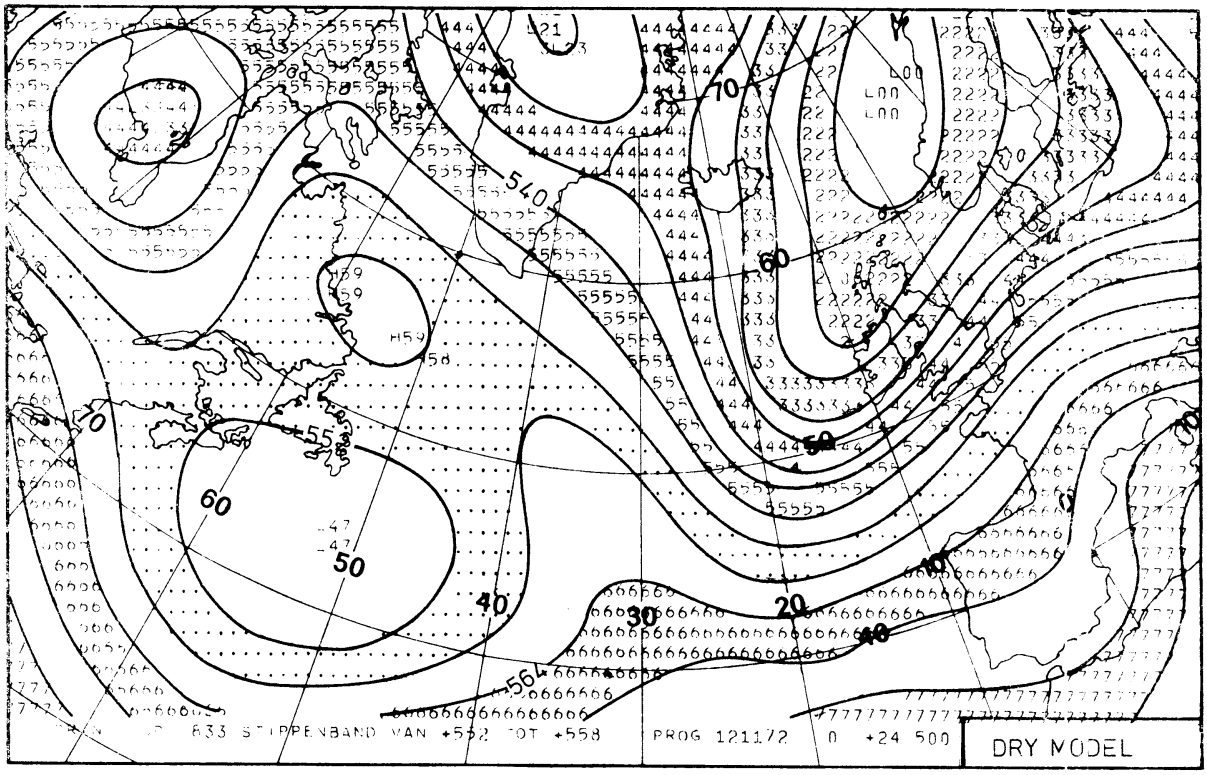

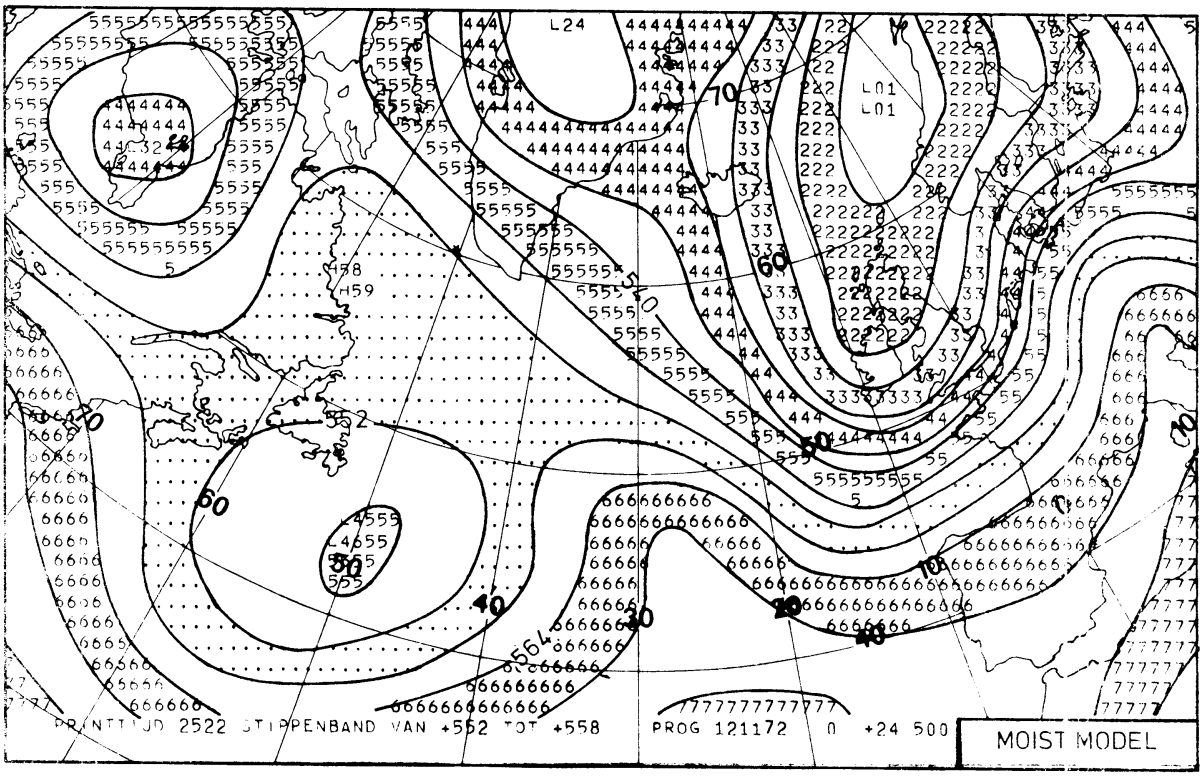

500 MBAR + 24 PROG, VALID 00.00 GMT, 13-11-'72

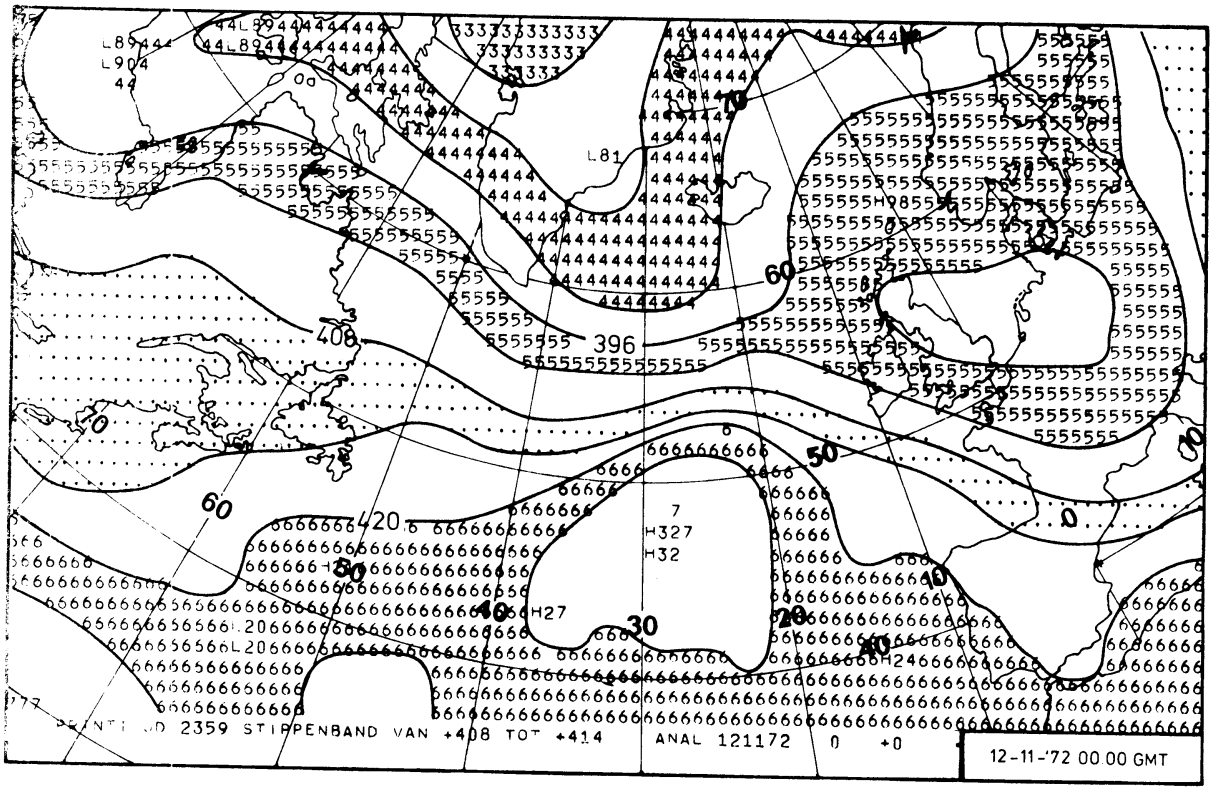

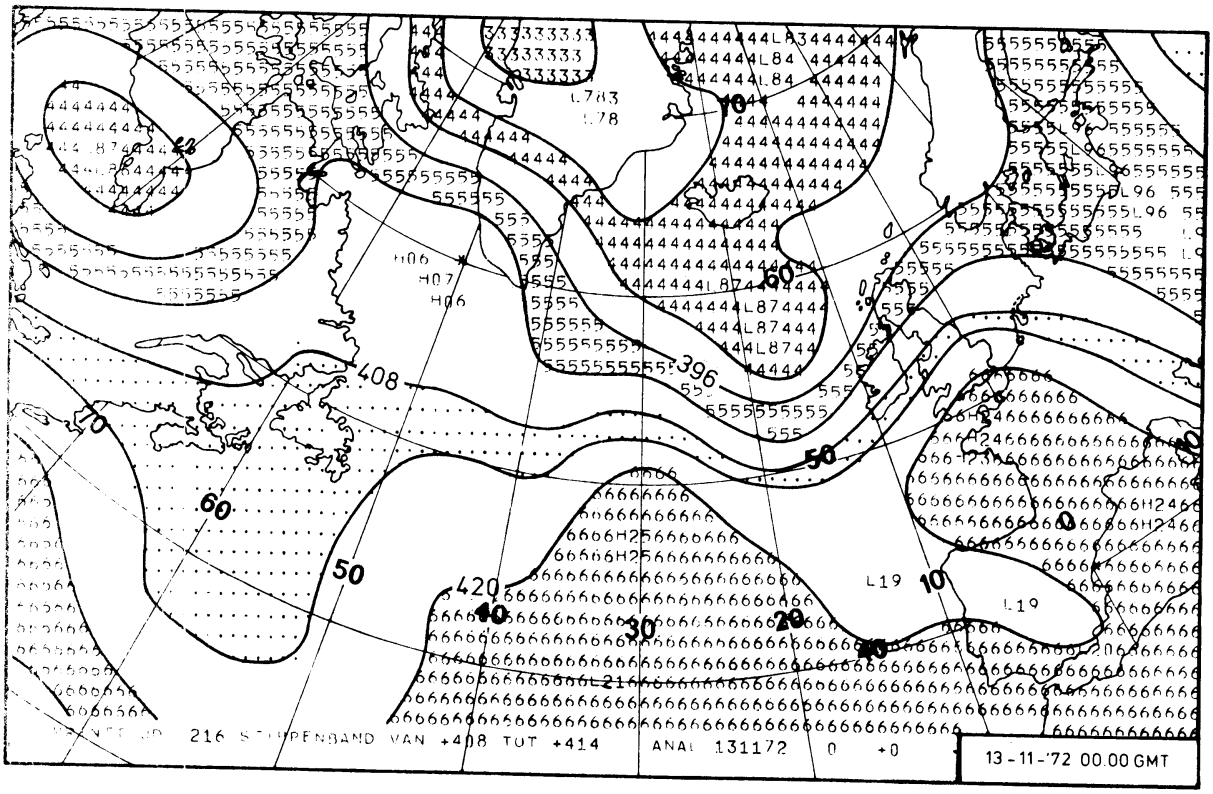

850-500 MBAR ANALYSIS 00.00 GMT

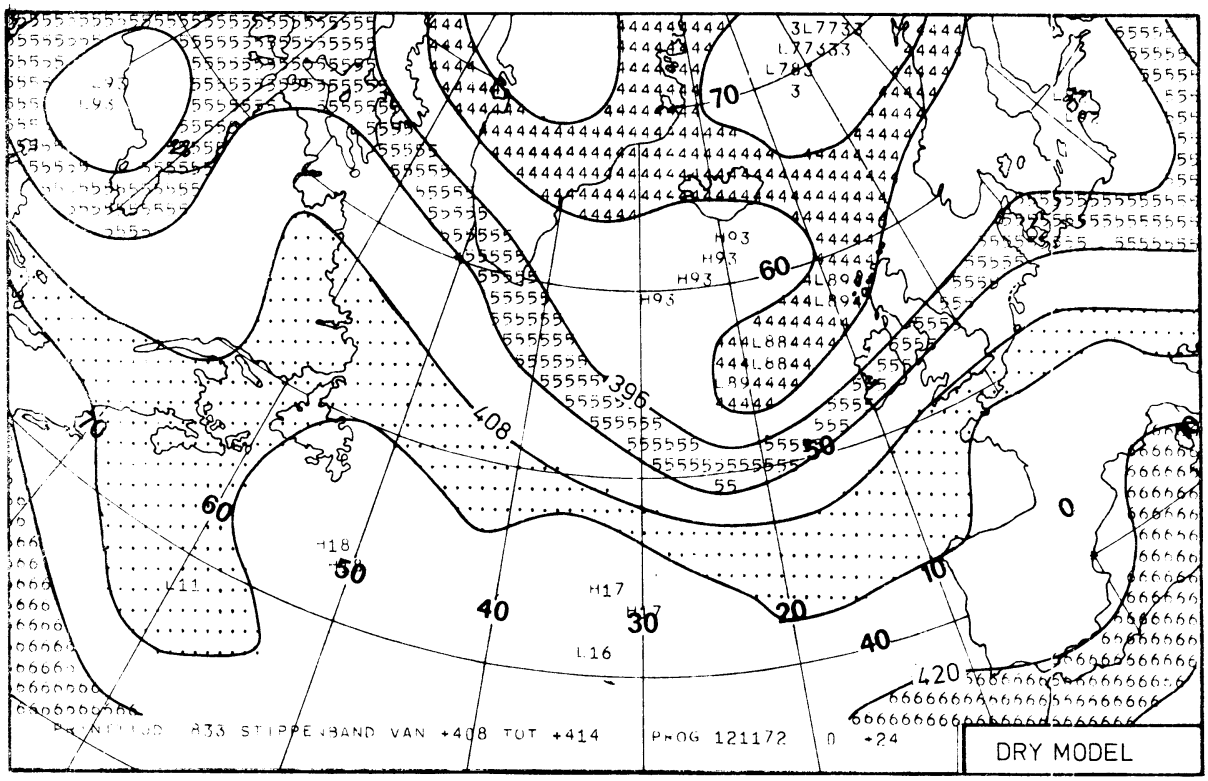

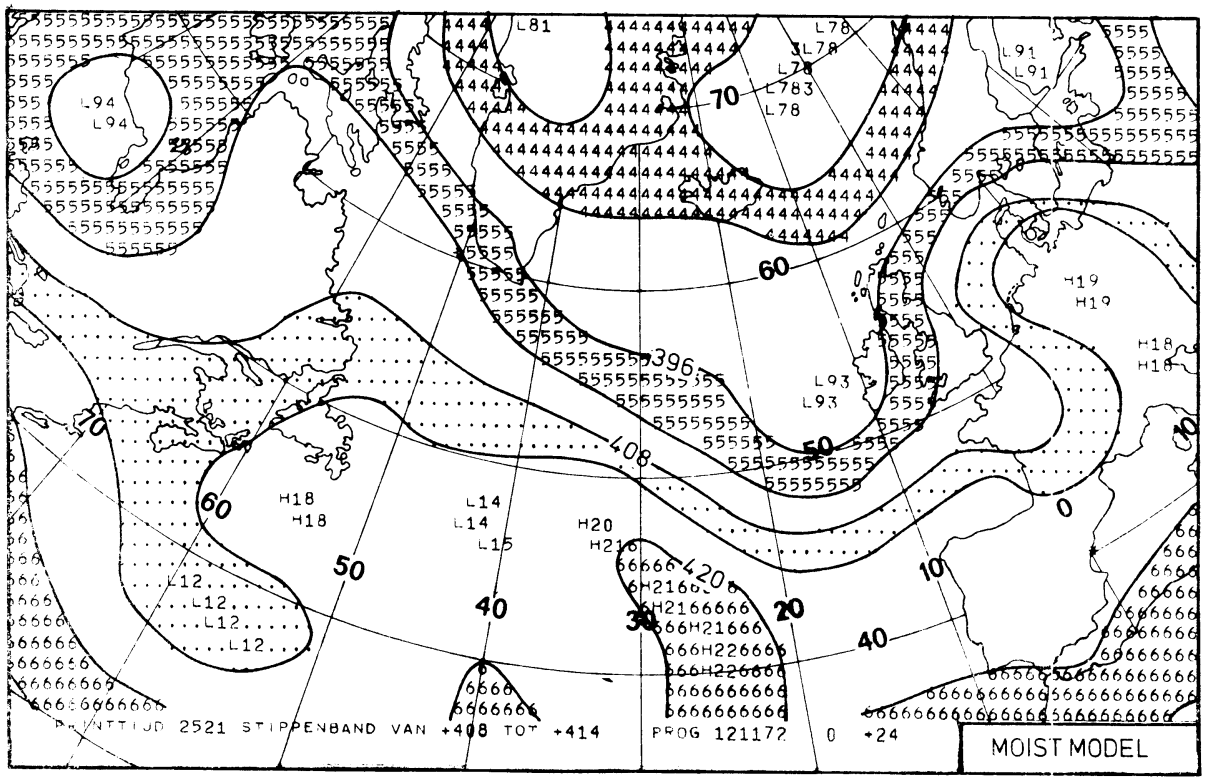

850-500 MBAR + 24 PROG, VALID 00.00 GMT. 13-11-72

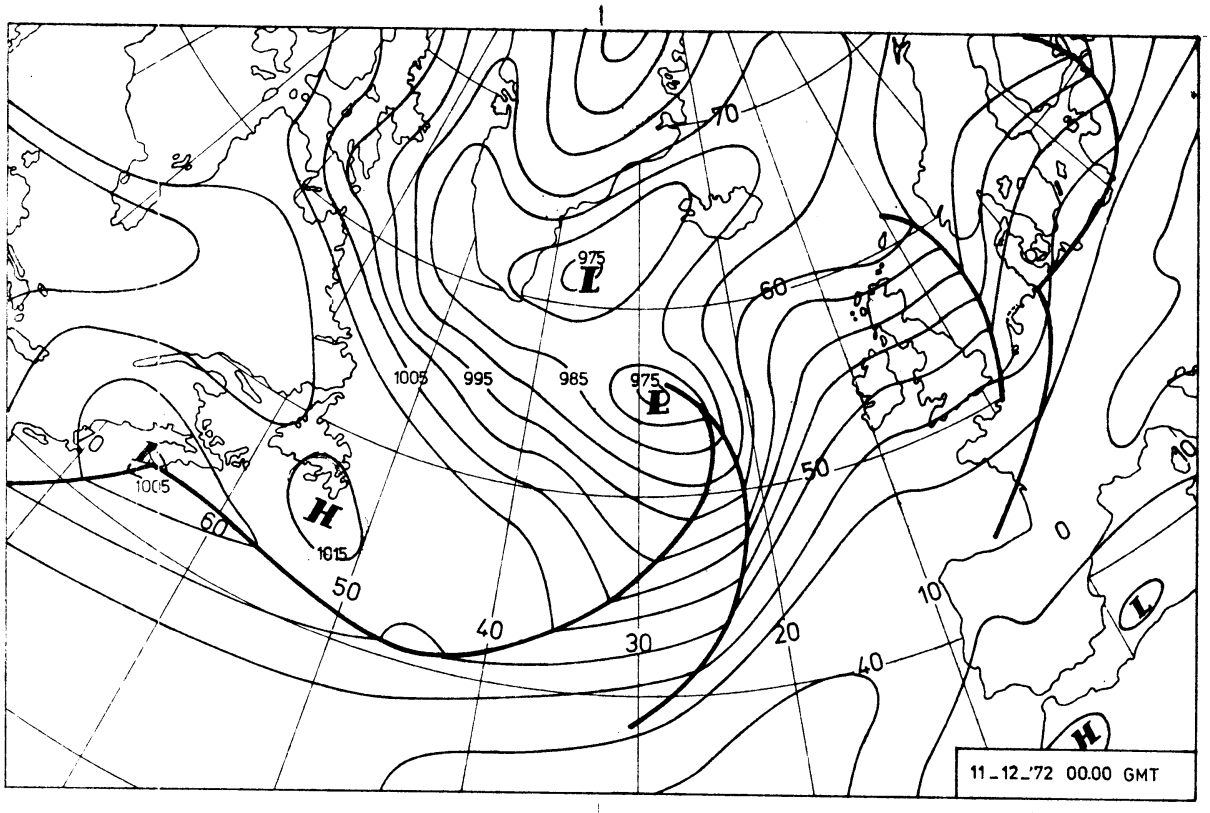

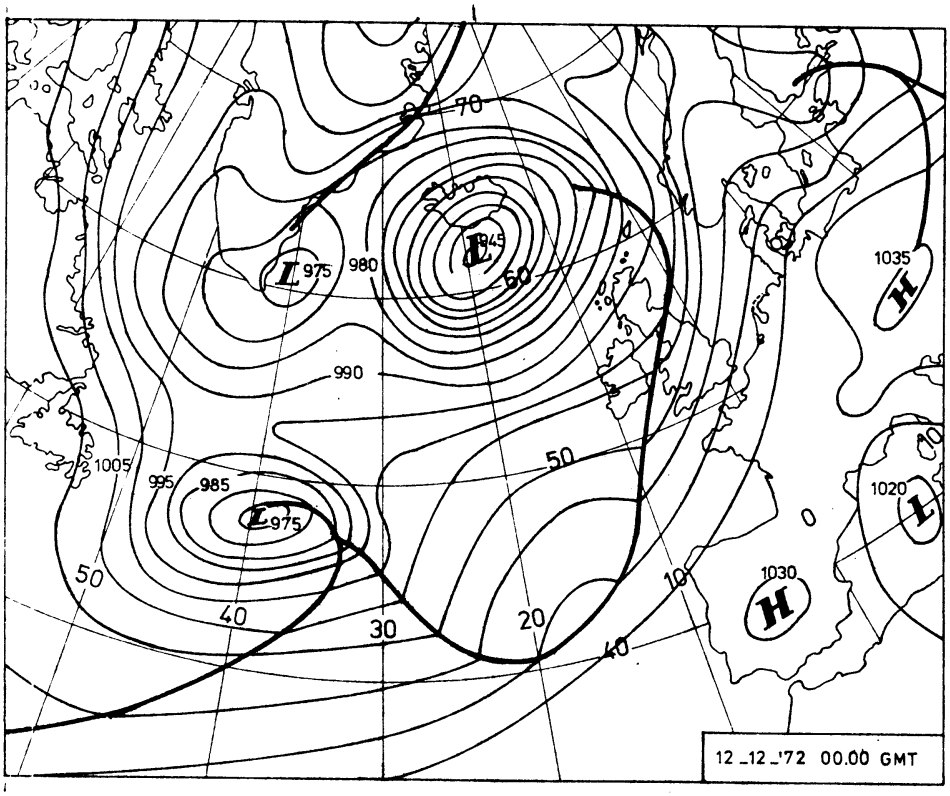

SURFACE ANALYSIS

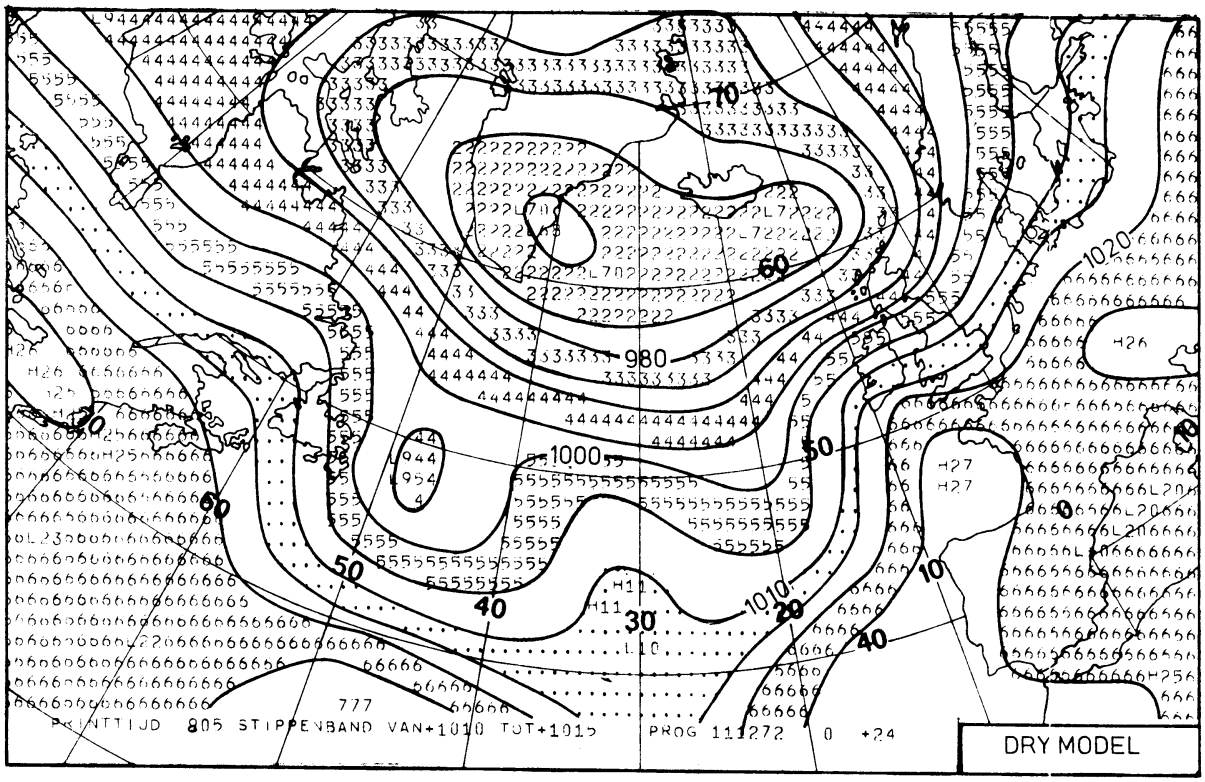

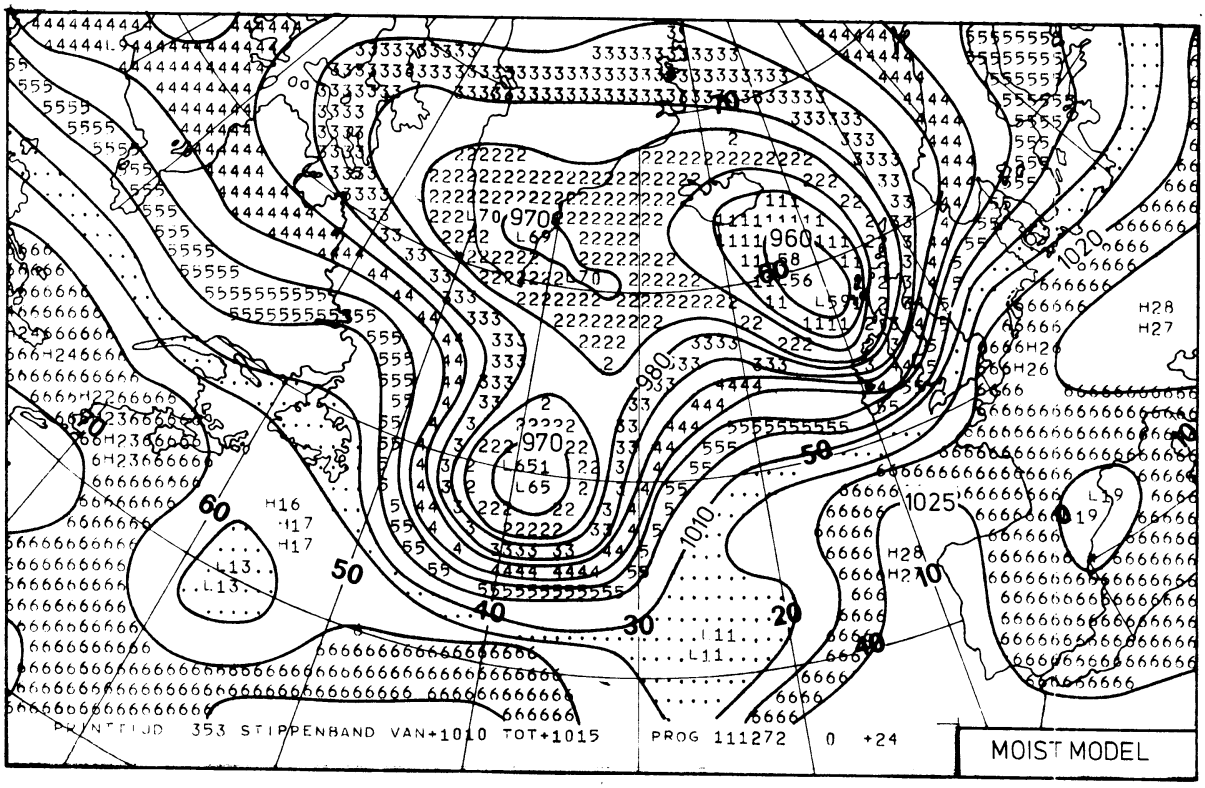

SURFACE + 24 PROG. VALID 00.00 GMT. 12-12-72

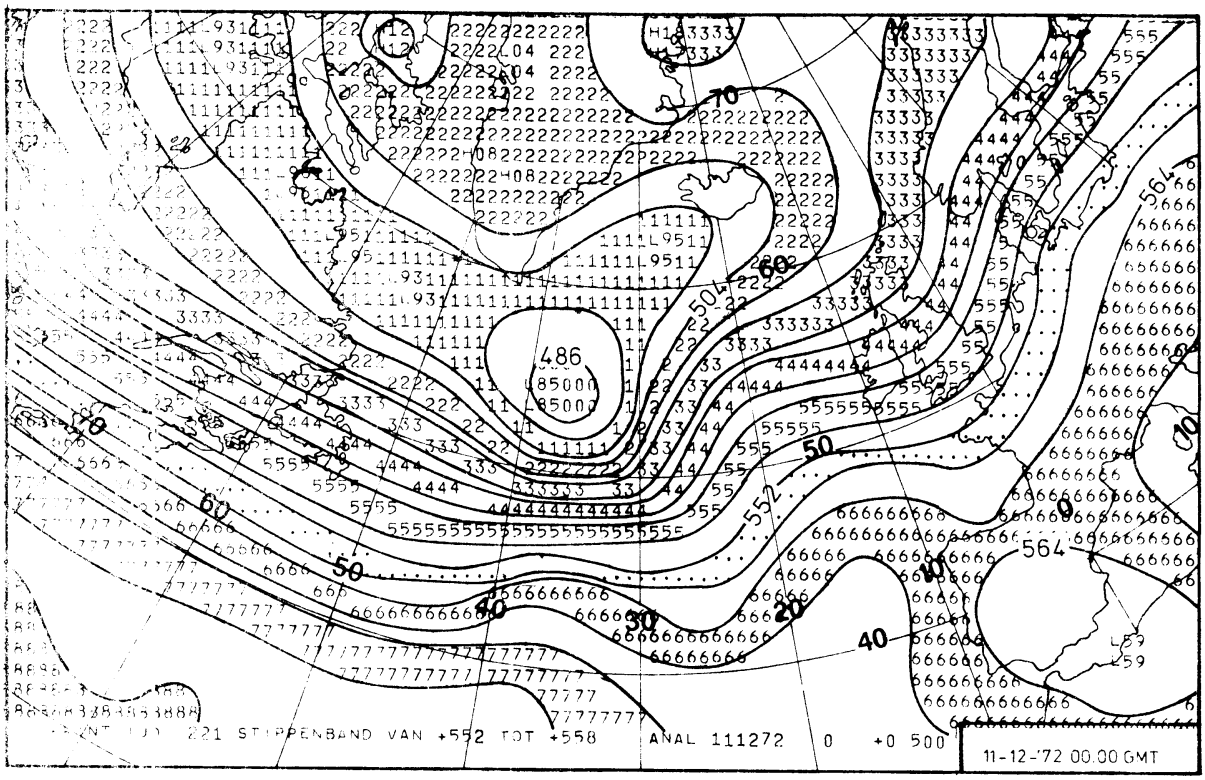

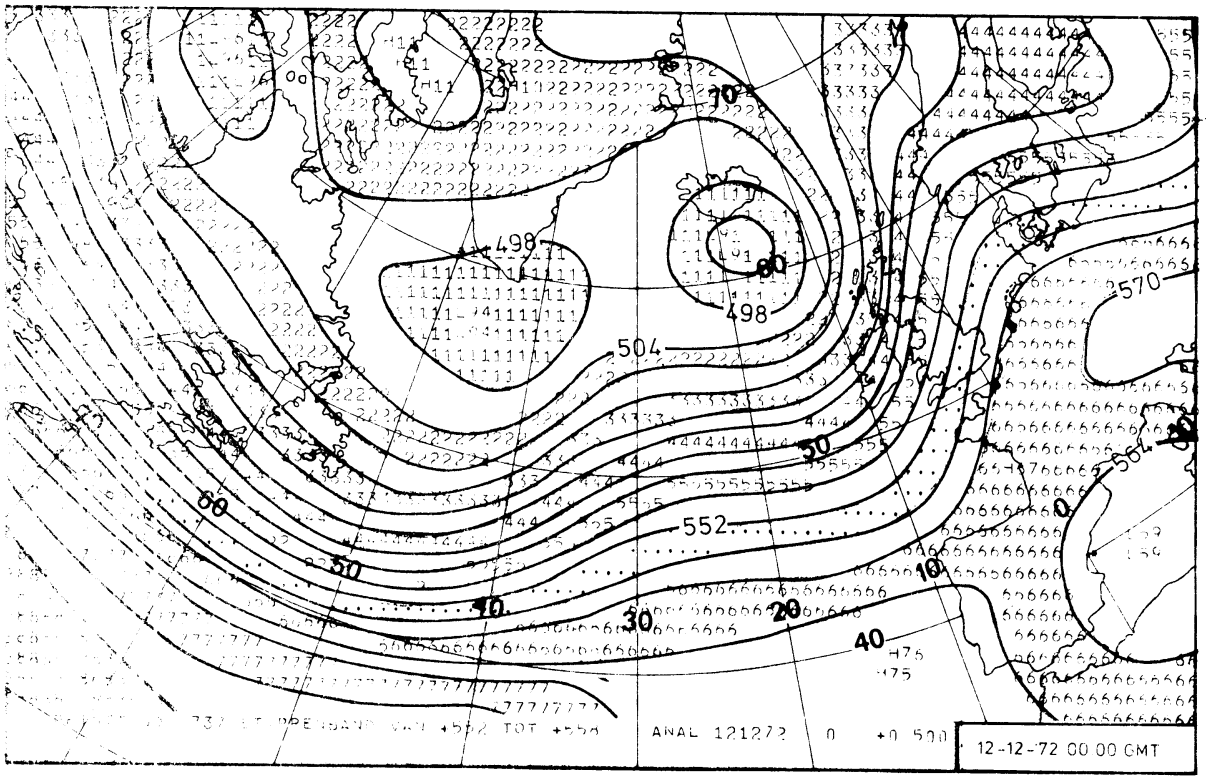

500MBAR ANALYSIS 00.00 GMT

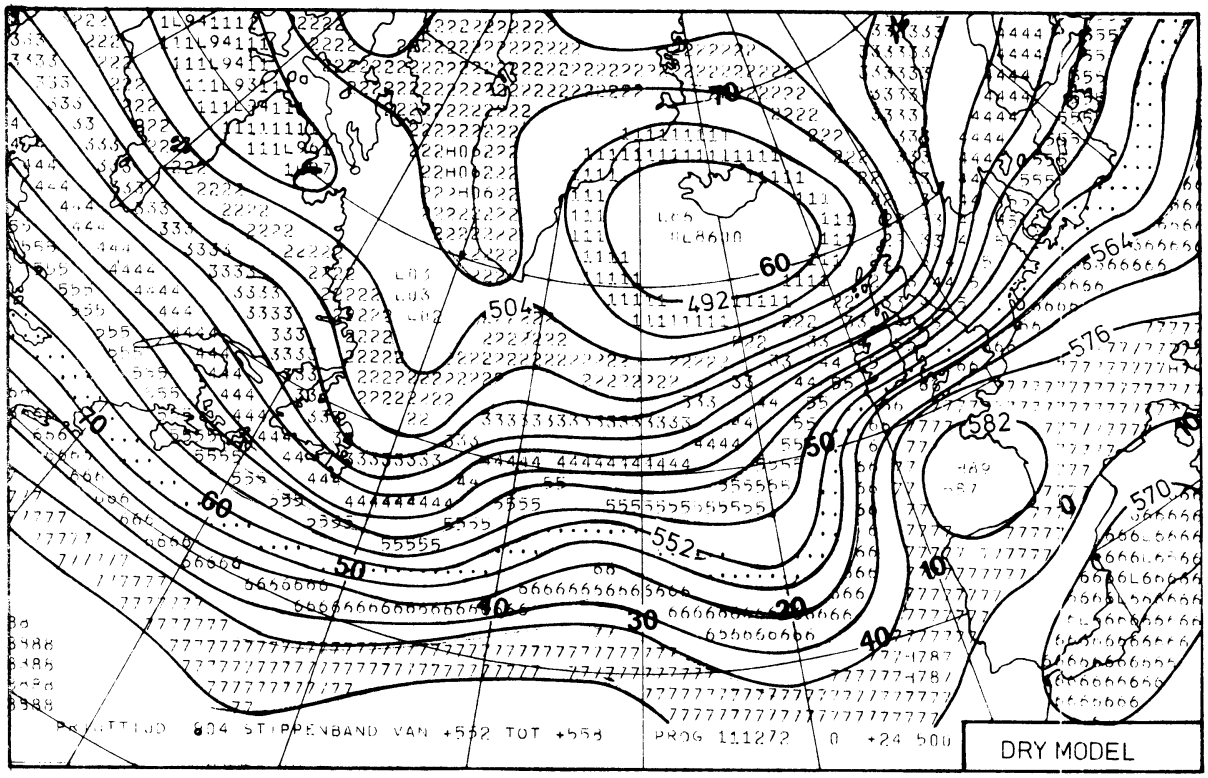

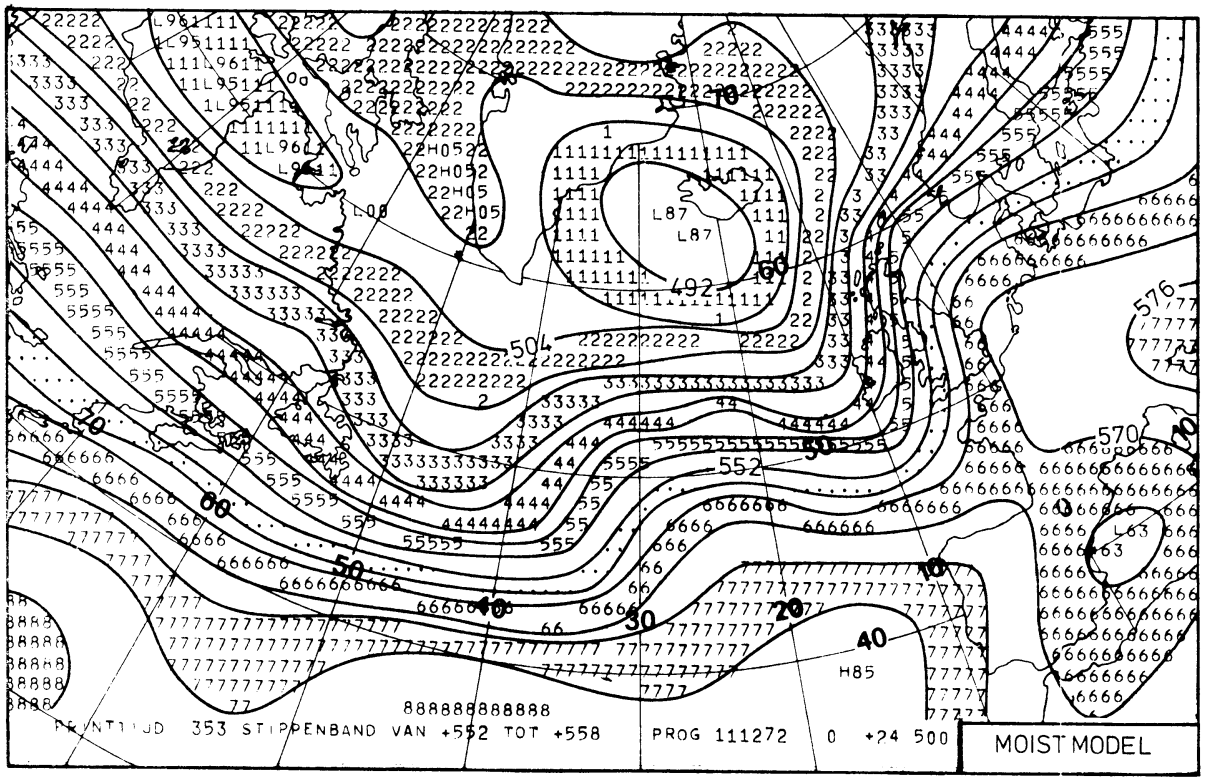

500MBAR + 24 PROG. VALID 00,00 GMT 12-12-72

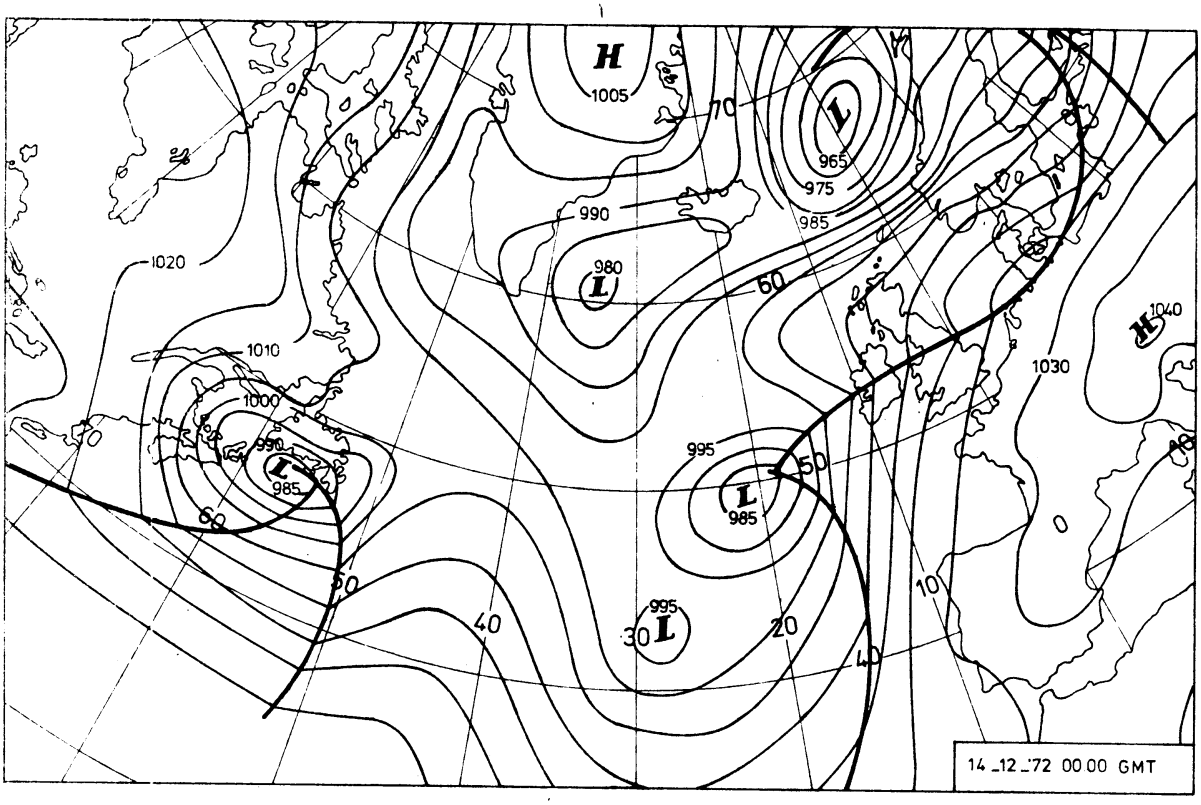

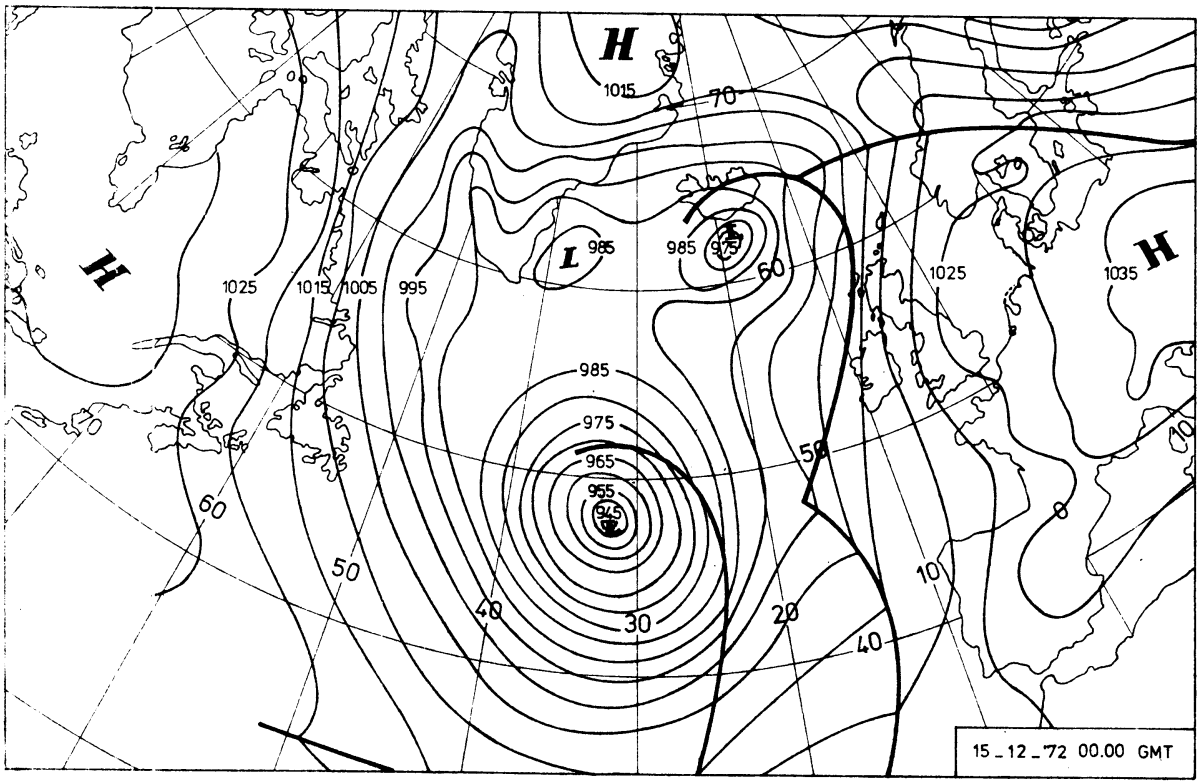

SURFACE ANALYSIS

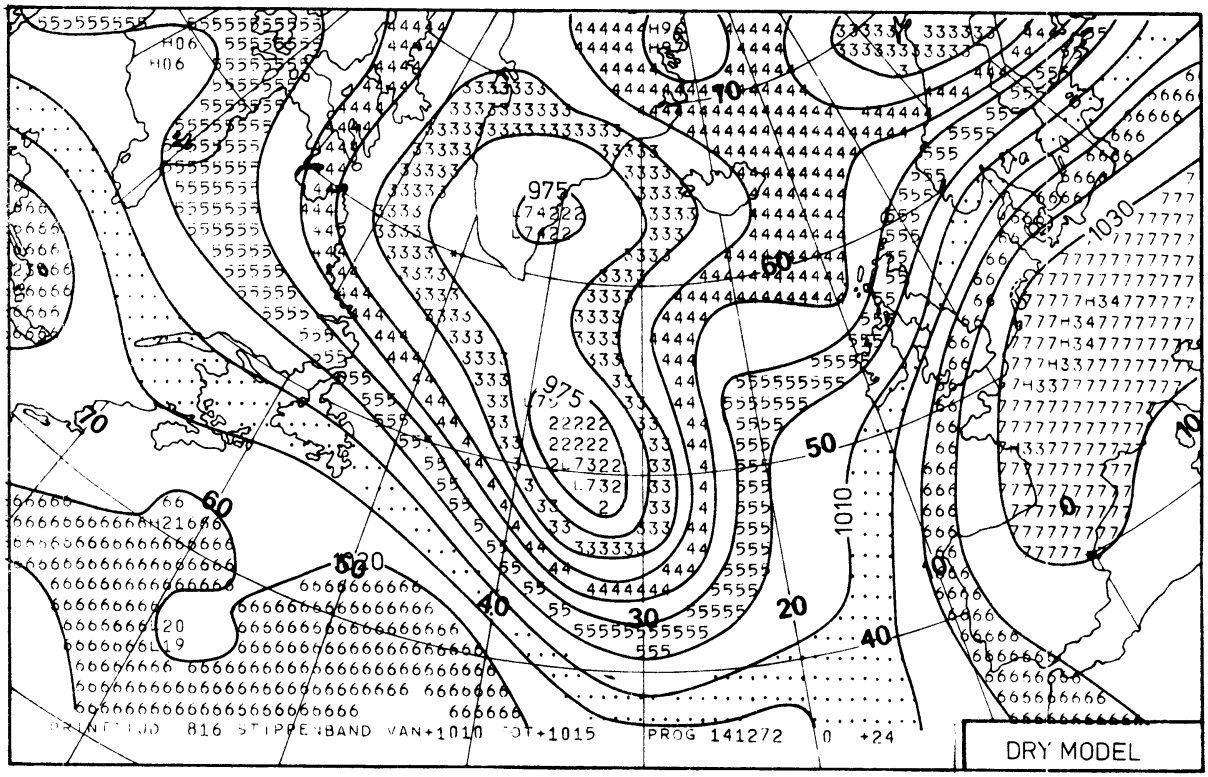

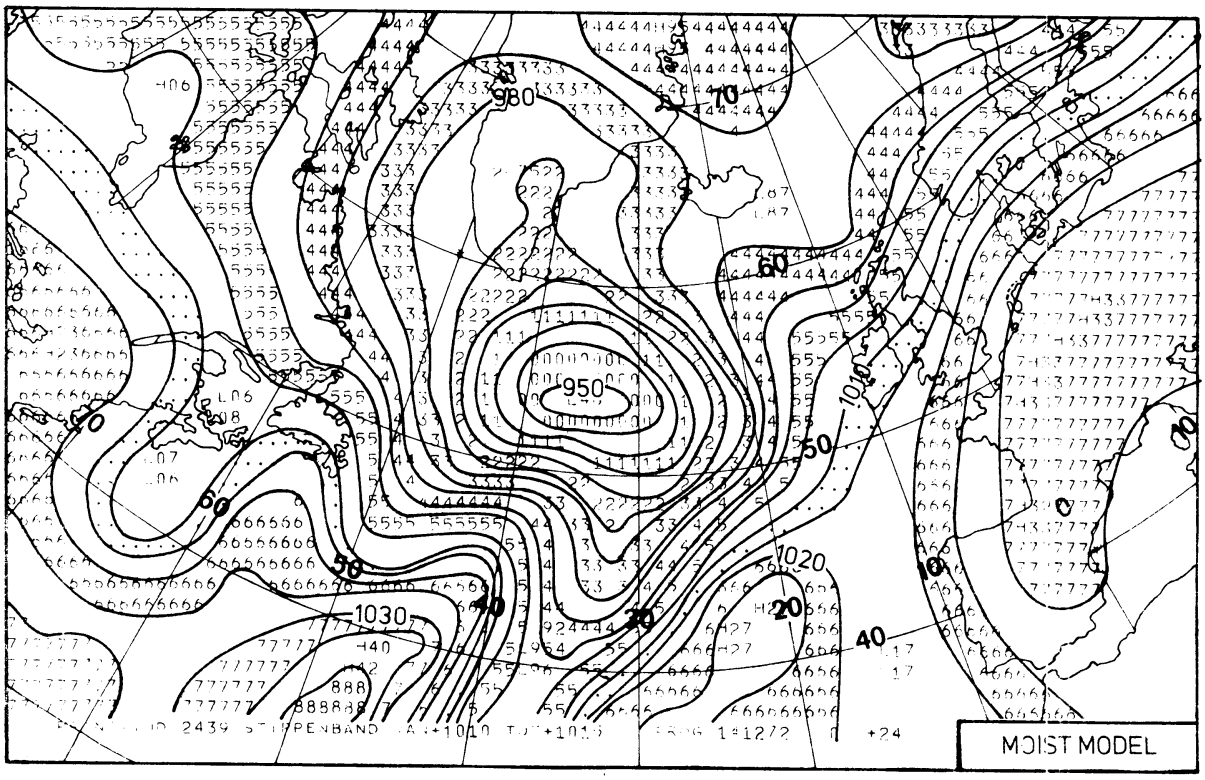

SURFACE + 24 PROG., VALID 00.00 GMT. 15-12-72

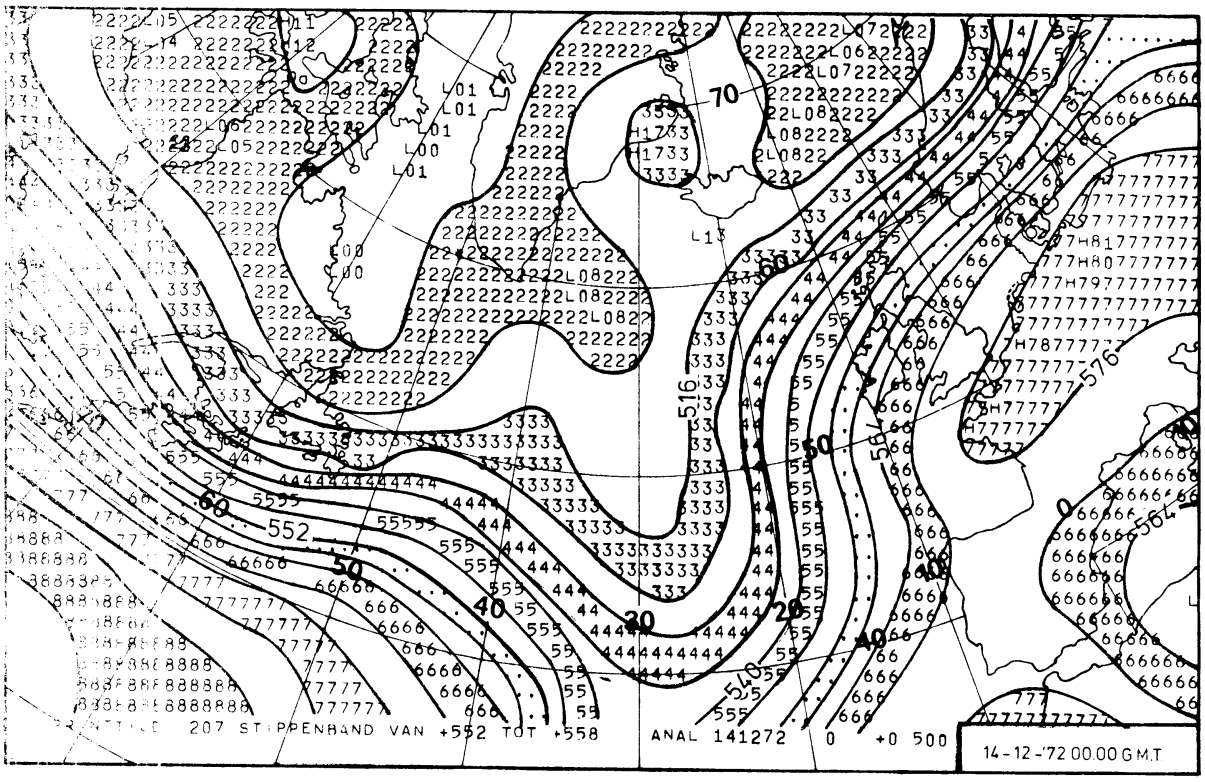

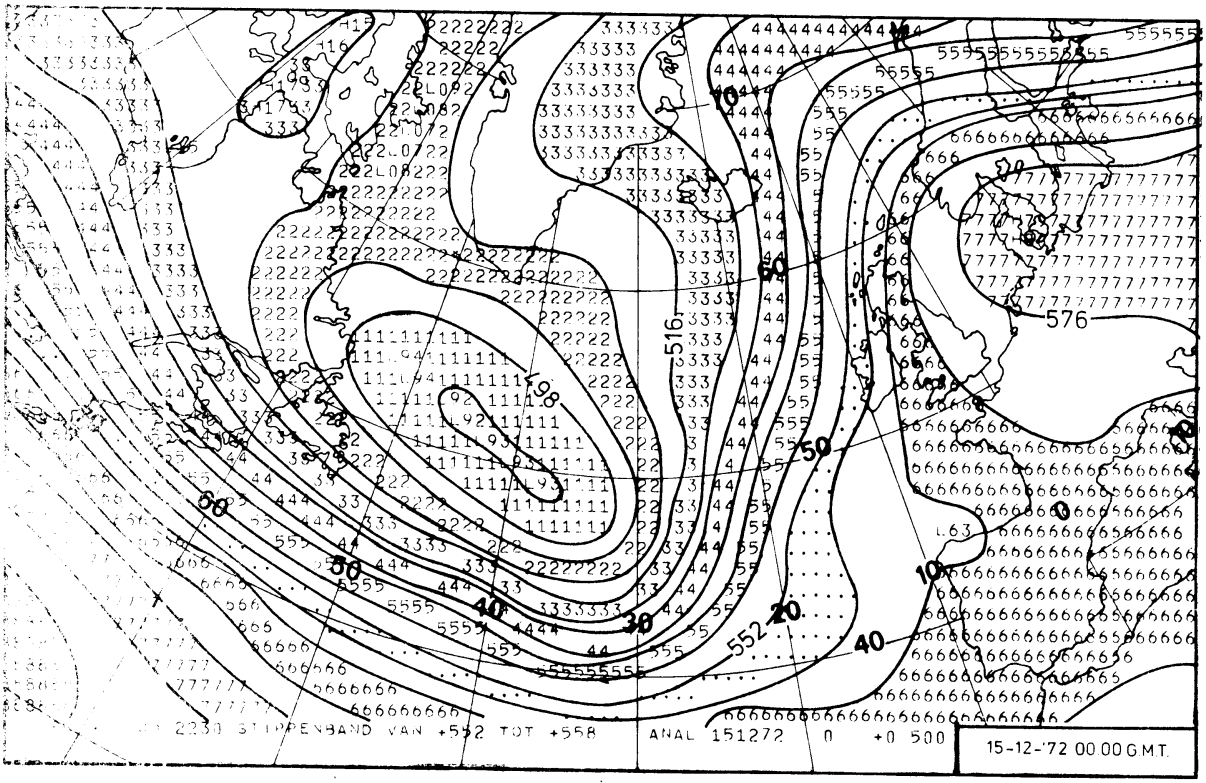

500MBAR ANALYSIS 00.00 GMT

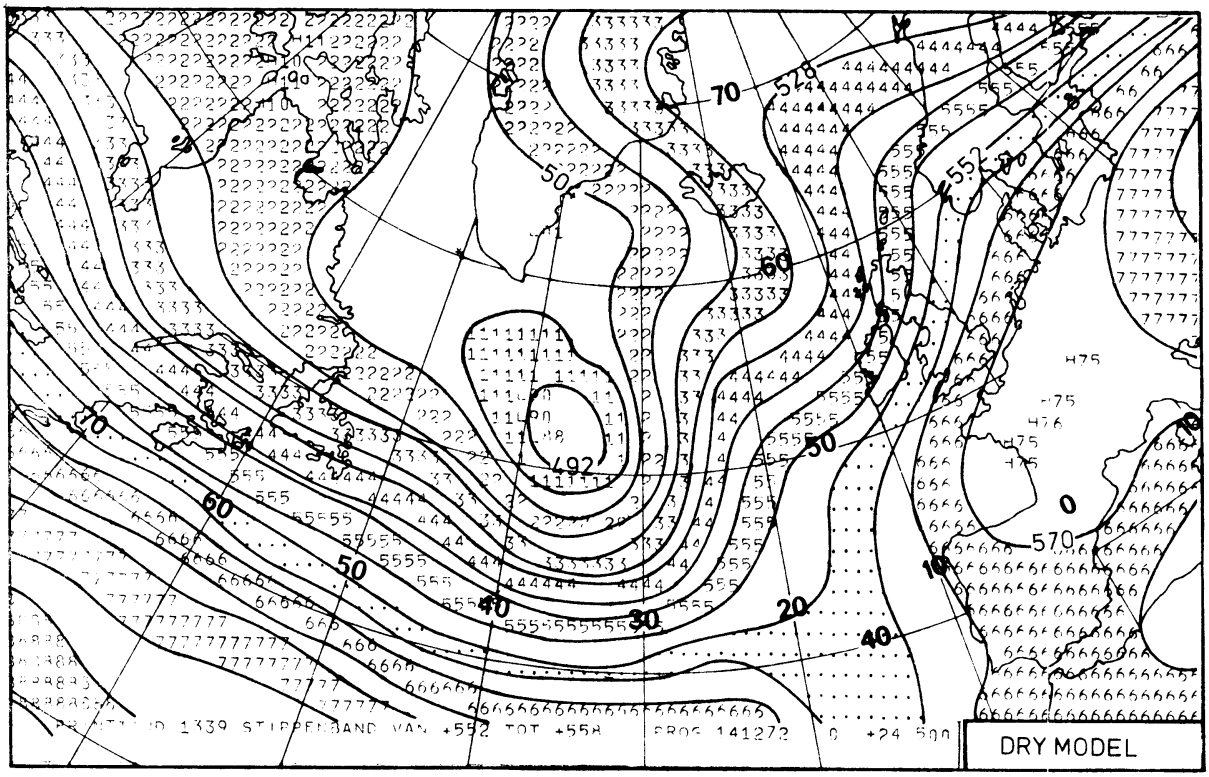

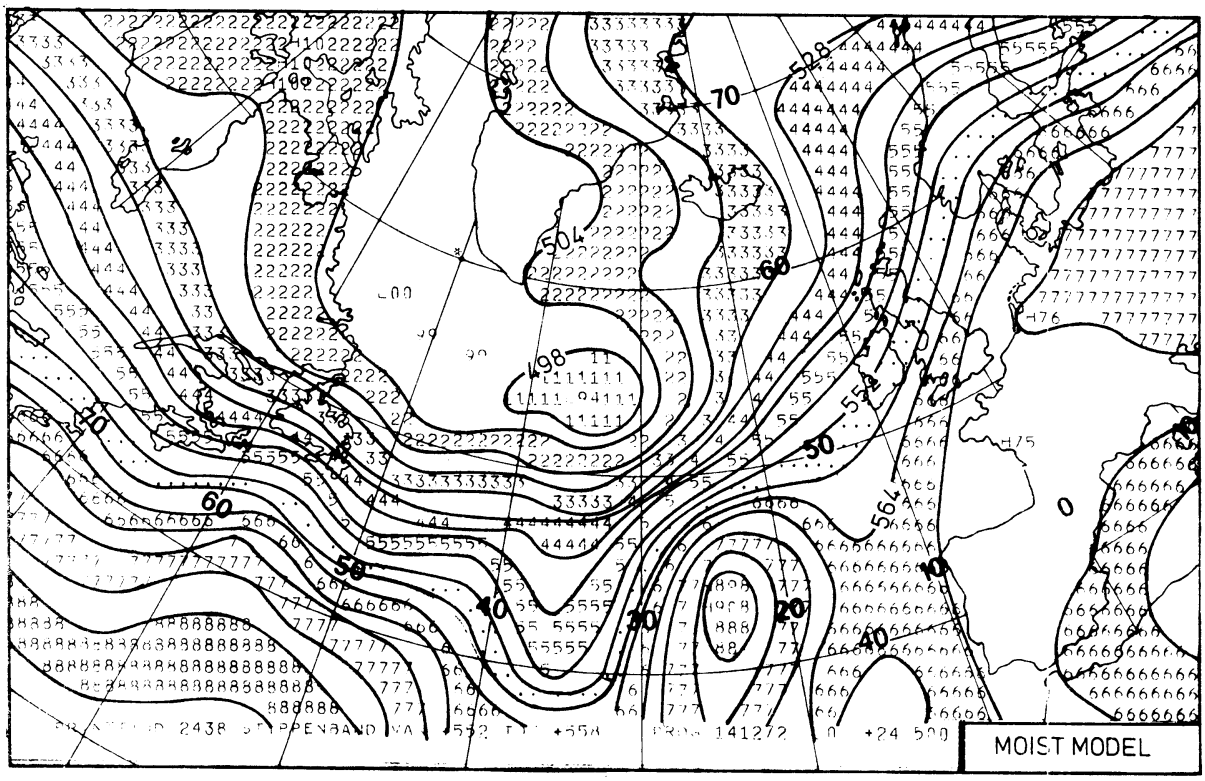

500MBAR + 24 PROG. VALID 00.00 GMT. 15-12-'72.

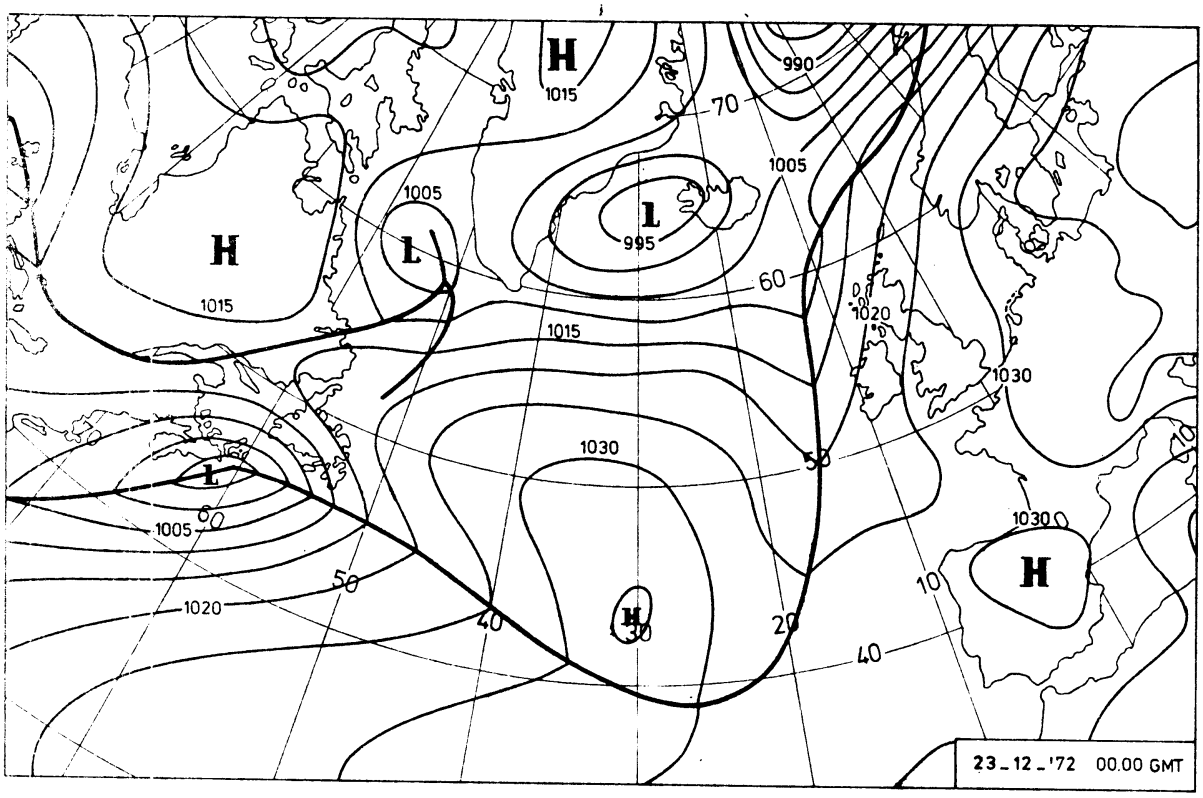

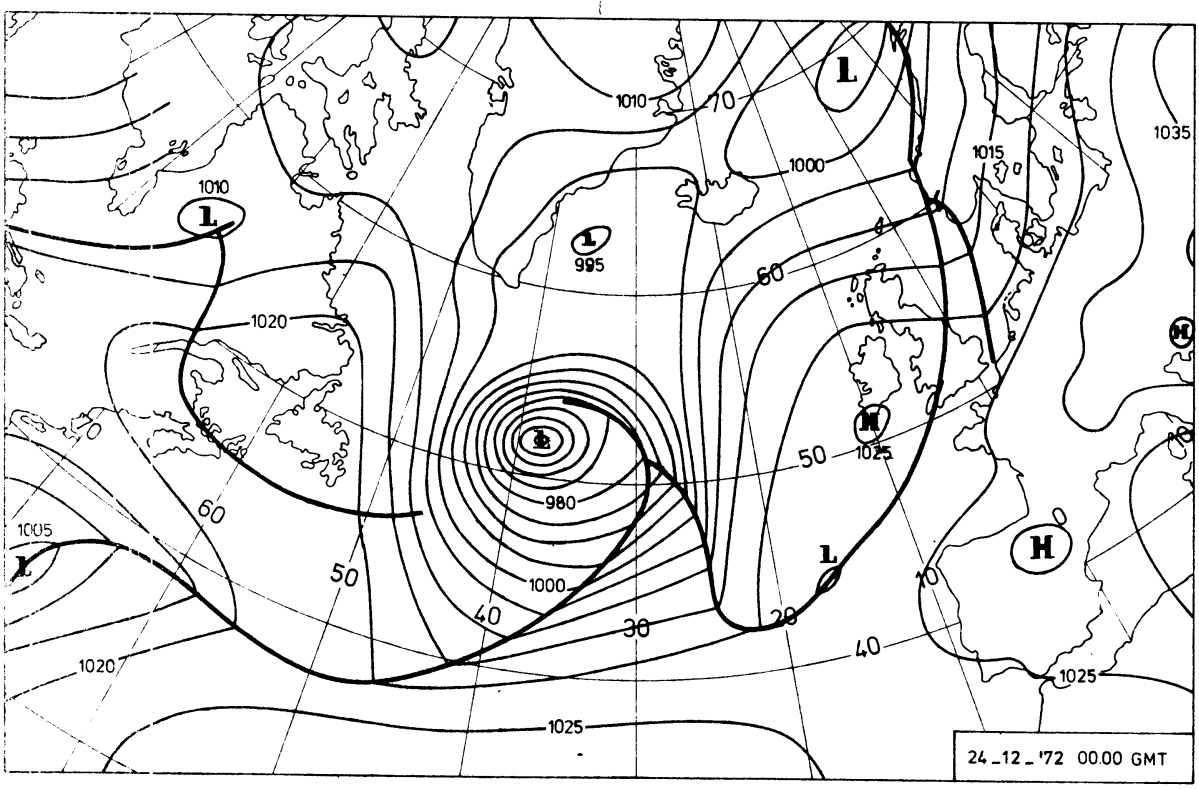

SURFACE ANALYSIS

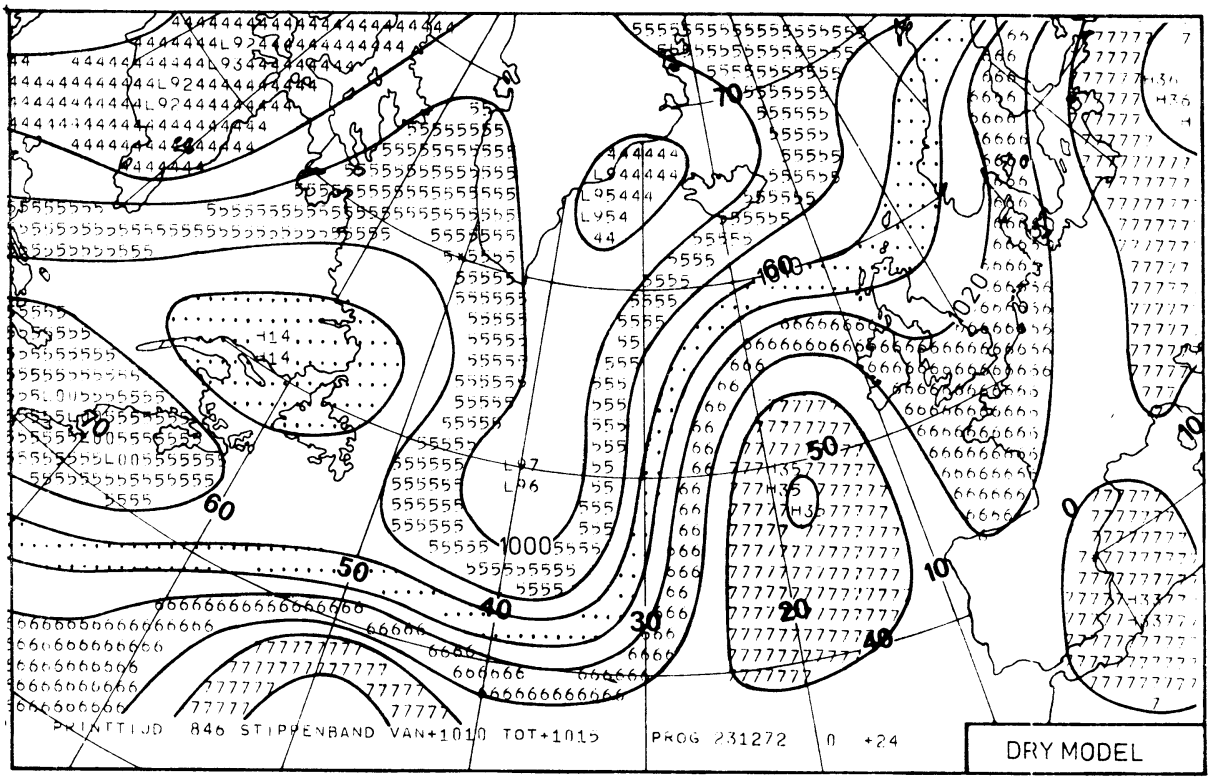

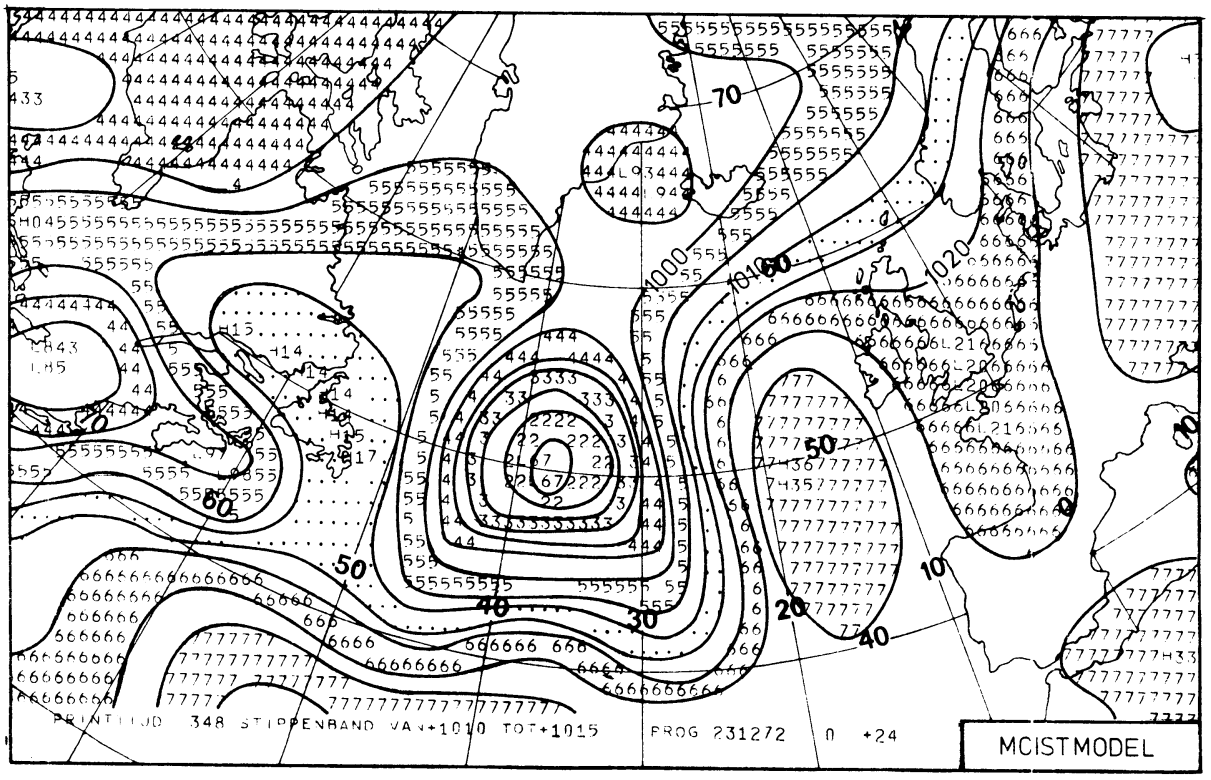

SURFACE + 24 PROG. VALID 00.00 GMT. 24-12-72

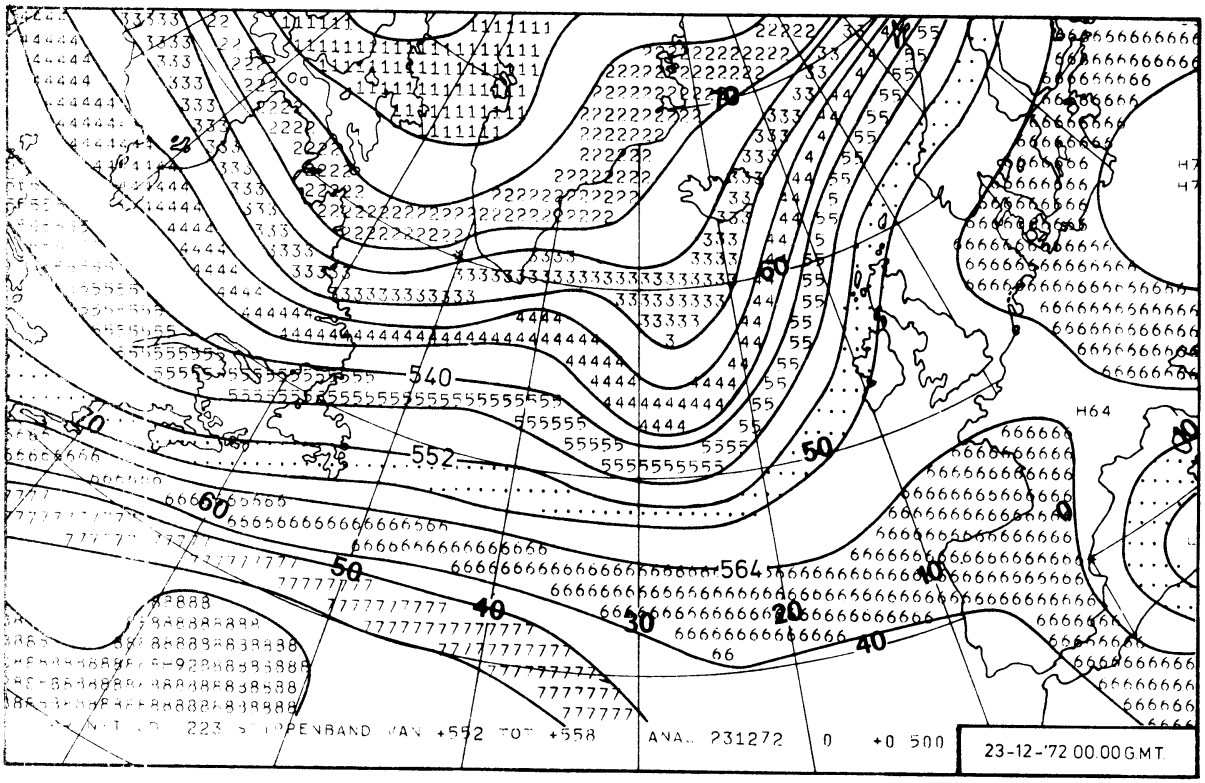

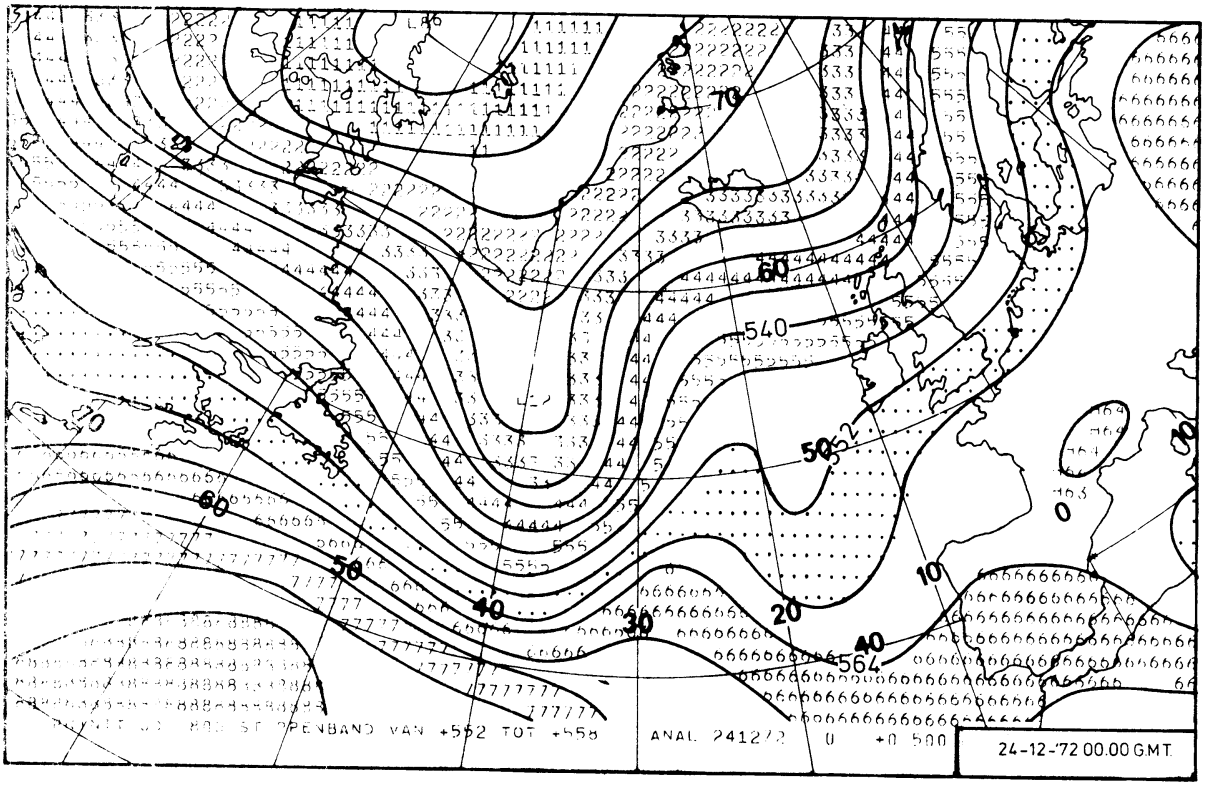

500MBAR ANALYSIS 00.00 GMT.

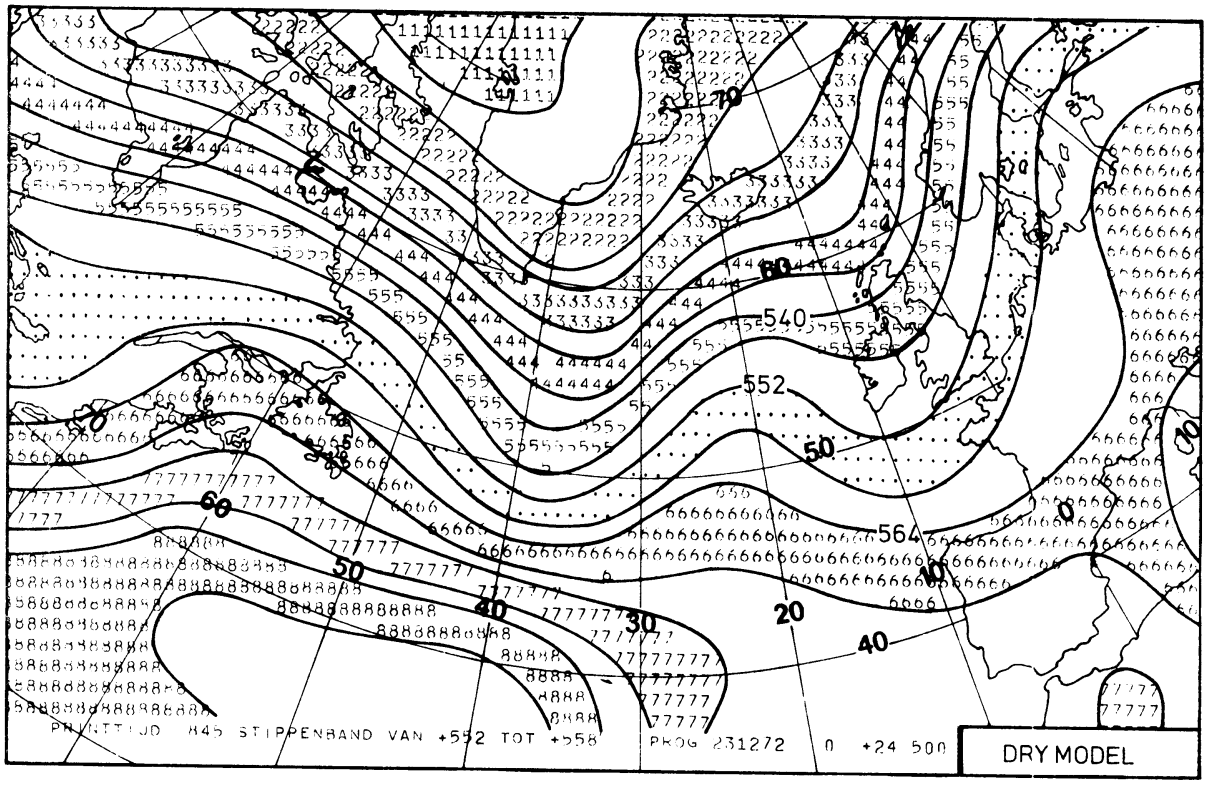

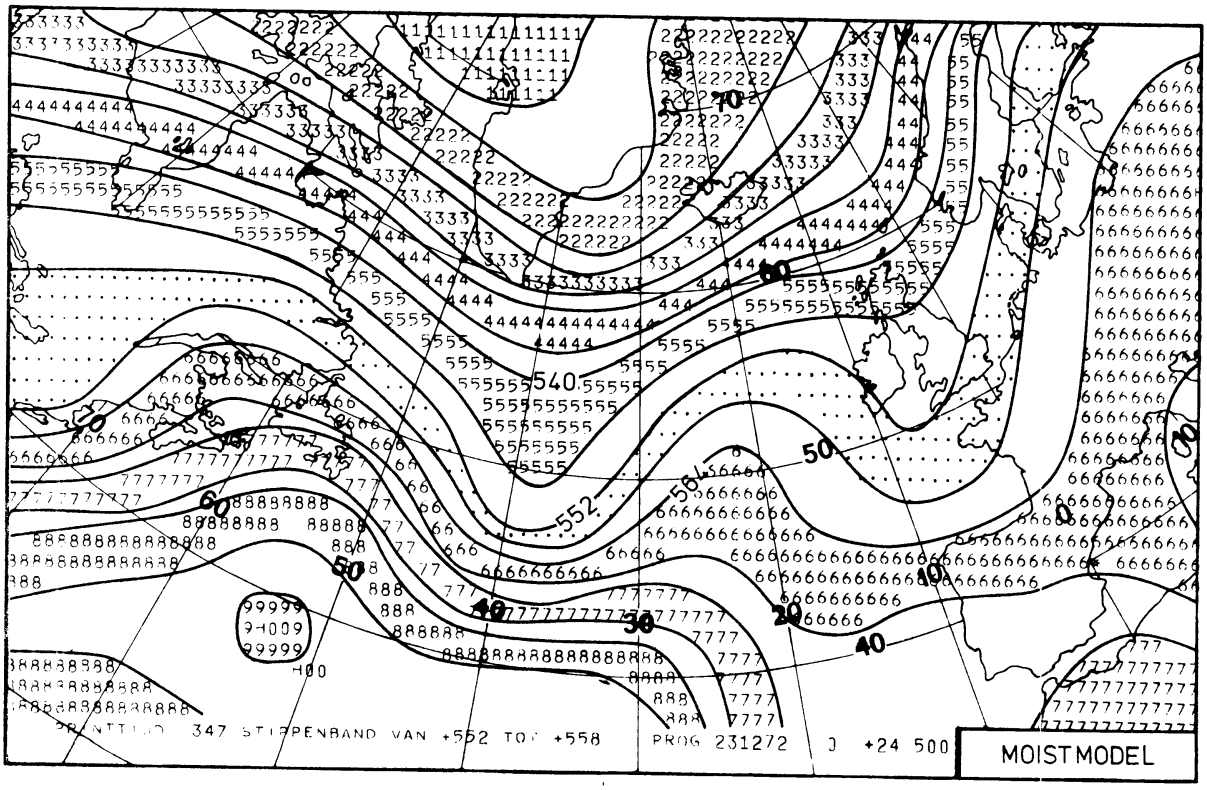

500MBAR + 24 PROG. VALID 00.00 GMT 24-12-'72

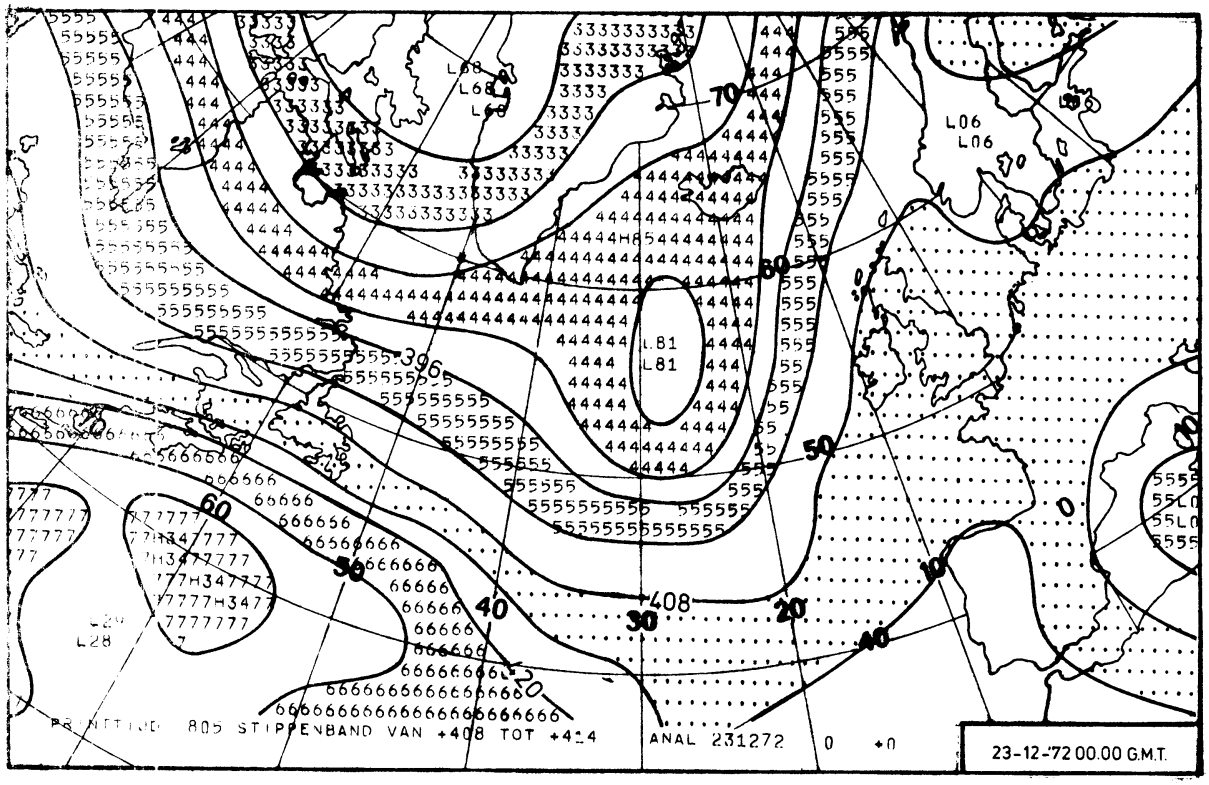

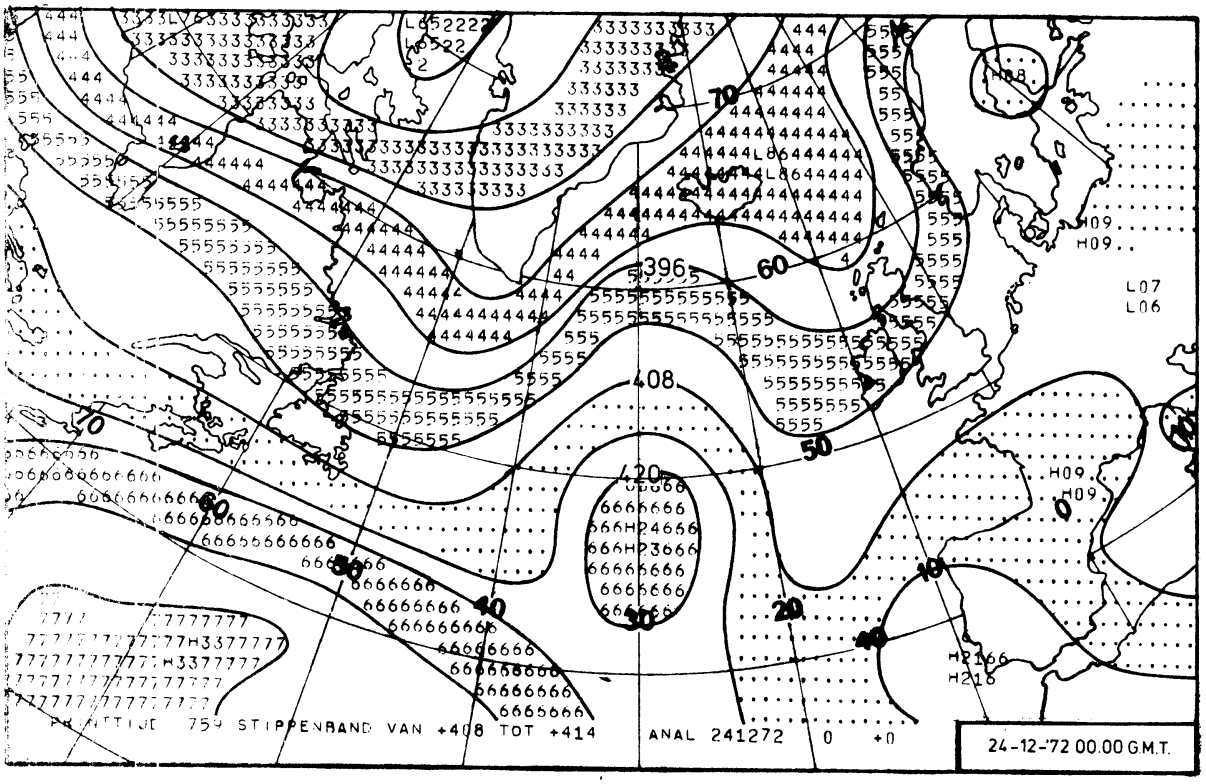

850-500 MBAR ANALYSIS 00.00 GMT

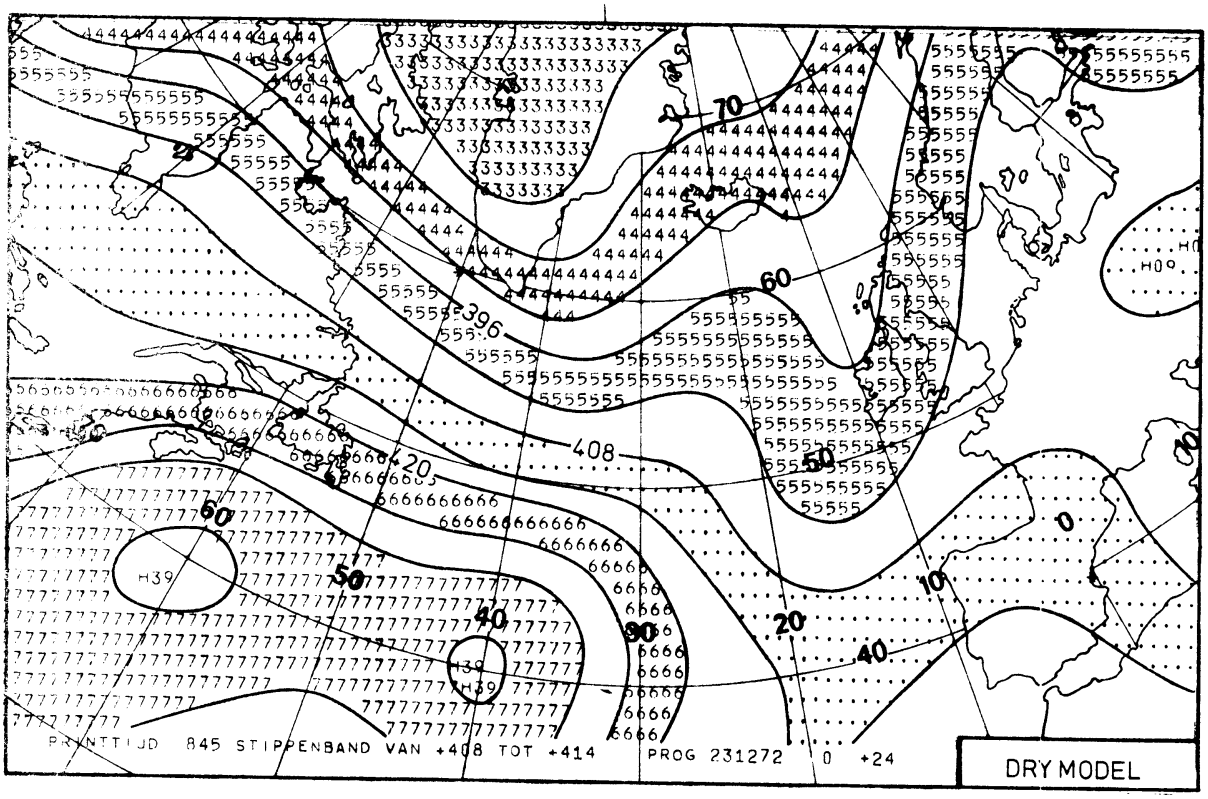

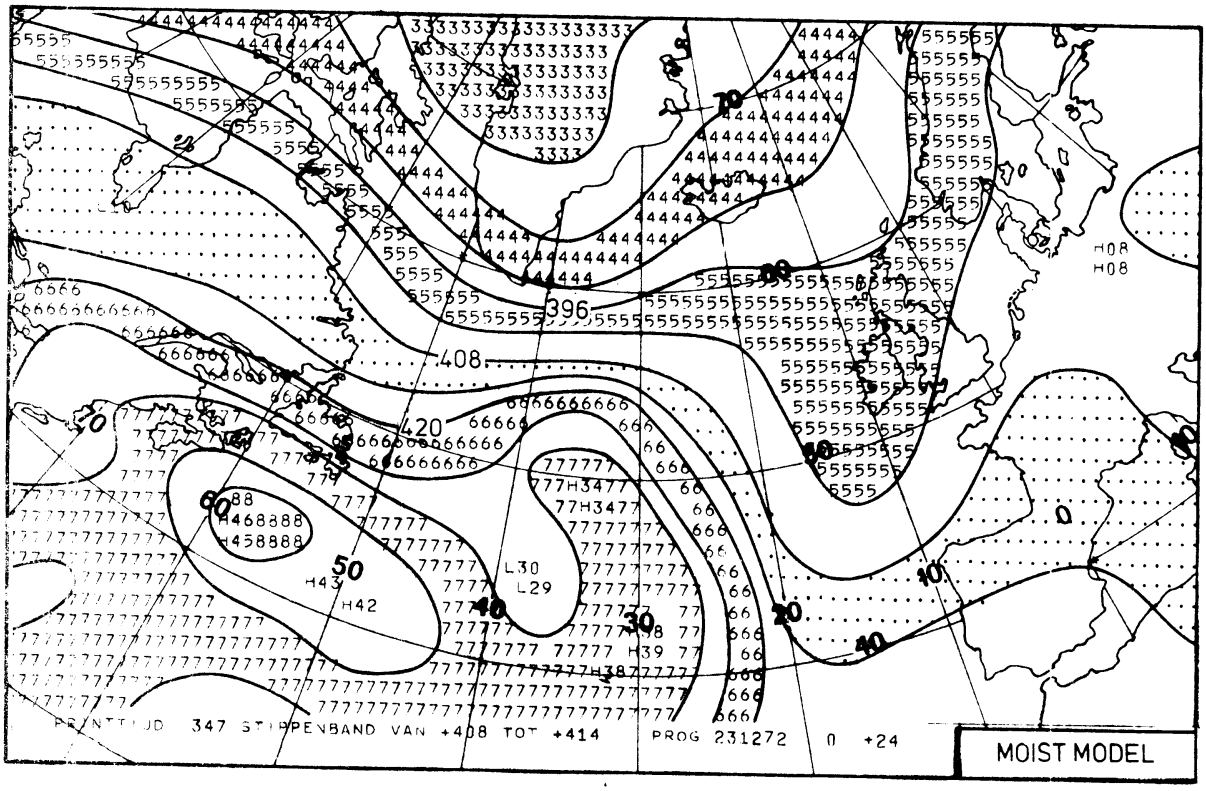

850 500MBAR + 24 PROG. VALID 00.00 GMT. 24 – 12 – '73

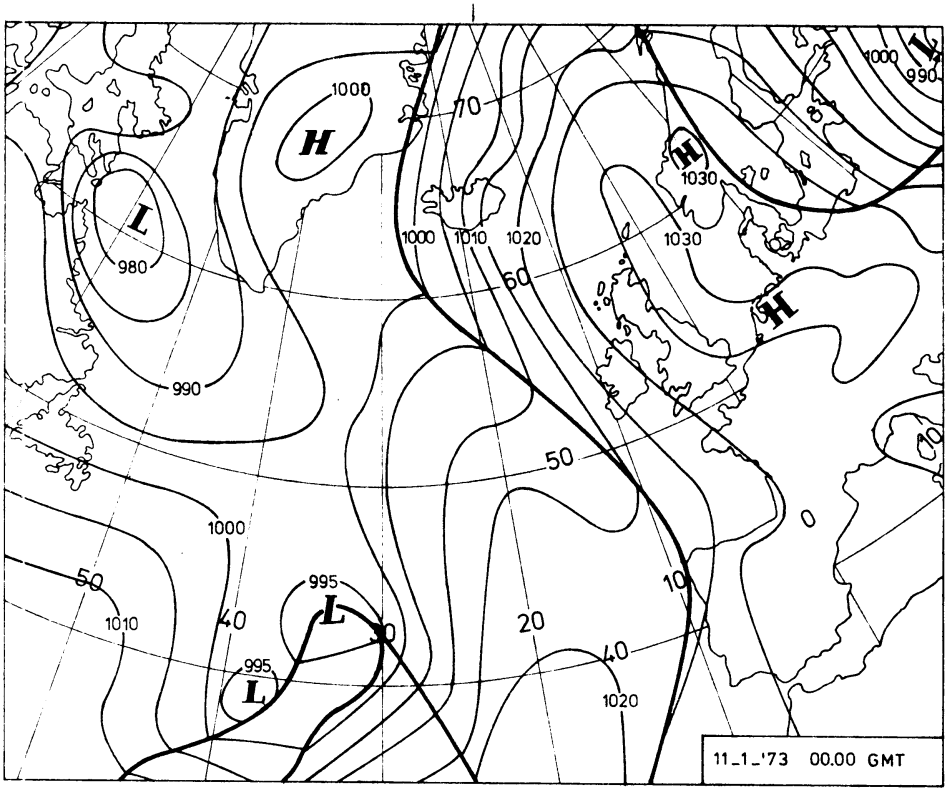

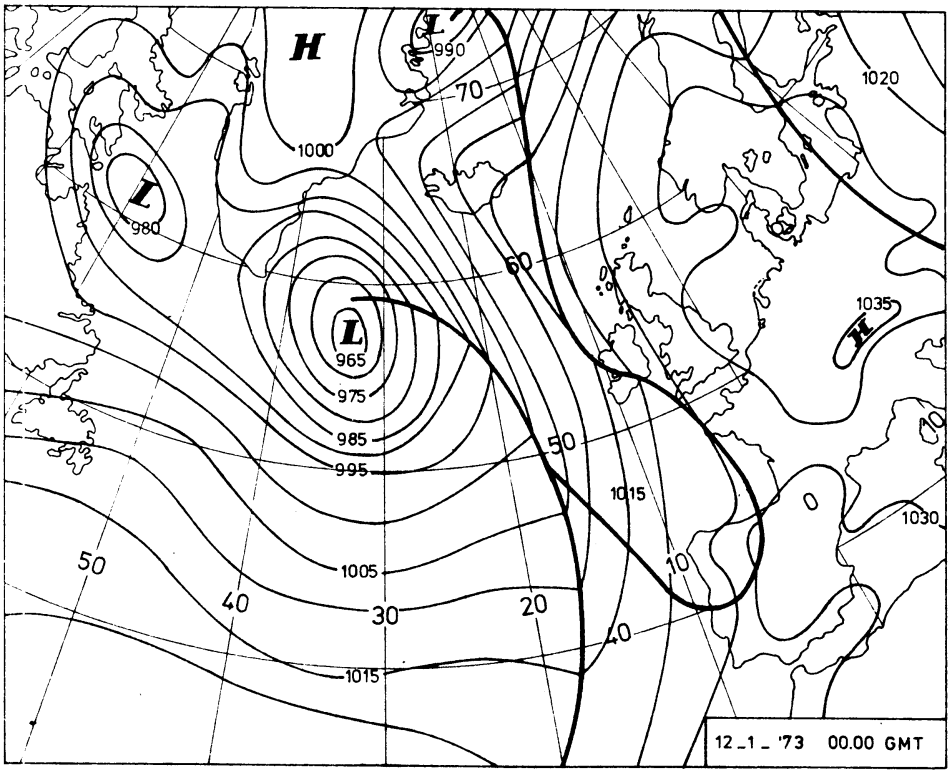

SURFACE ANALYSIS

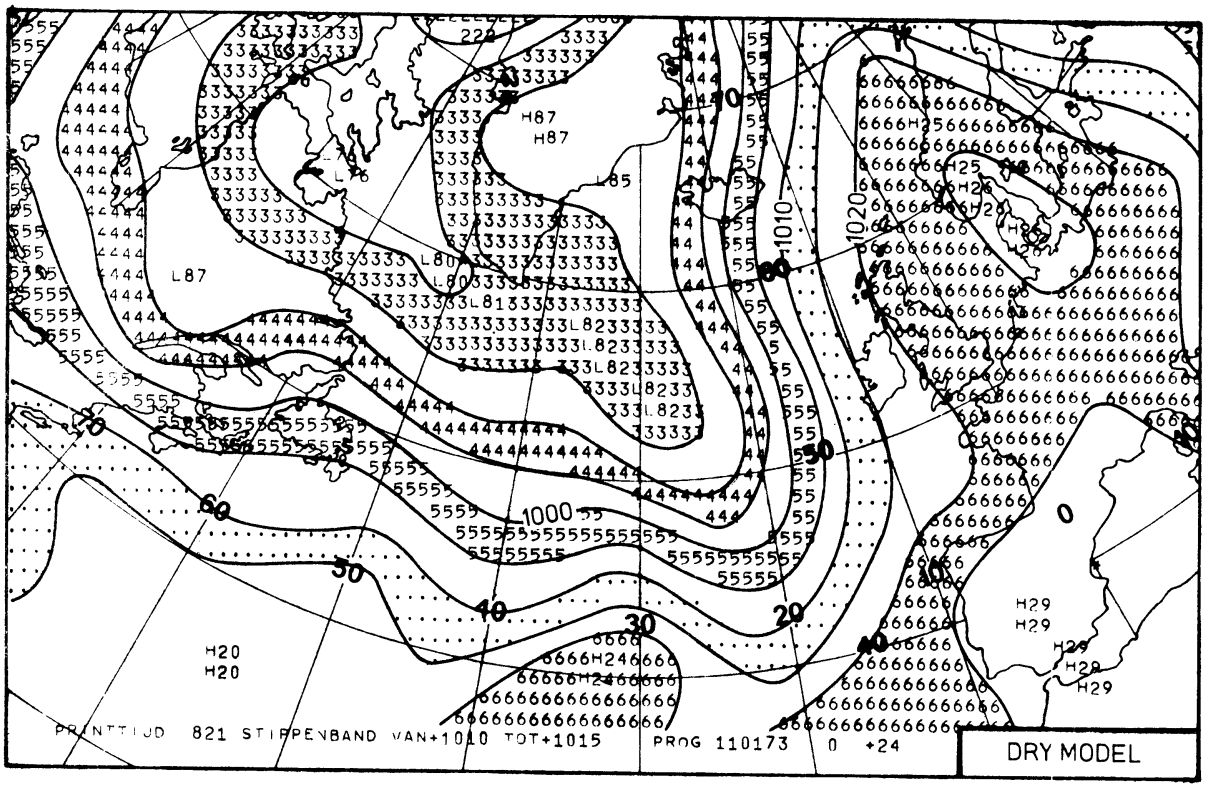

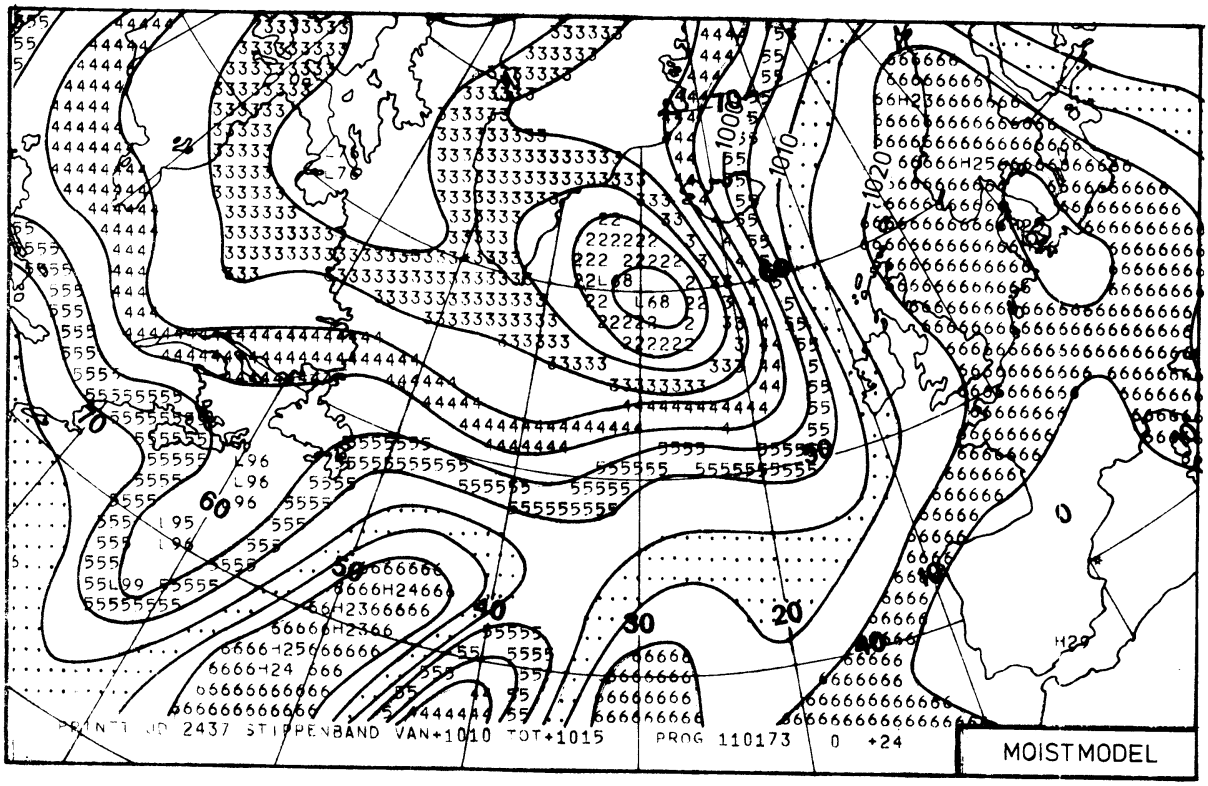

SURFACE + 24 PROG. VALID 00.00 GMT. 12-1-'73

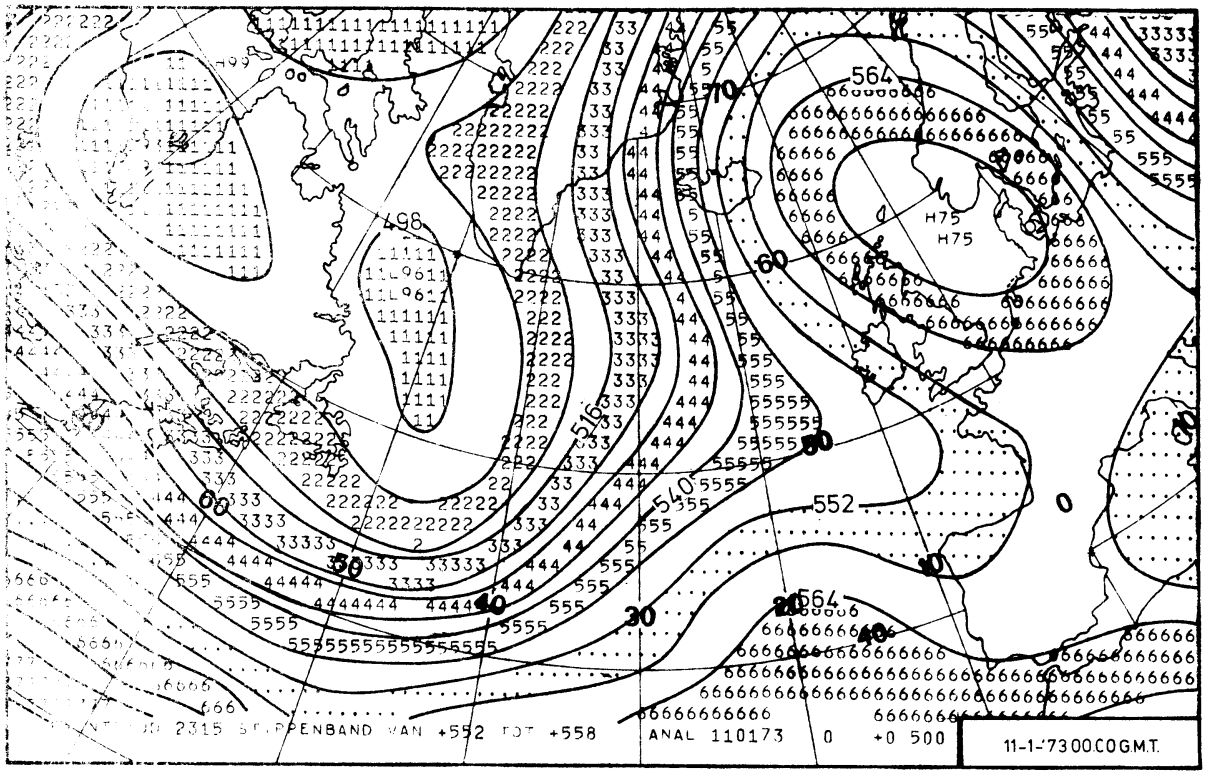

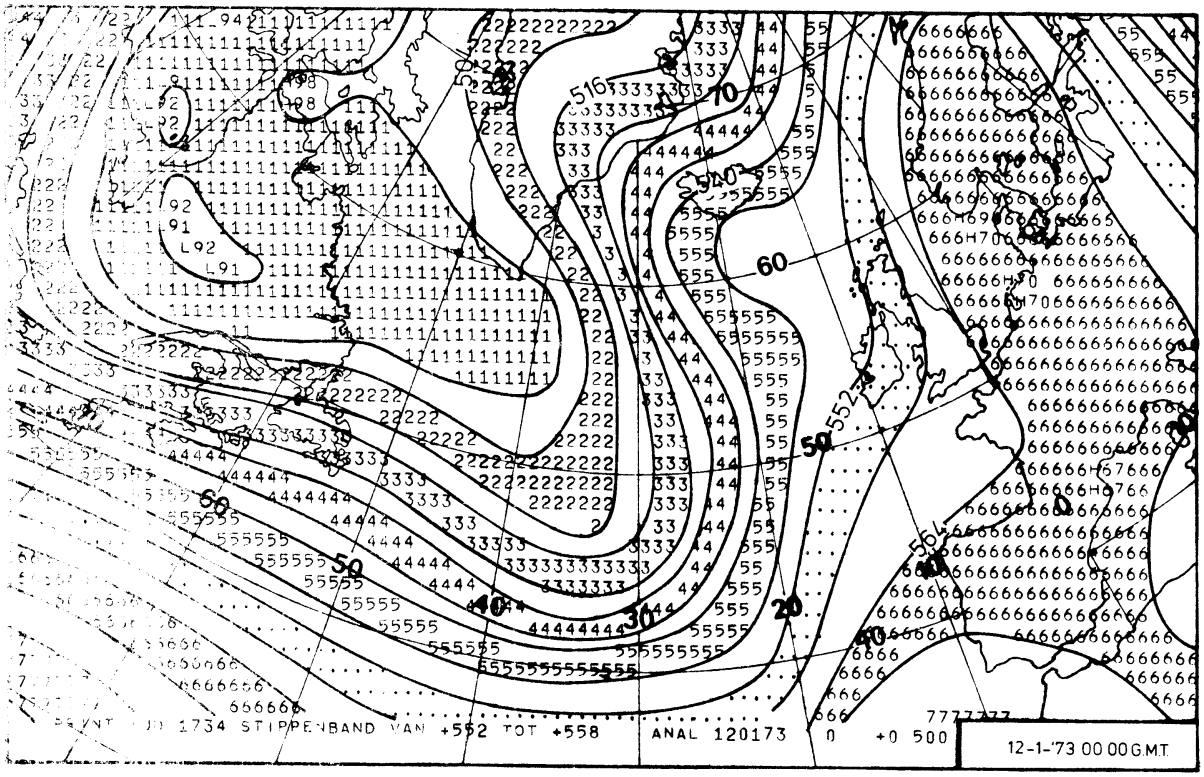

500MBAR ANALYSIS 00.00 GMT

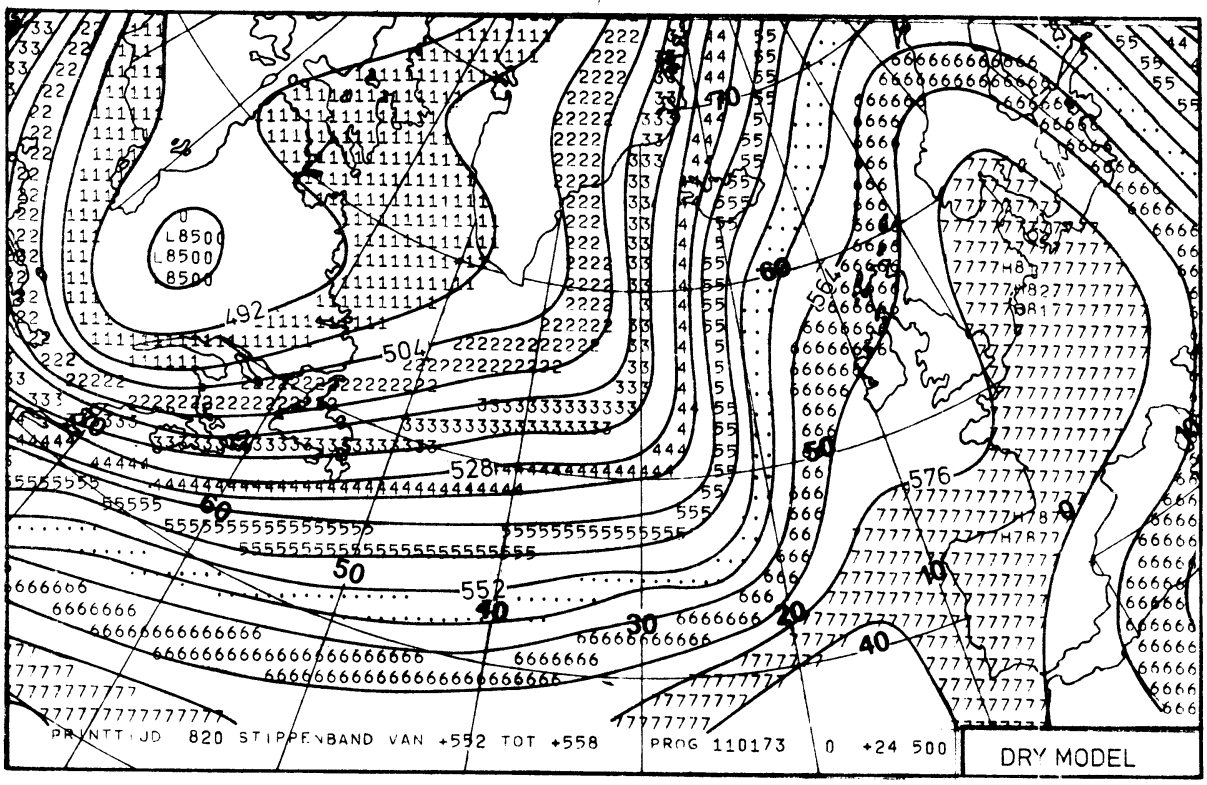

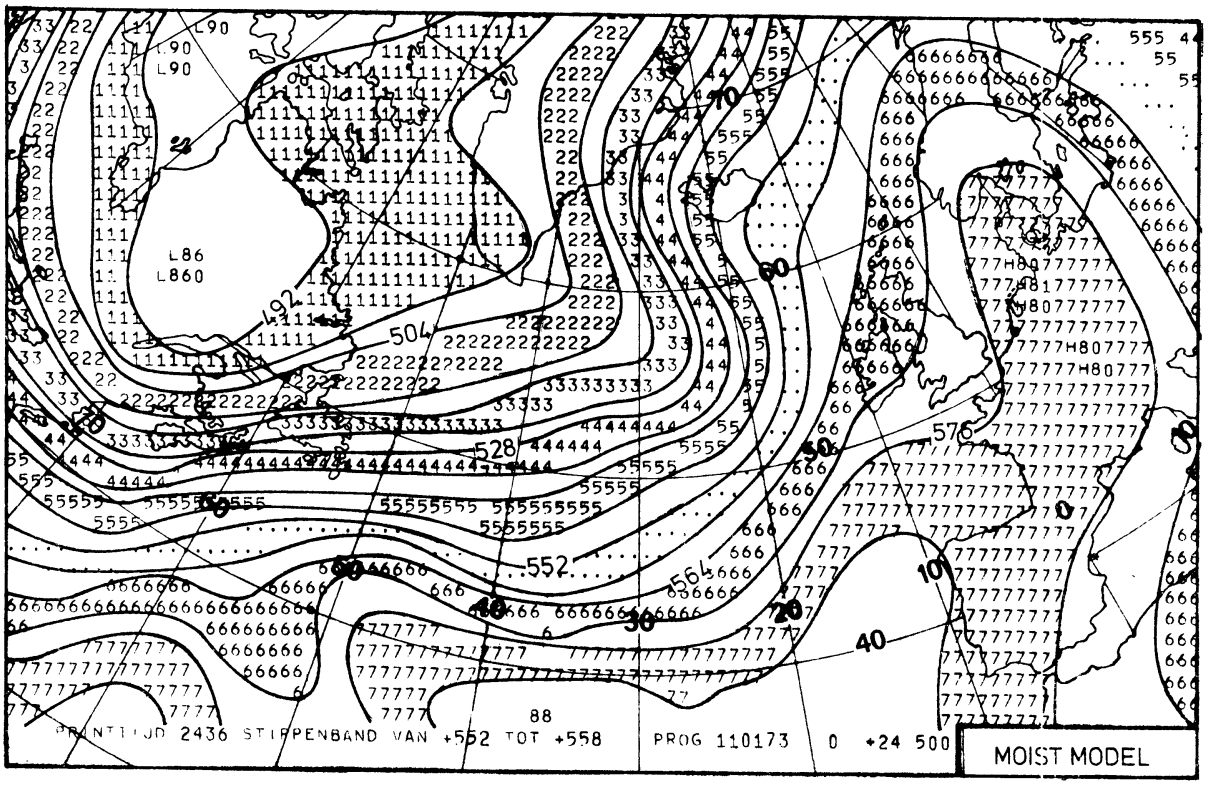

500MBAR + 24 PROG. VALID 00.00 GMT 12–1–'73

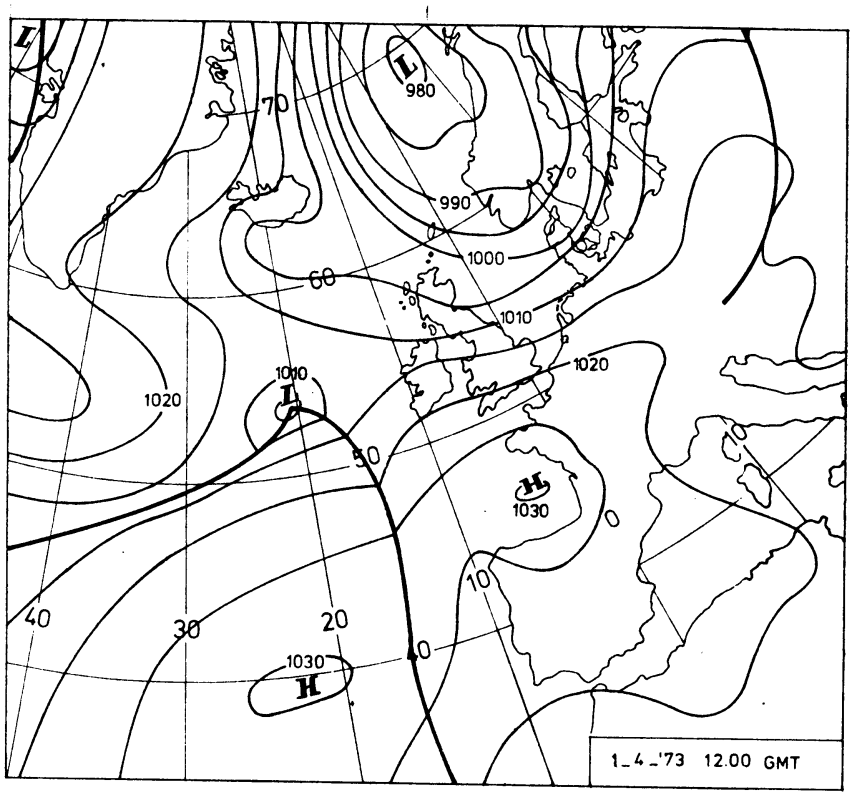

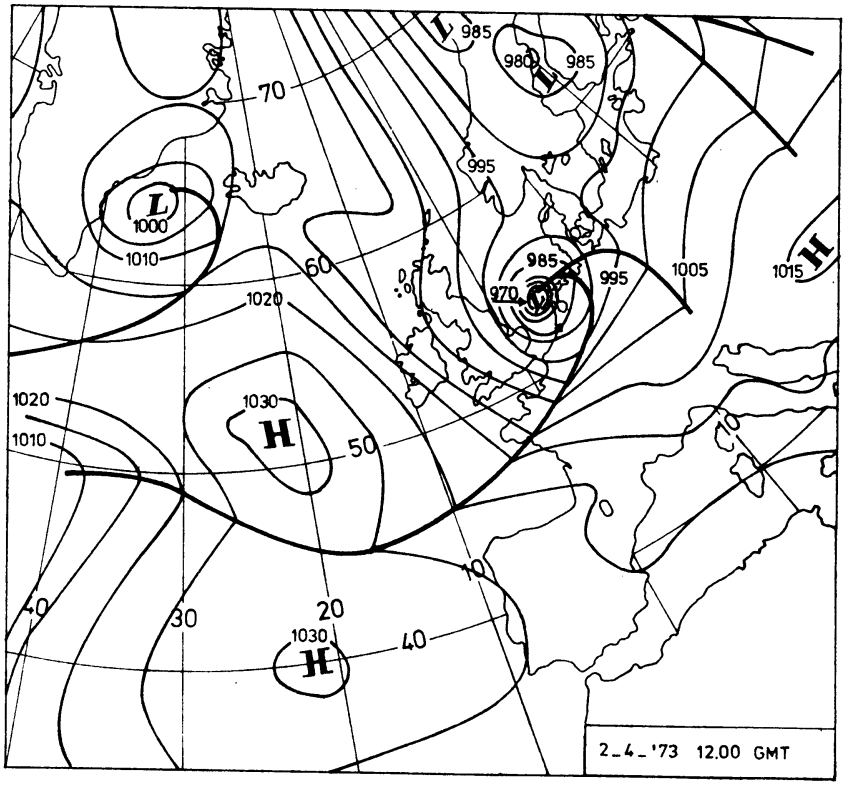

SURFACE ANALYSIS

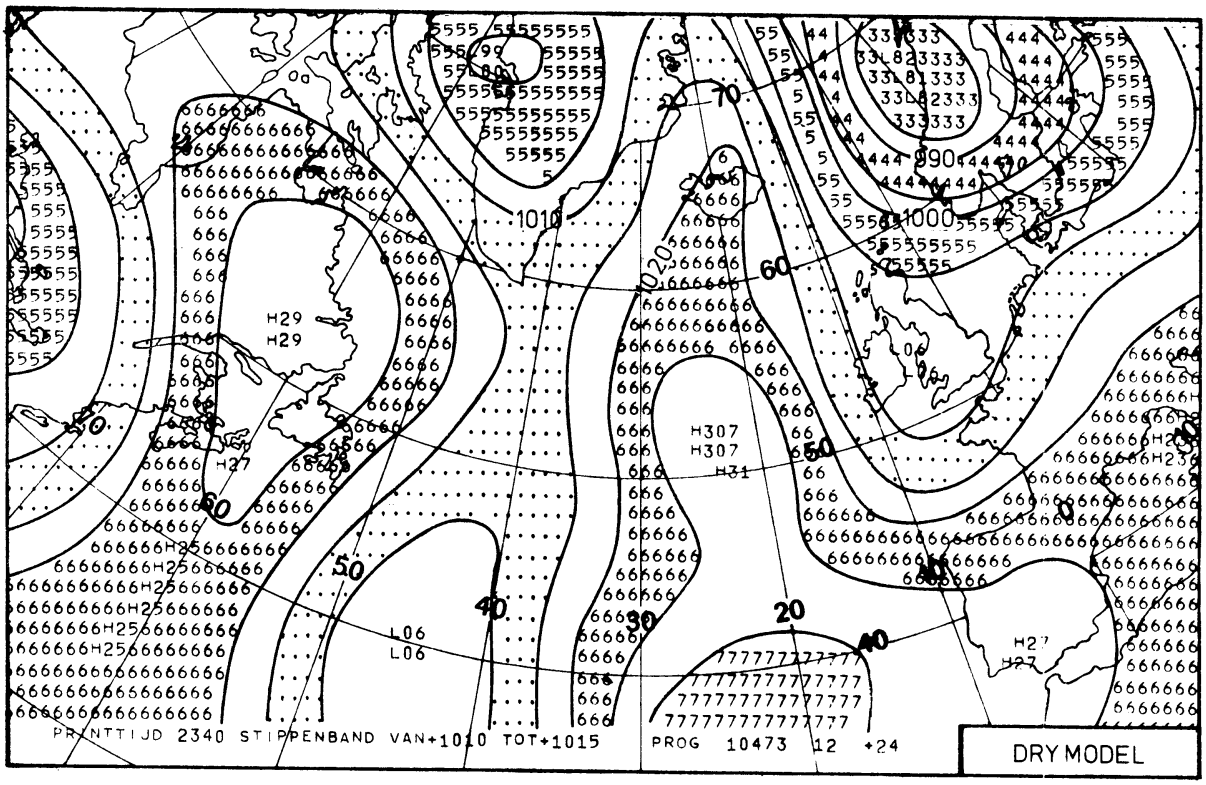

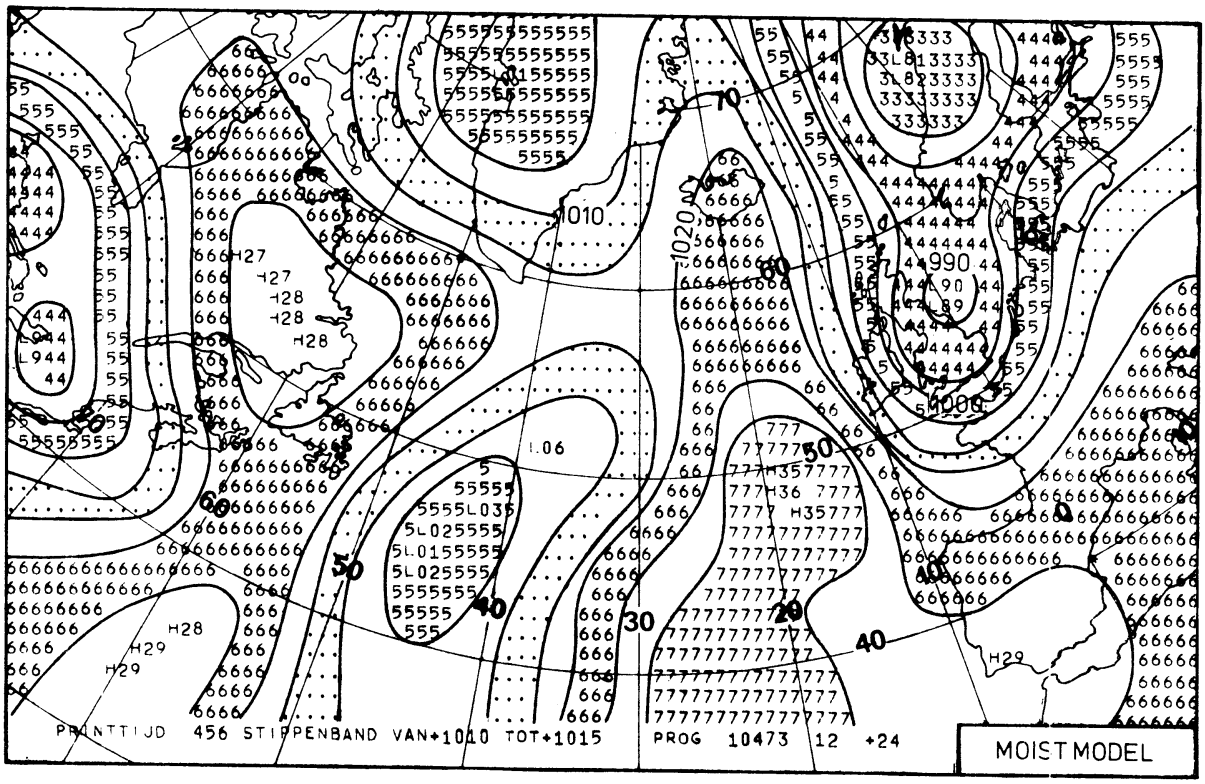

SURFACE + 24 PROG. VALID 12.00 GMT. 2-4-'73.

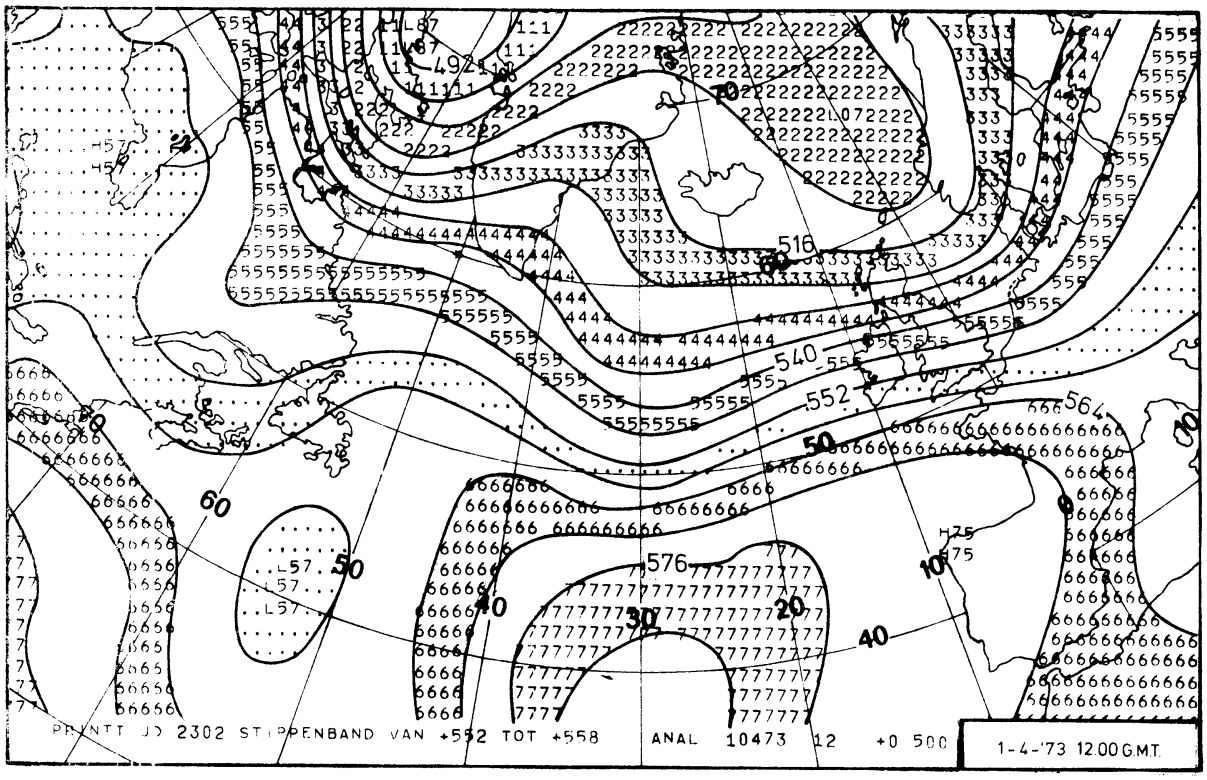

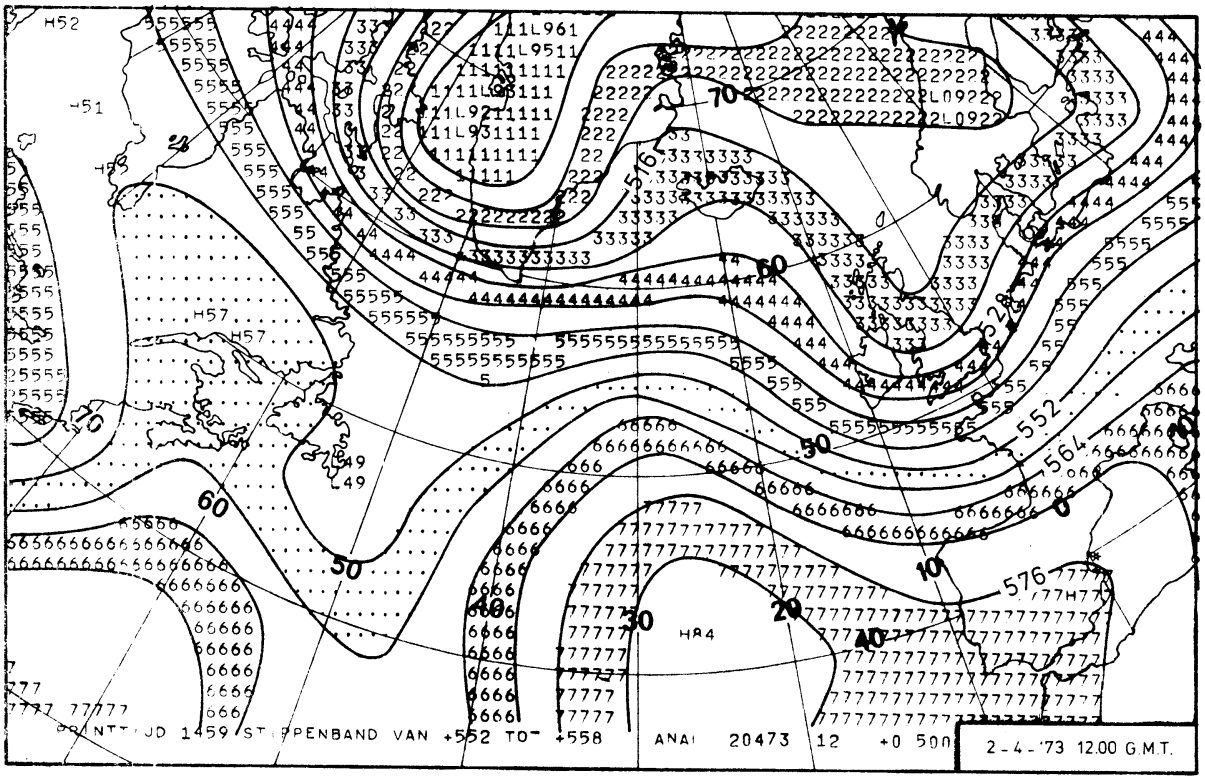

500MBAR ANALYSIS 12.00 GMT

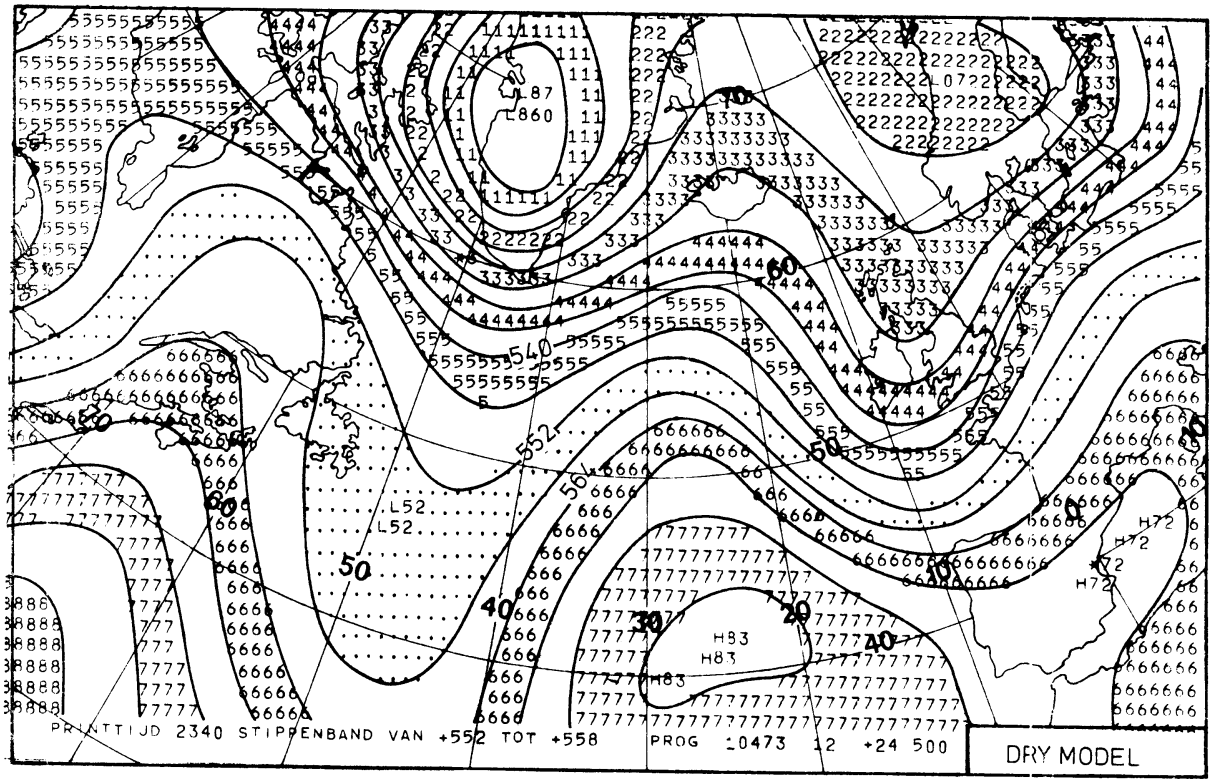

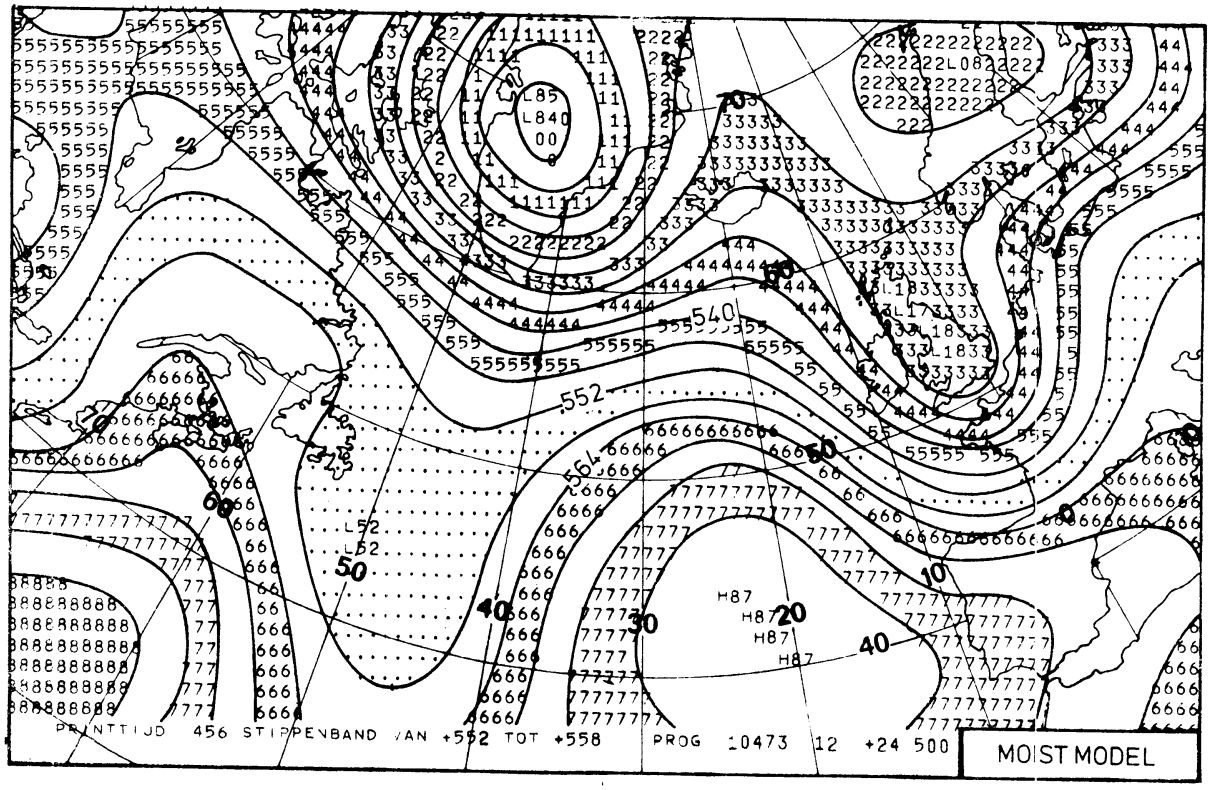

500MBAR + 24 PROG, VALID 12.00 GMT. 2-4-'73

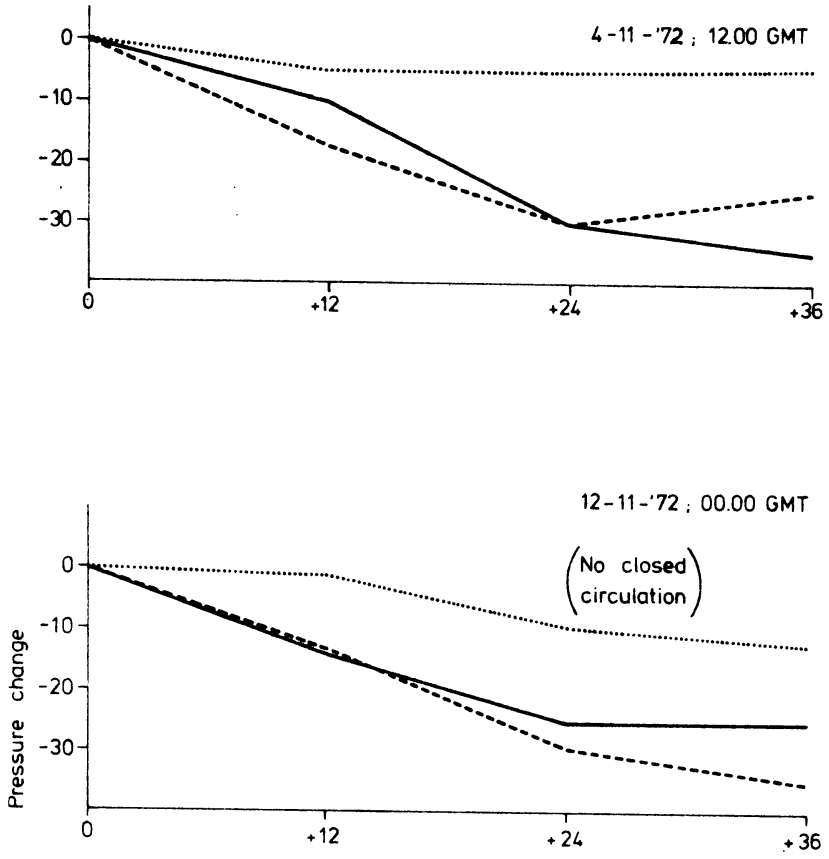

Comparison of predicted and observed pressure changes of the surface low centers.
The solid, dotted and dashed curves refer to the actual and the predicted dry and moist changes, respectively.

Figuur 2

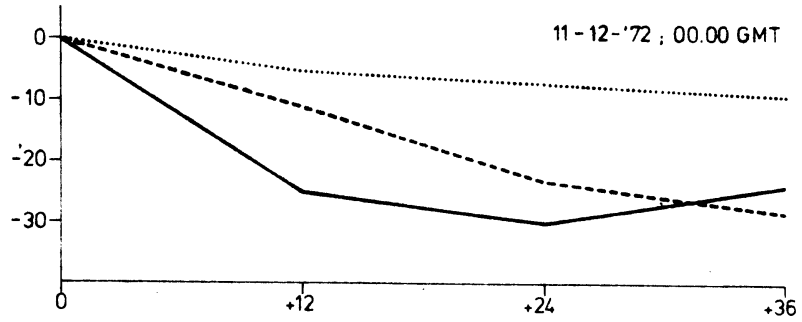
11-12-'72 ; 00.00 GMT
0
-10
-20
-30
0
+12
+24
+36

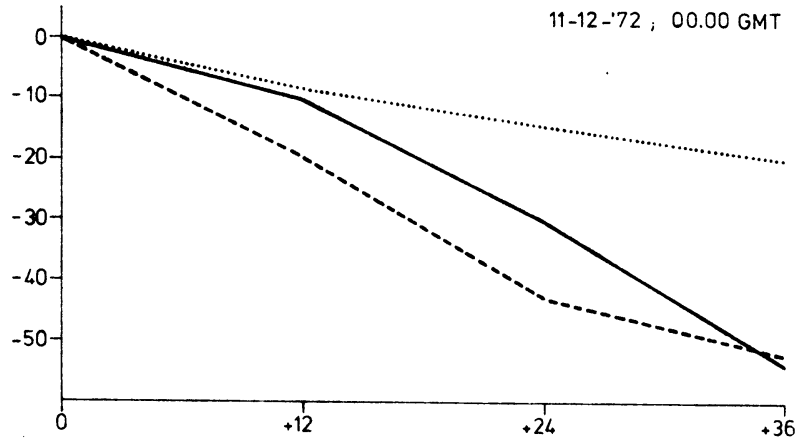
11-12-'72 ; 00.00 GMT
0
-10
-20
-30
-40
-50
0
+12
+24
+36

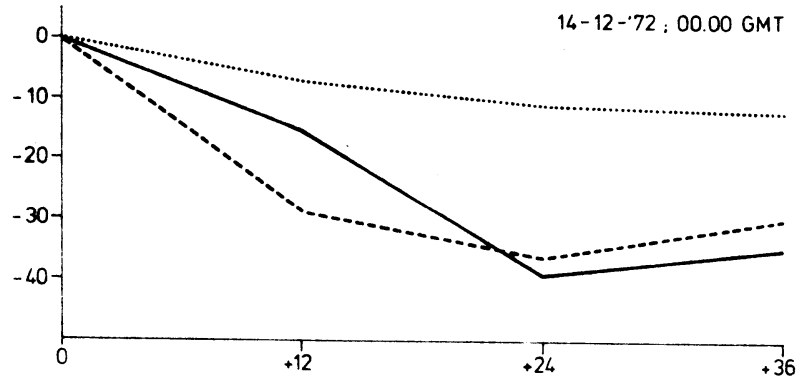
14-12-'72 ; 00.00 GMT
0
-10
-20
-30
-40
0
+12
+24
+36

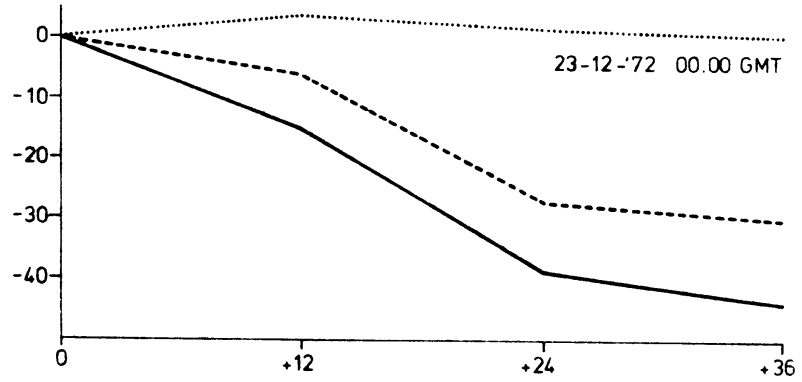
23-12-'72 00.00 GMT
0
-10
-20
-30
-40
0
+12
+24
+36

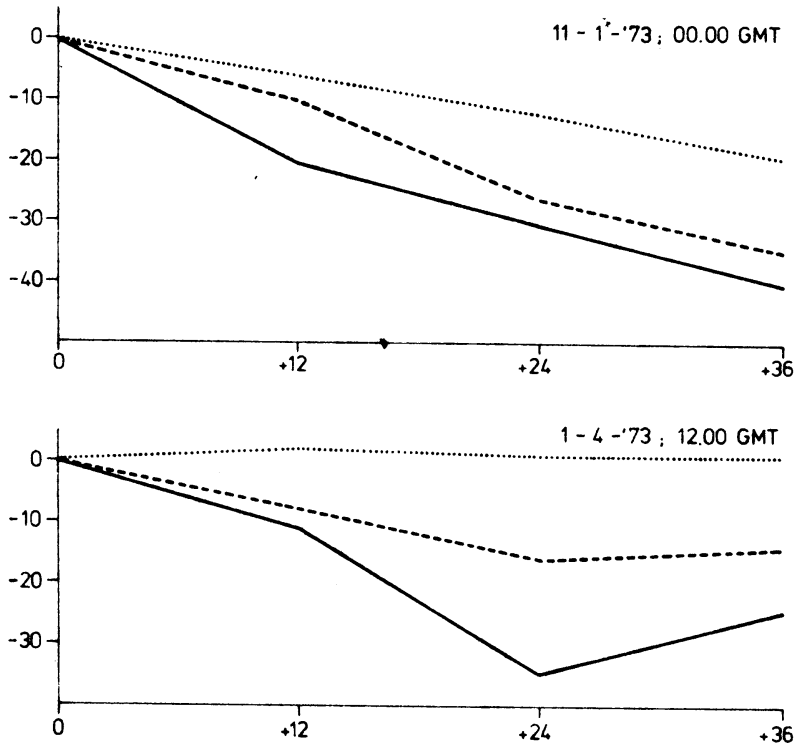
11 - 1 -'73 ; 00.00 GMT
0
-10
-20
-30
-40
0
+12
+24
+36
1 - 4 -'73 ; 12.00 GMT
0
-10
-20
-30
0
+12
+24
+36

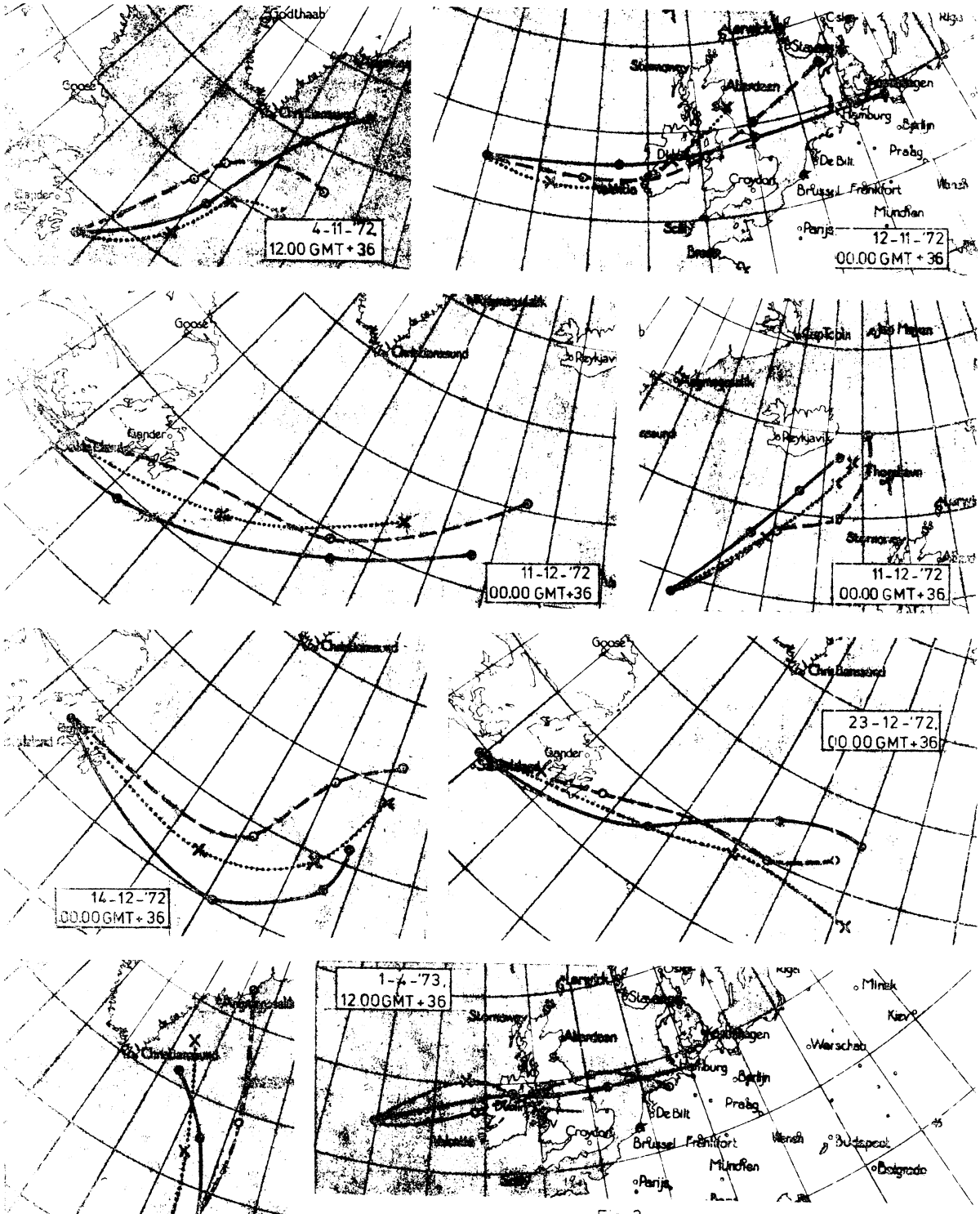

Fig. 3

Comparison of predicted and observed tracks of the surface low centers. The solid, dotted and dashed lines refer to the actual and the predicted dry and moist model tracks, respectively.

- ● actual position
- X dry model forecast
- ○ moist model forecast

} after 0, +12, +24, +36 hours